DISSERTATIONES
MEDICINAE
UNIVERSITATIS
TARTUENSIS
324

LAURA VIIDIK

3D printing in pharmaceutics: a new avenue for fabricating therapeutic drug delivery systems

DISSERTATIONES MEDICINAE UNIVERSITATIS TARTUENSIS
324

DISSERTATIONES MEDICINAE UNIVERSITATIS TARTUENSIS
324

LAURA VIIDIK

3D printing in pharmaceutics: a new avenue for fabricating therapeutic drug delivery systems

UNIVERSITY OF TARTU
Press
1632

Institute of Pharmacy, Faculty of Medicine, University of Tartu, Estonia

Dissertation is accepted for the commencement of the degree of Doctor of Philosophy (Pharmacy) on December 15th, 2021 by the Council of the Faculty of Medicine, University of Tartu, Estonia.

Supervisors	Associate professor Ivo Laidmäe PhD, Institute of Pharmacy, Faculty of Medicine, University of Tartu, Estonia; Institute of Biomedicine and Translational Medicine, Faculty of Medicine, University of Tartu, Estonia
	Associate professor Karin Kogermann PhD, Institute of Pharmacy, Faculty of Medicine, University of Tartu, Estonia
	Professor Jyrki Heinämäki PhD, Institute of Pharmacy, Faculty of Medicine, University of Tartu, Estonia
Reviewed by	Associate professor Tarmo Tamm PhD, Institute of Technology, Faculty of Science and Technology, University of Tartu, Estonia
	Professor Ursel Soomets PhD, Institute of Biomedicine and Translational Medicine, Faculty of Medicine, University of Tartu, Estonia
Opponent	Professor Thomas de Beer PhD, Department of Pharmaceutical Analysis, Faculty of Pharmaceutical Sciences, Ghent University, Belgium
Commencement	March 15th, 2022

The work was funded by the Estonian Research Council projects PUT1088, PRG726, and IUT-34-18; and Nordic POP, project #85352 by NordForsk.

ISSN 1024-395X
ISBN 978-9949-03-808-4 (print)
ISBN 978-9949-03-809-1 (pdf)

University of Tartu Press
www.tyk.ee

CONTENTS

LIST OF ORIGINAL PUBLICATIONS

This thesis is based on the following original publications referred to in the text by Roman numerals (I–III).

I **Viidik, L.**, Seera, D., Antikainen, O., Kogermann, K., Heinämäki, J., Laidmäe, I. 3D-printability of aqueous poly (ethylene oxide) gels. *European Polymer Journal*, 2019; 120, 109206. DOI: https://doi.org/10.1016/j.eurpolymj.2019.08.033

II **Viidik, L.**, Vesala, J., Laitinen, R., Korhonen, O., Ketolainen, J., Aruväli, J., Kirsimäe, K., Kogermann, K., Heinämäki, J., Laidmäe, I., Ervasti, T. Preparation and characterization of hot-melt extruded polycaprolactone-based filaments intended for 3D-printing of tablets. *European Journal of Pharmaceutical Sciences*, 2021; 158, 105619. DOI: https://doi.org/10.1016/j.ejps.2020.105619

III Anderspuk, H.*, **Viidik, L.***, Olado, K., Kogermann, K., Juppo, A., Heinämäki, J., Laidmäe, I. Effects of crosslinking on the physical solid-state and dissolution properties of 3D-printed theophylline tablets. *Annals of 3D Printed Medicine*, 2021, *Volume 4, 100031*. DOI: https://doi.org/10.1016/j.stlm.2021.100031
* Equal contribution to this publication.

Contribution of **Laura Viidik** to these publications

I Participation in the study design; viscosity measurements, designing, 3D printing and characterisation of the model lattices, FTIR spectroscopy studies; participation in data analysis; writing the manuscript.

II Participation in the study design; participation in filament preparation and test printing, physical appearance, mechanical properties, and stability testing of filaments; data analysis for performed experiments; writing the manuscript.

III Participation in the study design; material preparation, 3D printing of tablets, UV-crosslinking, and *in vitro* dissolution testing; data analysis for performed experiments; principal component analysis; writing parts of the manuscript.

LIST OF ABBREVIATIONS

2D	Two-dimensional
3D	Three-dimensional
4D	Four-dimensional
API	Active pharmaceutical ingredient
ARA	Arabic gum
CAD	Computer-aided design
CT	Computed tomography
DDS	Drug delivery system
DSC	Differential scanning calorimetry
EXT	Extrudate
FDA	United States Food and Drug Administration
FDM	Fused deposition modelling
FFF	Fused filament fabrication
FTIR	Fourier-transform infrared
HBP	4-hydroxybenzophenone
HER2	Human epidermal growth factor receptor 2
HME	Hot melt extrusion
HPLC	High performance liquid chromatography
IBU	Ibuprofen
IND	Indomethacin
IP	Intellectual property
MS	Microsoft
MW	Molecular weight
NIR	Near-infrared
ODT	Orally disintegrating tablet
PAM	Pressure assisted micro-syringe
PC	Principal component
PCA	Principal component analysis
PCL	Polycaprolactone
PEO	Polyethylene oxide
PETA	Pentaerythritol tetra acrylate
PM	Physical mixture
QbD	Quality-by-design
RH	Relative humidity
SD	Standard deviation
SLS	Selective laser sintering
SNV	Standard Normal Variate
STL	Standard tessellation language, stereolithography
THEO	Theophylline
USP	United States Pharmacopeia
UV	Ultraviolet
XR(P)D	X-ray (powder) diffraction

1. INTRODUCTION

It has been known for a while that the "one size fits all" concept does not always apply in medicine. Precision (also known as personalised) medicine is an approach to enhance the prevention, diagnosis, and treatment of diseases to benefit a specific group of patients. This approach includes, e.g., improved diagnostics by biological markers, pharmacogenetics, and more detailed evaluation of clinical responses. Using this knowledge to select the most suitable active pharmaceutical ingredients (APIs) and doses enables to achieve the optimal therapeutic efficiency. This applies to both specific diseases and patient populations, i.e., children and elderly, who need API dose and/or dosage form different from the average.

Another strategy to achieve an optimal drug treatment is to combine multiple otherwise simultaneously administered APIs into one drug delivery system (DDS). The growing number of medicines administered by a single patient is one of the reasons for a poor patient compliance. Such combined medicines called "polypills" are already on the market in the treatment of hypertension. While the combination of APIs is a step towards the right direction, it can still provide only a few average dose combinations. This is because the conventional industrial-scale manufacturing technologies (e. g., tablet compression), while being established and cheap, are not intended for producing small-scaled batches of personalised medicines. Therefore, the aim of pharmaceutical scientists is to find novel and more flexible methods to better meet the requirements of precision medicine.

Three-dimensional (3D) printing is an additive manufacturing technique that has been proposed as a solution for this challenge. In the first stage of 3D printing, computer-aided design (CAD) is used for creating a desired shape and size for the object to be printed. Next, the design is sliced into a layer-by-layer pattern by which the 3D printer will build up the object. There are various printing technologies using for example powdered, semisolid or molten materials for the creation of designed objects. Depending on the technique used, additional considerations, such as thermal stability and viscosity of the materials might need to be taken in to account. The 3D printing technologies have been studied since the 1980s, but they have gained wider popularity in recent years. Today, 3D printing technologies are widely used in different fields, such as in electronics, automotive industry, modular design, food industry, arts and jewellery making, and, of course, in medicine and pharmaceutics.

Patient-specific prostheses, models for practical studies, bioprinted cells, tissues, and printed medical gadgets are only a few examples of the implementation of printing technologies in medicine and biotechnology. Today, printing is also of great interest in pharmaceutical science. As 3D printing enables the layer-by-layer fabrication of DDSs, the API dosage can be readily modified by either increasing or decreasing the size or infill of the system. By using different carrier polymers and excipients, it is also possible to modify the drug release

behaviour. Therefore, 3D printing is considered as a possible future technology for fabricating more complex patient-specific DDSs. While this novel technique is promising, there is still a lot of understanding and knowledge to be gained. Further understanding of the 3D printing process, various printing technologies, printable materials and process parameters is crucial in successful development and manufacture of safe and stable personalised printed DDSs.

In the present doctoral research work, micro-extrusion-based and fused deposition modelling (FDM) 3D printing were investigated in fabricating novel pharmaceutical solid dosage forms. The aims of the research work were to gain understanding of the critical process parameters of these 3D printing methods, and to investigate the applicability of some commonly used polymeric excipients in 3D printing process.

2. LITERATURE REVIEW

2.1. The concepts of precision medicine

Precision medicine is a combination of methods to achieve the successful prevention, diagnosis, and treatment of diseases in a way that would benefit a specific patient group the most (Ashley, 2016). Figure 1 illustrates the dynamics from a common "one size fits all" concept to a novel precision medicine concept, and from the larger group of various patients towards detecting the needs of patient subgroups and a single patient. Some established approaches, such as blood type compatibility for transfusion (Landsteiner and Levine, 1927), have been used in medicine for almost a century and they have become a common practice. In the recent decades, however, a lot of research has focused on finding new strategies for precision medicine. Not only are patients categorised to subgroups by specific clinical features (Trusheim et al., 2011, Trusheim et al. 2007), but individual features, medication history and lifestyle habits can be considered when deciding on the medical treatment (Gray et al., 2019; Mutie et al., 2017).

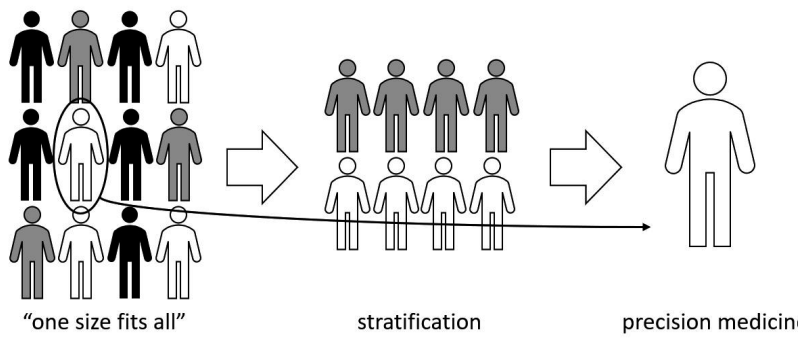

Figure 1. The idea and process of personalisation in medicine.

It is well known that if we focus only on a single patient, the medical treatment may not be cost-effective. Therefore, patient similarity and the possibility to create new clinically meaningful patient subgroups have been discussed in the literature (Brown, 2016; Parimbelli et al., 2018). Such medical treatment tailoring was intended also by the United States (US) National Research Council, when they implemented the term "precision medicine" in contrast to "personalised medicine" which implies to a patient-specific treatment (US National Research Council, 2011). Both precision and personalised medicine involve the overall idea of focusing on a smaller group of patients and their individual features, and therefore parallel terminology can be found in the state-of-the-art literature.

The volume of data and our knowledge of analysing and interpreting is ever growing (Hulsen et al., 2019). In the recent years, the application of precision medicine has been reported e.g., in the fields of cardiology (Antman and Loscalzo, 2016), oncology (Hamamoto et al., 2020; Li et al., 2020), and autoimmune diseases (Conrad et al., 2020; Giacomelli et al., 2021). An increased understanding of the individual therapeutic response and outcome in patients has opened a door for more personalised DDSs, and consequently, changes in dosage, drug release behaviour and API combination(s) (Cerda et al., 2020; Shaban A. Khaled et al., 2015; Robles-Martinez et al., 2019). As the overall goal of a healthcare system is not only to diagnose and treat, but also prevent diseases, it is not surprising that parallel to personalised DDSs and precision medicine, a new field of precision health is also emerging (Gambhir et al., 2018; Hekler et al., 2020; Khoury et al., 2016). The precision health approach involves the early-stage assessment of clinical risk and preclinical conditions. This concept very much relies on the technological advances of omics (Ahmed, 2020; Chen and Snyder, 2013; Garay and Gray, 2012; Long et al., 2018; Olivier et al., 2019), but also on the daily and commonly understandable methods, such as the implementation of wearable monitoring devices to everyday life (Ho et al., 2019; Jeong et al., 2019).

For years, the concept of drug delivery (i.e., the systems designed for delivering API(s) into the body to obtain desired clinical response) has evolved into the usage of complex modified or targeted DDSs with an ultimate goal to achieve the personalisation of drug treatment(s) (Florence and Lee, 2011). In many aspects, precision medicine and precision pharmacotherapy can be regarded as a similar concept – more thorough decisions are made by the aid of genetic and biological markers to achieve optimal results. Personalised medicine as such can be considered quite a historical approach, since pharmacists have been compounding extemporaneous preparations intended for specific patients' needs for centuries (Falconer and Steadman, 2017). Today, if precision medicine is discussed, in most cases pharmacogenomics is meant (Lee et al., 2020).

The US Food and Drug Administration (FDA) has published a list of over fifty APIs that need considerations when administering to specific patient subgroups of certain genetic variants, or genetic variant-inferred phenotypes (FDA, 2020). It is not surprising that the majority of the variations listed are related to cytochrome P450 enzyme family, as they are responsible for the biotransformation of approximately 75% clinically used APIs (Lynch and Price, 2007; Zanger and Schwab, 2013). Yet, the first personalised treatment was targeted at human epidermal growth factor receptor 2 (HER2), that is associated with worse prognosis for breast cancer (Ross et al., 2009; Whenham et al., 2008).

The further development of conventional methods for tailoring API doses and dosage forms should not be underestimated. The need for age-appropriate doses for paediatric and geriatric patients is well understood, but this approach still remains a challenge for the pharmaceutical industry (Galande et al., 2020; Walsh et al., 2018). Problems can arise for example in finding oral solid dosage forms with suitable size (Forough et al., 2018; Ranmal and Tuleu, 2013; Schiele

et al., 2013; Stegemann et al., 2012). Oral liquid formulations are often developed and administered to both children and elderly patients to overcome this barrier. However, the two major formulation challenges related to such oral liquids are their limited stability (Haywood and Glass, 2013) and dose-related variations/errors (Grießmann et al., 2007; Wang et al., 2020; Williams et al., 2019; Yin et al., 2016). In addition, palatability, mouth feel and taste are of most importance for the use of oral liquids (Andrews et al., 2021; Mistry and Batchelor, 2017; Ternik et al., 2018). Moreover, from the safety point of view the careful selection of excipients is crucial in paediatric formulations (Binson et al., 2019; Buckley et al., 2018; Nellis et al., 2016).

As the amount of information for making medical decisions is rapidly growing and evolving, the methods used in medical treatment and drug therapy need to keep up. The most common manufacturing technologies used in the pharmaceutical industry are intended for large-scale manufacture, thus lacking flexibility. The process flexibility and reliability are being improved via the implementation of quality-by-design (QbD) concept to produce improved DDSs (Tahara, 2020; Zhang and Mao, 2017). In addition, 3D-printing as a novel manufacturing technology holds great promises in filling the gap between the conventional batch-wise and modern flexible continuous manufacturing methods (Prendergast and Burdick, 2020).

2.2. Additive manufacturing – 3D printing

Three-dimensional (3D) printing is an additive manufacturing technique for the layer-by-layer creation of pre-designed structure of any shape. It was first described by Charles W. Hull in 1980s as a "system for generating three-dimensional objects by creating a cross-sectional pattern of the object to be formed at a selected surface of a fluid medium" (Hull, 1986). Additive manufacturing holds great promises in fabricating customised healthcare products, since it enables to reduce environmental impact and simplifies a supply chain (Huang et al., 2013). Even more, 3D-printing has shown its advantages in quick adaption to current needs during the COVID-19 pandemics (Choong et al., 2020; Cox and Koepsell, 2020; Oladapo et al., 2021; Tarfaoui et al., 2020).

The overall process schematic of 3D printing from design to final object is shown on Figure 2.

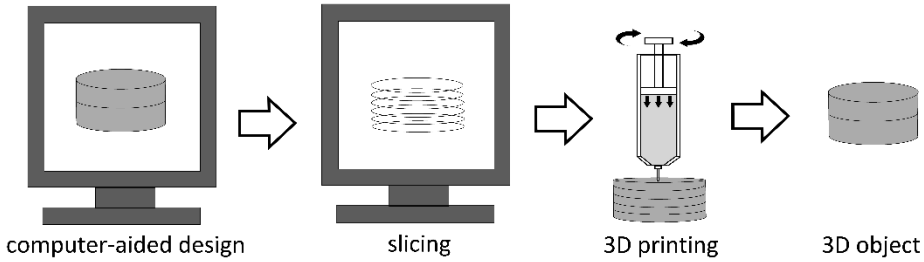

Figure 2. Simplified schematic of additive manufacturing exemplified by extrusion-based 3D printing setup.

The object to be printed is first created by computer-aided design (CAD). CAD enables to design the final DDS with a wide range of properties regarding size, shape and drug release behaviour (Curti et al., 2020). The design can also be obtained by 3D scanning (Willis et al., 2007), which to date has also been widely applied in the medical field (Goyanes et al., 2016; Haleem and Javaid, 2019). In the next step, the design is sliced by a computer software to separate layers and a specific printing itinerary is created. The STL (standard tessellation language, also called stereolithography) file provides the approximation of the original model using planar geometry via tessellation. Such pre-processing of the design instructs the printer on how to optimally prepare the model object, and in some cases it can be challenging (Oropallo and Piegl, 2016). The designed object is then fabricated either by layer-by-layer addition of (semisolid, molten) printing material, or by layer-by-layer manipulation of printing bed (powder, polymeric) via thermal or laser treatment. The formation of object from CAD file is also called rapid prototyping. Depending on the process and material(s) used, additional post-print curing may be needed.

The theoretical basis for 3D printing was described already more than a hundred years ago by an Italian mathematician Guido Fubini (Fubini, 1907). He proved that any real-life 3D object can be replicated by two-dimensional (2D) layers. According to Fubini's theorem, any object of n dimensions can be portraited by a spectrum of layers of shapes of $n\text{-}1$ dimensional layers. In practice, the well-known bottleneck for the use of 3D-printing in medical applications is finding suitable biocompatible polymers as carrier materials (Paul et al., 2018; Yan et al., 2018). These material considerations are discussed in detail in subchapter 2.4.2.

Two-dimensional (2D) and four-dimensional (4D) printing have also found uses in pharmaceutical and medical applications. 2D (or inkjet) printing is familiar to common users as a method to print text or images onto paper or other surfaces. In medical field this concept has been used by replacing office supplies with eatable or biodegradable carrier surface (e.g. paper/film/mats), and by introducing API-loaded biocompatible ink (Daly et al., 2015; Tian et al., 2019). 4D printing refers to the phenomena where the dimensions of a 3D-printed

object are changed when in contact with certain medium, such as water (Gladman et al., 2016; Joshi et al., 2020; Momeni et al., 2017).

2.2.1. 3D-printing technologies

Additive manufacturing technologies are classified differently in the literature – often based on either the state of substance material, or the additive shaping principle. The latter is also used by the International Organization for Standardization in a first international standard (ISO/ASTM 52900:2015 Standard Terminology for Additive Manufacturing – General Principles – Terminology, 2015). In this standard, 3D printing process techniques are categorised into seven groups:

1) Binder jetting
2) Directed energy deposition
3) Material extrusion
4) Material jetting
5) Powder bed fusion
6) Sheet lamination
7) VAT photopolymerization

The layer formation principle of these printing methods is summarised in Table 1. As the names of printing methods may vary in the literature, it is important to understand the basic mechanisms of given technique. Some variations are also introduced in this thesis. It is worth to mention that not all printing methods listed in Table 1 are applicable for fabricating pharmaceutical dosage forms, and the selection of a printing method is primarily based on the physicochemical characteristics of API (Garcia et al., 2018; Yu et al., 2008).

Table 1. Printing technologies and their characterisation

Technology	Layer formation
Binder jetting	spraying of solution binds solid particles to one another
Directed energy deposition	material is deposited onto surface and then melted, using a laser, electron beam or plasma arc
Material extrusion	molten material is deposited onto surface, layers build up on solidified material
	deposition of viscous liquids/semisolids, layers build up from dried material
Material jetting	liquid material is deposited onto surface, then cured/hardened
Powder bed fusion	powder layers are melted and fused using a laser or electron beam
Sheet lamination	material layers are stacked using welding, adhesive, heat, or pressure
VAT photopolymerization	UV light cures/hardens the layers

Micro-extrusion-based printing, fused deposition modelling (FDM), binder jetting, selective laser sintering (SLS) and stereolithography (STL) are the most common printing methods used in pharmaceutics today (Trenfield et al., 2018).

Bioprinting is a special printing technique in which bioengineered structures are generated by assembling living and non-living materials to predesigned 2D or 3D placement (Groll et al., 2016; Moroni et al., 2018). According to the literature, 3D-bioprinting techniques are classified to the following four categories: material jetting, VAT photopolymerization, material extrusion and bioassembly (Lee et al., 2018).

By taking these 'classical' methods and improving their portability, novel printing pens for possible *in situ* 3D printing have been developed (Han et al., 2014).

In the present dissertation, two material extrusion methods, micro-extrusion-based 3D-printing and FDM, were used for fabricating pharmaceutical oral solid dosage forms.

2.2.2. Micro-extrusion-based printing

In micro-extrusion-based 3D-printing, viscous solutions or semisolid materials are used to create layered constructs (Zhou et al., 2020). The method has also been called pressure-assisted micro syringe (PAM) printing in the literature (El Aita et al., 2020; Elbadawi et al., 2021). Both names are well-descriptive of the method setup as illustrated in Figure 3.

A syringe-like printing head containing the printing material is moved around the printing plate at a pre-set speed and trajectory. The material is pushed out of the printing head at a set force level aided by either a screw, piston or pneumatic movement (Zhang et al., 2020). The selection of a proper driving mechanism can be important when printing living cell-incorporated materials (Ning et al., 2020). The material deposited on the printing plate needs to be dried/solidified before the addition of a subsequent layer.

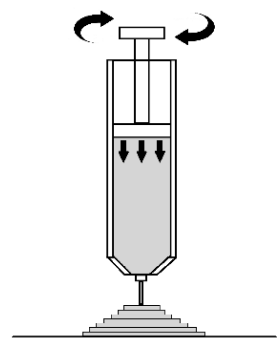

Figure 3. Schematic illustration of micro-extrusion-based 3D printing head setup

If needed, both the printing plate and printing head compartment can be heated. The use of elevated temperatures with this method is not necessary, making this a suitable method for use in pharmaceutics (El Aita et al., 2019; Elbadawi et al., 2021), food printing (Liu et al., 2017; Piyush et al., 2020; Voon et al., 2019) and bioengineering (Chia and Wu, 2015; Groll et al., 2016; Kyle et al., 2017; Moroni et al., 2018; Ozbolat and Hospodiuk, 2016). Relevant material considerations when using micro-extrusion-based 3D printing are further discussed in subchapter 2.5.

2.2.3. Fused deposition modelling

Fused deposition modelling, FDM (also known as fused filament fabrication, FFF) requires premade filaments, which are commonly prepared by hot melt extrusion (HME). HME itself is also a widely used pharmaceutical method for producing DDSs via mixing and jointly melting the carrier system and API together to create an homogenous extrudate (Patil et al., 2016; Simões et al., 2019). The recent increase in 3D-printing applications has also extended the use of HME in this area (Awad et al., 2018; Azad et al., 2020; Dumpa et al., 2020; Giri et al., 2020; Melocchi et al., 2020b, 2016; Tan et al., 2018; Vo et al., 2020; Yan et al., 2018).

HME process integrated in FDM 3D-printing sets strict requirements for the selection of a filament-forming polymer due to the use of elevated temperatures (Goyanes et al., 2015a; Kempin et al., 2018). In FDM, these filaments are applied in most cases as an intermediate product. Novel FDM 3D printing approaches, however, have also made it possible to print solids without using any HME filaments as an intermediate product (Fanous et al., 2020; Goyanes et al., 2019).

In the integrated HME and FDM 3D-printing approach, the extruded filament is fed into FDM printing head and subsequently melted in a heated chamber (Figure 4). Then, the molten material is used to deposit a layer on the printing plate at the set speed and trajectory of the printing head.

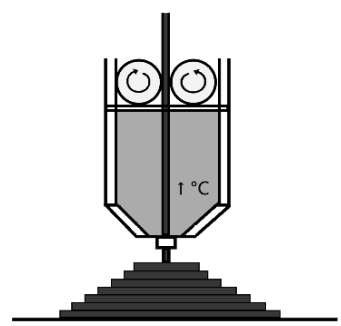

Figure 4. Schematic illustration of FDM 3D printing head setup

Today, FDM is probably one of the most widely used 3D printing methods with widespread applications also in pharmaceutics (Cailleaux et al., 2021; Melocchi et al., 2020a).

2.3. 3D printing in medicine and pharmaceutics

In the past recent years, 3D printing is increasingly used in various medical disciplines. Some of those applications and outcomes could have previously been considered even like science fiction. One specific field in medicine, where 3D printing has found wide use and advances is surgery (Pugliese et al., 2018). Modern 3D printing principles were also used before implementing 3D printing in the successful manual recreation of urinary bladder (Yoo et al., 1998). Further automation in 3D printing has replaced a slow and complicated manual construction process.

Printing technologies have found applications also in the other medical specialities, such as cardiology (Luo et al., 2017; Vukicevic et al., 2017), dentistry (Lin et al., 2019), urology (Huri et al., 2020; Parikh and Sharma, 2018), and plastic surgery (Lin and Yarholar, 2020). Some of these examples have similar features compared to the abovementioned surgical interventions. Another emerging printing application is bioprinting (Groll et al., 2016; Moroni et al., 2018). The goals and applications of bioprinting are often closely linked to surgical operations. The desired result of working organ replacements could also be beneficial in solving the emerging crisis in donor organ transplantations (Mills and Mills, 2020; Munoz-Abraham et al., 2016; Sreekala et al., 2020).

In pharmaceutical technology, 3D-printing holds great promises as a potential flexible fabrication method suitable for personalised medicines. The focus of pharmaceutical 3D printing has been on creating more complex systems with a combination of APIs (polypills), controlling the drug release behaviour, and printing the medicinal products on demand with accurate dose for specific patient groups. Patient adherence has an important role in successful medical treatment. Adherence among the patients with high drug burden can be improved by using polypills – a combination of APIs fused into one DDS (Baumgartner et al., 2020). 3D printing has been used to produce such polypills containing five and more APIs (Shaban A Khaled et al., 2015; Robles-Martinez et al., 2019). Not only are the APIs combined into one system, but also the drug release behaviour of each separate component can be modified (Shaban A Khaled et al., 2015; Shaban A. Khaled et al., 2015). In addition, the dimensions and geometry of the printed DDS affect the dissolution profile of API (Goyanes et al., 2015b; Kyobula et al., 2017a; Sadia et al., 2018).

A milestone was hit in 2015 with the FDA approving the first 3D-printed drug product, an orally disintegrating tablet (ODT) Spritam® by Aprecia Pharmaceuticals (Norman et al., 2016). Spritam® ODTs are fabricated by a powder-based ZipDose® 3D-printing technology enabling the creation of a porous tablet structure, which presents significantly shorter disintegration time

compared to conventional ODTs. Such behaviour has also been described in scientific literature (Fina et al., 2018b). Up to date, Spritam® has remained the only 3D-printed pharmaceutical product on the market.

2.4. Quality aspects of 3D printed objects

The 3D printability of materials can be defined as the capability of a 3D printer to reproduce a given model produced by CAD. The accuracy and precision of a printing process will determine the final quality of the printed product. In the literature, the printability has been evaluated by the determination of e.g., the width of the printed scaffold filament (Habib et al., 2018; Li et al., 2016), filament collapsing (Habib et al., 2018), overlaps in sharp corners (He et al., 2016), area (He et al., 2016), the properties of the lattice gap (Habib et al., 2018; Ouyang et al., 2016), visual appearance (Yang et al., 2018), and surface roughness (Rocha et al., 2014) of the printed 3D object. Moreover, the internal structure and density of the 3D-printed objects have been studied with (X-ray) micro computed tomography (CT) (du Plessis et al., 2018; Vasarhelyi et al., 2020).

In the development of 3D printed pharmaceuticals, it is of outmost importance that the final product is reproducible and complies all quality specifications set for the printed product (e.g., the dimensions and shape, mechanical properties, and drug release *in vitro*). According to the literature, the variations and defects in the shape of printed DDSs can result in an inadequate drug dosing and delivery (Kyobula et al., 2017b; Yu et al., 2008). The possible technological shortcomings in accuracy and resolution are discussed in chapter 2.2, yet the materials used play an equally important role.

The printability and quality aspects of hydrogels are widely reported in the state-of-the-art literature (Gao et al., 2018; Habib et al., 2018; He et al., 2016; Li et al., 2016). With 3D-printed pharmaceuticals, it is essential to conduct a complete pharmaceutical qualitative and quantitative analyses relevant to the present manufacturing technology to ensure the final quality of 3D printed DDS (Melocchi et al., 2021).

2.5. Material considerations in 3D printing

Materials used in medical and pharmaceutical applications need to be biocompatible, biodegradable, and non-toxic. Moreover, the materials need to comply with the technical requirements set by the printing technology used. Therefore, the chemical and physical properties of the carrier materials are of vital importance (Chia and Wu, 2015; Habib et al., 2018).

If semisolids such as gels and pastes are used as printing materials, viscosity is one of the key parameters affecting the printing process. Therefore, the rheological tests are critical for assessing the applicability of such materials for

printing (Aho et al., 2015; He et al., 2016; Kyle et al., 2017; Paxton et al., 2017). The material needs to be viscous enough to maintain structural integrity after printing. With the materials being too viscous, higher force is needed to eject it through the printing head nozzle. For printing, a shear thinning behaviour of the material is beneficial. Other material properties affecting the printability of solutions and semisolid materials include the gelation mechanism, surface tension, density and thermal properties (He et al., 2016; Joshi, 2011).

The use of elevated temperatures in FDM 3D printing will become one of the key concerns, and consequently strategies to lower the HME and/or printing temperature for thermolabile APIs are needed (Kollamaram et al., 2018).

For ensuring the pharmaceutical quality of the final 3D-printed product, it is crucial that the HME filaments as intermediate products are uniform in terms of their geometrical, physical solid-state and pharmaceutical properties. High temperatures are used during HME process, therefore the carrier polymer(s) used need to be thermostable (Kempin et al., 2018). The addition of plasticizer can increase the extrudability of the carrier polymer (Desai et al., 2018). In addition, APIs used in the printing formulation can act as plasticizers, thus enhancing the process (Siepmann et al., 2006). The key HME process factors affecting the properties and performance of final extruded products are the extrusion temperature, screw speed and size, and feed rate (Thiry et al., 2015).

2.5.1. Polyethylene oxide

Polyethylene oxide (PEO) is a hydrophilic, thermoplastic semicrystalline synthetic polymer obtained by the polymerisation of ethylene oxide monomer (Herzberger et al., 2015).

It can be used either on its own, in the composition of copolymers or in combination with other polymers. For example, Pluronic block-copolymer (consisting of PEO – polypropylene oxide – PEO) allows the 3D printing of vascularised tissue constructs (Kolesky et al., 2014). On its own, PEO has been used in FDM for printing radiator-like shaped oral dosage forms (Isreb et al., 2019) and in SLS for printing gyroid lattices (Fina et al., 2018a). PEO has also been used as the viscosity enhancer for printing polyurethane elastomers (Hung et al., 2014).

2.5.2. Polycaprolactone

Polycaprolactone (PCL) is a biodegradable and water-insoluble polymer with a relatively low melting point of approximately 50 to 60 °C (Murphy et al., 2012). In the literature, PCL has been reported as a suitable carrier polymer for FDM-assisted 3D printing (Beck et al., 2017; Fu et al., 2018; Ramanath et al., 2008). For pharmaceutical/medical applications, PCL has been used in patient-specific 3D-printed antimicrobial wound dressings (Muwaffak et al., 2017), intrauterine

implants (Holländer et al., 2016), and biodegradable/bioabsorbable stents (Guerra and Ciurana, 2018).

2.6. Regulation and legislation aspects of 3D-printing

In 2011, a Berlin-based designer Ronen Kadushin published an open design for stylised intra-uterine device called Bearina. The mock-DDS consisted of similar polymers as its role models, and a euro cent was used as the source of Cu^{2+} ions. The fabrication of the present prototype costs 2.50€ each (Kadushin, 2011). While the author stresses that this device is by no means intended for therapeutic use, such projects became available for everyone due to large open-source design banks and cheaper 3D printers (Rayna and Striukova, 2016).

Today, 3D-printing as a novel technology is not yet very much regulated. With the method emerging, it would be important to pay attention to this soon. Currently, the main issues are related to the intellectual property (IP) and the corresponding legislation. More precisely, the problem is two-fold, the protection of (1) CAD files and (2) printed final object.

Taking a step towards the adoption of 3D printing in pharmaceutical manufacturing, we still need more comprehensive studies on the scale-up possibilities of this method (Jamróz et al., 2018). The pharmaceutical industry is thoroughly regulated by both national and international regulatory bodies, making the changes in manufacturing challenging and time consuming. The methods for the compounding of extemporaneous preparations in Estonian pharmacies are not enacted by either Medicinal Products Act (RT I 2005, 2, 4) nor the regulation of the Manufacturing of Medicinal Products (RT I, 19.12.2014, 6) issued by Minister of Health and Labour. The future application of 3D printers in practice have been discussed in the literature (Beer et al., 2021). Recently, it has been suggested that the individual patients could print their own medicines, but this can be a great risk for the safety and compliance of medicines. The experts have found that the most likely scenario is the implementation of 3D printers in hospital pharmacies or compounding community pharmacies. This, however, would require a paradigm shift in the way how extemporaneous preparations are being seen by the pharmacists, doctors, and regulatory bodies. This is also valid for any novel technology or method to be adopted in use in medicine and pharmacy.

3. SUMMARY OF THE LITERATURE

To conclude, the layer-by-layer fabrication during 3D printing allows the introduction of flexibility in future fabrication of novel and more patient-specific DDSs. Dosage form design is a multistage process, and the implementation of new techniques can add various material and process considerations. Often new in-house quality control methods and regulations need to be developed.

The choice of material dictates many of the properties of the final 3D printed product, irrespective of the used printing method. Both PEO and PCL are being studied as carrier polymers for API-loaded electrospun nanofibers in the Institute of Pharmacy, University of Tartu (Hakkarainen et al., 2019; Lanno et al., 2020; Preem et al., 2017; Ramos et al., 2021). Previous knowledge and experience with the chosen materials also aid the application of them in 3D printing.

Further understanding of the 3D printing process, different printing technologies, printable materials and process parameters is crucial in successful development, manufacture, and quality control of safe and stable 3D printed DDSs.

4. AIMS OF THE STUDY

The overall aim of the present thesis was to gain understanding of the applicability and critical process parameters of extrusion-based 3D printing methods in fabricating pharmaceutical oral solid dosage forms. Aqueous-based micro-extrusion 3D printing and HME-integrated FDM 3D printing were used as novel methods for fabricating pharmaceutical DDSs. The "green manufacturing"-related goal of the study was to design pharmaceutical 3D printing formulations without using any organic solvents.

The specific aims were:

(1) to find at least one feasible composition of carrier polymer(s) and API(s) for both pharmaceutical micro-extrusion based, and FDM 3D printing
(2) to gain knowledge of the critical material and process parameters of micro-extrusion based, and FDM 3D printing
(3) to investigate the effects of printing head speed and printing plate temperature on the micro-extrusion-based 3D printability of a model aqueous polymer solution
(4) to gain knowledge on the impact of plasticizer and API(s) on the formation, mechanical properties, homogeneity, and 3D printability of HME filaments intended for FDM 3D printing
(5) to evaluate the effects of tablet geometry and post-printing treatment (crosslinking) on the drug release behaviour of 3D-printed tablets.

5. MATERIALS AND METHODS

5.1. Materials (I, II, III)

Aqueous gel-like solutions (further referred also to as gels) of polyethylene oxide (PEO, MW approx. 900,000, Sigma-Aldrich, USA) were used in micro-extrusion-based 3D printing. Polycaprolactone (PCL, Purasorb PC 08, Corbion Purac, USA) was used as a polymeric base in the HME filaments applied as an intermediate product in a FDM 3D-printing process.

The three model APIs used in the 3D-printing experiments were selected based on their different physicochemical properties and water solubility. Indomethacin, IND (Acros Organics, UK), anhydrous theophylline, THEO (Sigma-Aldrich, Germany) or ibuprofen, IBU (Hangzhou Dayangchem Co. Ltd, China) were loaded in the HME filaments intended for FDM 3D printing. Anhydrous THEO (Sigma-Aldrich, Switzerland) was also used in micro-extrusion-based 3D-printing.

Arabic gum, ARA (Sigma-Aldrich, USA) in powder form was used as plasticizer in HME filaments.

For the crosslinking of PEO, 4-hydroxybenzophenone, HBP (Sigma-Aldrich, USA) was used in powder form as a photo-initiator.

5.2. Preparation of 3D-printing materials

5.2.1. Preparation of printing solutions (I, III)

The gels referred to as 10%, 15%, and 20% (coded as PEO10, PEO15, PEO20) were prepared by dissolving either 1 g, 1.5 g, or 2 g of PEO in 10 ml of distilled water, respectively. PEO was dissolved for at least 12 hours in distilled water at ambient room temperature to form a viscous gel. The pure polymeric gels were printed as such, unless otherwise stated.

For preparing the API-loaded gels (PEO_THEO, 80:20 ratio), 0.375 g of THEO was added to 15 ml of distilled water and heated until fully dissolved. Then, 1.5 g of PEO was added, mixed, and subsequently allowed to dissolve overnight similarly to that with pure polymeric gels. For crosslinking, HBP was mixed into the aqueous printing solution (at the concentration of 10% w/w from a polymer PEO weight in the gel) prior to the 3D-printing.

5.2.2. Preparation of physical mixtures (II)

The physical mixtures (PMs) for HME were prepared using a ‘geometric dilution’ protocol. The powders were first manually ground by mortar and pestle before mixing. Three batches of PMs were made with the content of API (IND, THEO or IBU) either 20%, 30% or 40% (w/w). All PMs contained 10% (w/w) of plasticizer (ARA), and the amount of PCL was varied in accordance with the API content.

5.2.3. Hot-melt extrusion (II)

The filaments were extruded from PMs using a Filabot EX2 (Filabot, USA) single-screw hot-melt extruder. The most suitable extrusion temperature was screened and selected individually for each formulation. The extrusion speed was manually optimised during the process. The samples were stored in a dry cabinet (containing silica gel) at room temperature (22 ± 2 °C). The extruded filaments are considered as printing materials in this work since they are used as an intermediate product for further 3D printing.

5.3. Characterisation of printing materials and 3D-printed objects

5.3.1. Viscosity measurements (I)

The viscosity measurements of the pure PEO gels were conducted with a Physica MCR 101 rheometer (Anton Paar, Austria) using a cone-plate geometry. The measurements were carried out at 25 °C. The viscosity was measured in a rotational shear test at the controlled shear rates between 100 s^{-1} and 0 s^{-1}. All measurements were carried out in triplicates.

5.3.2. Injectability of printing solutions (III)

Brookfield CT3 Texture Analyzer (Middleboro, MA, USA) together with TexturePro CT software (AMETEK Brookfield, Middleboro, MA, USA) was used for measuring the injection force needed for pushing the printing solutions through a 21G needle. PEO + THEO 80:20 printing solution and reference solutions (PEO15 and PEO10) were tested. A 3-ml Luer lock Norm-Ject® syringe was filled and fixed at 2 ml of test solution. The syringe was securely placed between the fixtures of the texture analyzer, and a continuous speed of 1.0 mm/s was used for material extrusion from the syringe. All measurements were carried out in triplicates at room temperature (22 ± 2 °C).

5.3.3. Fourier-transform infrared spectroscopy (I, II, III)

The Fourier-transform infrared (FTIR) spectra of the samples were obtained using an IRPrestige-21 spectrophotometer (Shimadzu Corp., Japan) and Specac Golden Gate Single Reflection attenuated total reflection ZnSe crystal (Specac Ltd., UK). The analytical range was from 600 cm^{-1} to 4000 cm^{-1}. All measurements were in triplicates. A single spectrum was an average of 60 spectra, normalised and baseline corrected.

5.3.4. Differential scanning calorimetry (II, III)

The thermal behaviour of pure substances intended for extrusion, PMs and HME filaments were studied using the TA DSC2500 system (TA Instruments, USA). The samples of approximately 2–8 mg were placed in crimped aluminium pans with a pinhole on the lid. The samples were analysed under a nitrogen purge of 50 ml/min. In the cooling unit, a purge of 200 ml/min was used. The heating was conducted at 10 °C/min with a starting temperature at 25 °C. The end temperature was 170 °C for IND and IND extrudates, 150 °C for ARA, 75 °C for PCL, 280 °C for THEO, 270 °C for 20% THEO extrudate and 275 °C for 30% and 40% THEO extrudate.

The melting temperature (T_m) and other thermal properties for pure materials (THEO and PEO), PMs and micro-extrusion-based 3D-printed multilayered tablets were determined by using a PerkinElmer DSC 4000 Differential Scanning Calorimeter (PerkinElmer, Inc, Waltham, MA, USA). Samples of 4 mg were placed in sealed aluminum standard pans and an empty pan was used as a reference. The samples were heated (10 °C/min) from 20 °C to 300 °C under a nitrogen gas purge at the flow rate of 20 ml/min. The data were analysed using Pyris software (PerkinElmer, Inc, Waltham, MA, USA). All measurements were performed in triplicate.

5.3.5. Near infrared spectroscopy (III)

To study the drying of 3D-printed DDSs, near-infrared (NIR) spectra were measured with a AvaSpec-NIR256-2.2 spectrometer (Avantes, The Netherlands) equipped with a 256-pixel GaAs detector and tungsten halogen lamp (AvaLight-HAL). The NIR spectra were collected on the pure materials, PMs (freshly prepared and stored at 40 °C and 75% relative humidity (RH), and a drop of water added on the top of mixture) and 3D-printed tablets (FRESH, the tablet immediately after 3D-printing, and AGED, the tablet stored for a week in a desiccator in a refrigerator at 2–8 °C). All measurements were carried out in triplicate.

5.3.6. X-ray powder diffraction (I, II)

The powder samples, extruded filaments, PEO model squares, and 3D-printed tablets were studied by means of X-ray powder diffraction (XRPD) using a Bruker D8 Advance diffractometer (Bruker AXS GmbH, Germany) with Ni filtered CuKα radiation, 0.3° divergence slit, two 2.5° Soller slits and LynxEye line detector, operated at 40 kV and 40 mA. Scanning steps of 0.019° 2θ from 3 to 55° 2θ and a total counting time of 175 s per step were used.

5.3.7. Three-point bending test (II)

The mechanical properties of HME filaments were evaluated by a three-point bending test using a texture analyser (AMETEK Brookfield CT3, USA) at room temperature (22 ± 2 °C). The filament samples were cut in 5 cm pieces, and

their diameter was measured by a digital calliper. The general placement of the sample within batch (beginning, middle, end) was considered. The distance between horizontal probes was 3 cm, trigger load was set at 10 g, and test speed was 1 mm/s. All measurements were carried out in triplicate.

5.3.8. Filament homogeneity (II)

For evaluating the homogeneity of filaments, five to eight filament samples of 0.5 cm in length were cut from each original filament generated and weighed. The sample size differed due to practical reasons. The length of filaments was not the same with the different materials, and therefore the samples were collected in such a way that they could present the whole filament as much as possible. These samples were dissolved in 100 ml of acetonitrile by mixing in acetonitrile overnight. Aliquots (10 ml) were filtered (jet biofil 0.45 µm, Guangzhou Jet Bio-Filtration Co., China) and diluted (1:10) with a solution of acetonitrile and water (70:30 V/V). The concentration of API in the filaments was determined by high-performance liquid chromatography, HPLC (all Gilson, France) equipped with a 321 pump and 234 autoinjector, 506C System Interface Module, and UV/Vis-151 detector. A Gemini NX C18 250 mm x 4.60 mm HPLC column (Phenomenex, USA) equipped with a SecurityGuard pre-column (Phenomenex, USA) was used. The analytical wavelength used for IND and THEO was 270 nm and 210 nm, respectively. The mobile phase consisted of 70% of acetonitrile, 30% of water and 0.1% of trifluoroacetic acid (Sigma-Aldrich, USA), and the flow rate was adjusted to 1.2 ml/min (Ojarinta et al., 2017). Standard curves were prepared using an acetonitrile/water 70/30 (V/V) solution.

5.3.9. Physical stability of HME filaments (II)

The physical appearance and potential solid-state changes of the HME filaments were studied for 3 months with the filaments stored at the elevated temperature of 40 °C and 75% RH, or alternatively in a refrigerator at 3-8 °C and 0% RH. The XRPD solid-state analysis of the fresh and stored HME filaments was performed as described previously.

5.4. 3D-printing (I, II, III)

The semisolid materials were printed using a bench-top extrusion-based 3D-printing system (System 30M, Hyrel 3D, USA) equipped with a KRA-15 extrusion head and a 21G needle as a printing head nozzle.

During 3D printing, the printing head is moving at a set speed, and the printing material is extruded and forced through a nozzle system onto a printing plate. Following every printed layer, the printing plate is lowered by a pre-defined distance, thus allowing the printing head to create another layer of material on top of the printed object.

The printing experiments for 3D printability evaluation were carried out with three different PEO concentrations (X1): 10%, 15% and 20%. The effects of a

printing head speed (X2) and printing plate temperature (X3) on the overall printability of PEO gels were evaluated as independent process parameters (Table 2). The printing head speeds studied were 0.5 mm/s, 1.0 mm/s and 1.5 mm/s. The printing plate temperature was set at 30°C, 50°C or 70°C. All other process parameters, such as layer height, extrusion speed, needle size, and temperature in the printing head were kept constant. The layer height was set at 0.1 mm, 21G needle was used for the nozzle and the temperature in the printing head was held at 30°C.

Table 2. Full factorial design matrix (3^3) and the results (n=3).

Exp.	Independent parameter			Response		
	X1	X2	X3	Y1	Y2	Y3
1	-1	-1	-1	24.5 ± 12.1	162.7 ± 41.3	1.01 ± 0.26
2	-1	-1	0	30.2 ± 7.2	149.4 ± 4.9	0.93 ± 0.03
3	-1	-1	+1	47.0 ± 21.0	245.2 ± 79.8	1.52 ± 0.50
4	-1	0	-1	27.8 ± 0.6	202.0 ± 27.8	1.26 ± 0.17
5	-1	0	0	37.8 ± 19.6	195.2 ± 16.0	1.21 ± 0.10
6	-1	0	+1	26.4 ± 13.3	136.8 ± 25.7	0.85 ± 0.16
7	-1	+1	-1	25.6 ± 6.3	240.9 ± 82.4	1.50 ± 0.51
8	-1	+1	0	29.8 ± 1.9	152.8 ± 15.3	0.95 ± 0.09
9	-1	+1	+1	34.2 ± 4.9	169.8 ± 20.9	1.06 ± 0.13
10	0	-1	-1	44.3 ± 2.0	154.7 ± 33.4	0.96 ± 0.21
11	0	-1	0	43.8 ± 1.8	190.0 ± 32.1	1.18 ± 0.20
12	0	-1	+1	44.9 ± 3.3	186.0 ± 3.3	1.16 ± 0.02
13	0	0	-1	56.1 ± 13.6	230.7 ± 28.3	1.43 ± 0.18
14	0	0	0	44.4 ± 4.6	151.0 ± 26.5	0.94 ± 0.16
15	0	0	+1	45.8 ± 4.2	169.7 ± 31.8	1.06 ± 0.20
16	0	+1	-1	43.8 ± 7.3	281.7 ± 13.1	1.75 ± 0.08
17	0	+1	0	37.9 ± 5.8	141.9 ± 5.8	0.88 ± 0.04
18	0	+1	+1	43.6 ± 1.2	170.0 ± 27.4	1.06 ± 0.17
19	+1	-1	-1	76.8 ± 15.2	188.1 ± 20.9	1.17 ± 0.13
20	+1	-1	0	53.1 ± 11.3	153.3 ± 18.3	0.95 ± 0.11
21	+1	-1	+1	71.3 ± 9.6	171.8 ± 36.7	1.07 ± 0.23
22	+1	0	-1	56.4 ± 2.3	208.1 ± 98.8	1.29 ± 0.61
23	+1	0	0	46.2 ± 9.5	126.2 ± 5.8	0.78 ± 0.04
24	+1	0	+1	57.6 ± 11.1	112.5 ± 7.2	0.70 ± 0.04
25	+1	+1	-1	51.4 ± 1.6	210.9 ± 34.0	1.31 ± 0.21
26	+1	+1	0	53.7 ± 2.5	134.1 ± 7.7	0.83 ± 0.05
27	+1	+1	+1	57.8 ± 8.1	137.6 ± 4.1	0.86 ± 0.03

Key: X1 = Concentration of PEO solution: 10% (-1), 15% (0), 20% (+1); X2 = Printing head speed (mm/s): 0.5 (-1), 1.0 (0), 1.5 (+1); X3 = Printing plate temperature (°C): 30 (-1), 50 (0), 70 (+1).

The cylindrical-shaped model tablets were printed at a printing head speed of 0.5 mm/s and the printing plate temperature was 50 °C. Nine tablets were printed in one batch, and the number of material layers (i.e., tablet thickness referred to as TH for thin, or TK for thick) was varied in different batches. The tablet thickness was taken into consideration only for *in vitro* drug release testing. The tablets were kept in a desiccator in a refrigerator (2–8 °C) before crosslinking and subsequent dissolution tests.

Both the scaffold design and model tablet design for semisolid micro-extrusion-based 3D-printing were designed using Autodesk® 3ds Max® Design 2017 software (Autodesk, Inc., USA). For FDM 3D printing, similar cylindrical model tablet design was used. To alter the drug release, the model honeycomb tablets with equal weight but different surface area were designed using Solidworks software (Solidworks 2018, Dassault Systems, USA).

The FDM model printlets were manufactured by a ZMorph 3D-printing system (ZMorph, Poland). The temperature in printing was held at 175 °C and a printing plate temperature was kept in the range of 35 °C and 40 °C for IND tablets. The corresponding temperature levels used with the THEO tablets were 190 °C and 40 °C, respectively. The filaments and prepared 3D printed samples were stored in a dry cabinet (containing silica gel) at room temperature (22 ± 2 °C) before further analyses.

5.5. Crosslinking (III)

The PEO-based 3D-printed tablets were crosslinked using an UV transilluminator (GVM-20, 230V, 50Hz, 100W, 2A, ⌀5x20, Serial 964215, Syngene, UK). The irradiation time was 15 minutes for both sides of the tablets (30 minutes in total for one tablet). These tablets are further referred to as TH_UV30 and TK_UV30. Potential swelling or the degradation of the 3D-printed solids were evaluated visually. Gamma-radiation induced crosslinking was carried out in Scandinavian Clinics Estonia OÜ, Estonia. The measured radiation doses absorbed ranged from 31.3 kGy to 32.9 kGy. The tablets were gamma-radiated in either ambient air (TK_gamma) or nitrogen gas (TK_gammaN) environment to investigate the impact of environment during irradiation on the 3D-printed tablets.

5.6. Evaluation of printability (I)

The evaluation of 3D printability was based on the printed lattice weight, dimensions, and area measurements. The dimensions for a square-shaped 3D lattice were 20 x 20 x 1 mm. The surface area of the theoretical lattice (160.89 mm^2) was compared with the experimental areas of the 3D-printed lattices. Each printed PEO lattice was weighed with an analytical scale and photographed with a digital single-lens reflex camera (Nikon D3300, Nikon, Japan). The photographs were analysed with an ImageJ (National Institute of Health, USA) image

analysis software (version 1.51k). The area was automatically calculated from a black-and-white image based on a threshold value. This experimental value was then compared with the theoretical value of a designed lattice. The ratio of areas was calculated as the ratio of experimental area to the theoretical area (Equation 1).

$$r_s = \frac{s_e}{s_t} \qquad \text{Equation 1}$$

where r_s stands for the calculated ratio, s_e for the experimental area and s_t for the theoretical lattice area calculated from the designed lattice model.

The effects of PEO concentration (X1), printing head speed (X2) and printing plate temperature (X3) on over all printability of PEO gels were modelled using the following second-order polynomial Equation 2:

$$Y = a1 \cdot X1 + a2 \cdot X2 + a3 \cdot X3 + a4 \cdot X1 \cdot X2 + a5 \cdot X1 \cdot X3 + a6 \cdot X2 \cdot X3 + a7 \cdot X1^2 + a8 \cdot X2^2 + a9 \cdot X3^2 + constant \qquad \text{Equation 2}$$

where Y = response and a1...a9 = coefficients.

The model was simplified with a multi-linear backward, stepwise regression technique. The least significant terms were excluded from the model if the predictive power (Q^2) of the model was increasing (Table 3). The modelling was performed using MODDE® for Windows (Version 7.0.0.1, Umetrics AB, Sweden).

Table 3. The fitted models for unscaled coefficients and responses

Coefficient	Y1	Y2	Y3
a1	2.68	3.12	0.0186
a2	-6.46	152	0.940
a3	NS	-4.68	-0.0299
a4	NS	NS	NS
a5	NS	-0.110	-0.000667
a6	NS	-2.95	-0.0183
a7	NS	NS	NS
a8	NS	NS	NS
a9	NS	0.0821	0.000517
constant	11.2	215	1.36
R^2	0.746	0.682	0.681
Q^2	0.668	0.411	0.410

NS = not significant

5.7. Drug release (II, III)

The drug release of the FDM 3D-printed tablets was studied *in vitro* by a Sotax AT6 dissolution tester (Sotax AG, Switzerland) using the USP Paddle method with a paddle rotation speed of 50 rpm. The volume and temperature of the dissolution medium were 900 ml and 37 °C, respectively. The sample size was 5 ml. Immediately after sampling, 5 mL of pure buffer solution was added to the test sample to replace the volume. The sampling time points were at 15 min, 30 min, 1 hour, 2 hours, 4 hours, 6 hours, 8 hours, and 24 hours. The release of IND from the tablets was studied in a phosphate buffer (pH 7.2; USP). For THEO, the dissolution medium was HCl-buffer solution with sodium chloride (pH 1.2; USP). The dissolution tests were carried out in triplicate one week after printing.

The *in vitro* dissolution tests for micro-extrusion-based 3D-printed tablets were performed using a dissolution apparatus (Sotax AT7 Smart, Sotax, Switzerland) and a paddle method. The paddle speed was set at 50 rpm. The dissolution medium used was 500 ml of distilled water at 37 °C. The samples were assayed by UV spectrophotometry (Specord 200 plus, Analytik Jena, Germany) and compared to the calculated theoretical drug content of these tablets. Dissolution tests were carried out in three parallels. The residual samples were weighed after the test, if possible. Water uptake (%) was calculated from the weight gain of these samples. The dissolution behaviour of batch TK_UV tablets in water was visually compared with the dissolution of the corresponding round-shaped solvent-cast UV-crosslinked free films (with an equivalent composition, diameter, and thickness).

5.8. Data analysis (I, II, III)

Principal component analysis (PCA, Simca-P+ Version 12.0.1.0, Umetrics AB, Sweden) was applied for NIR spectra to evaluate the drying phenomena and process. Spectral range from 1200 to 2250 nm was used for multivariate data analysis. Standard Normal Variate (SNV) and the 1st derivative spectral pre-processing was performed. For the PCA model, the first three principal components (PC) were used to explain the data. The results are presented as scores plot and loadings plot where the scores reveal the spectral variation, and the loadings represent the spectral contribution to each PC.

All other statistical tests were carried out using MS Excel (Version 2110 Build 16.0.14527.20234). The influence of the process parameters on the 3D printability was evaluated using regression analysis. A two-tailed unpaired t-test was used to study the statistical difference between the groups.

6. RESULTS AND DISCUSSION

6.1. Rheological properties of the printing solutions

6.1.1. Viscosity of printing solutions (I)

The viscosity of aqueous PEO printing solutions increased as the polymer concentration was increased in the solutions at all shear rates studied (Figure 5). The viscosity of the present gels intended for extrusion-based 3D printing ranged from 24.4 ± 1.1 Pa·s to 186.7 ± 6.8 Pa·s at a shear rate of 10 s^{-1} (25 °C). We observed that by knowing the range of viscosity profiles of the solutions or gels suitable for micro-extrusion-based 3D printing, we can readily assess the expected 3D-printability of the material as well. The influence of PEO concentration (i.e., viscosity) on the 3D printability of tablets is discussed in more detail in chapter 6.3.

We found that the rheology of aqueous PEO gels followed a shear-thinning (also known as pseudoplastic) behaviour at all PEO concentrations studied. These results are in good agreement with the findings on the rheological behaviour of PEO gels reported in the literature (Ebagninin et al., 2009).

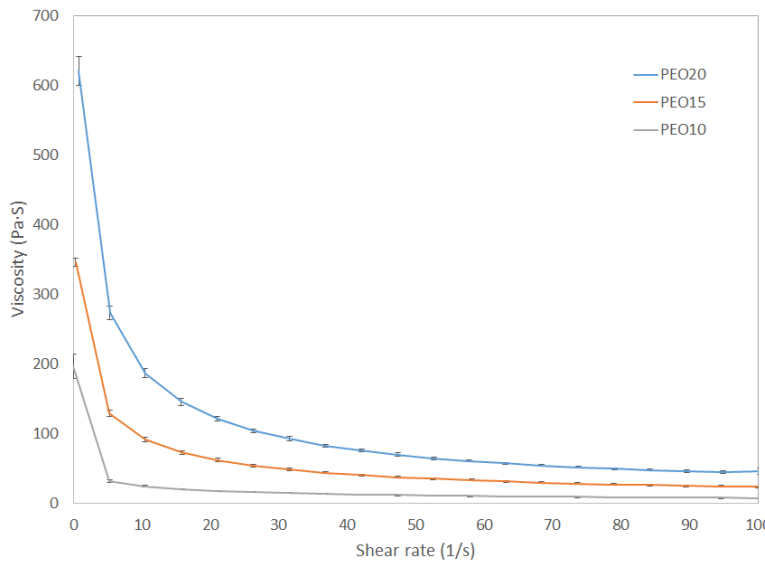

Figure 5. Viscosity of PEO gels (25 °C) intended for 3D printing.
Key: PEO10 = 10% aqueous PEO gel; PEO15 = 15% aqueous PEO gel; PEO20 = 20% aqueous PEO gel.

Perhaps surprisingly, the viscosity of aqueous PEO gels used in our study was even ten-to-hundreds time lower than those reported in the literature for 3D printing by using gels of different materials (Compton and Lewis, 2014;

Postiglione et al., 2015). However, Bakarich et al. (2013) reported that less viscous gels are also applicable for extrusion-based bioprinting. It is evident that the successful 3D printing with low-viscosity PEO gels is partially attributed to the shear-thinning rheology of PEO gel. A shear-thinning response and high near-zero viscosity have been reported as highly desirable in the context of liquid deposition modelling based 3D printing. In an extrusion-based printing, extrusion through a capillary nozzle at high shear-rates has been shown to decrease the viscosity of a printing material (Faes et al., 2015; Postiglione et al., 2015).

It is of outmost important to find the most suitable printing parameters for such polymer(s), and thus to gain understanding of the printing process. This will in turn contribute to finding more promising biocompatible polymers that can be applied in medical and/or pharmaceutical 3D printing. Pluronic F127 gels with different polymer concentrations (viscosity ranging from 30 mPa·s to over 60 × 10^6 mPa·s) were successfully applied in 3D printing (Chang et al., 2013). The known viscosity profile and 3D-printability correlation can be further taken into consideration when choosing the desired design pattern and printing parameters. According to the literature, crosslinking of polymer can also increase the viscosity, and consequently, also enhance the printing of low viscosity polymer inks (Chung et al., 2013).

6.1.2. Injectability of printing solutions (III)

The injectability test method was used to investigate the effects of drug-loaded semisolids and their rheological properties on a 3D-printing process. Table 4 shows the maximum injection force values for the aqueous PEO, and drug loaded PEO gel samples in the test. The maximum injection force for the aqueous PEO10 and PEO_THEO solutions was 43.7 ± 6.2 N and 52.9 ± 2.2 N, respectively. The difference of these two maximum forces, however, was not statistically significant ($p = 0.057$). A slight increase in the maximum force with the PEO_THEO solution is obviously due to the higher concentration of solids in the mixture. The PEO15 solution was found more challenging to load into the syringe due to higher viscosity of the solution. As shown in Table 4, the PEO15 solution presented also the highest maximum force value of 95.7 ± 5.9 N in the injectability test. The difference to the force values obtained with PEO10 and PEO_THEO solutions was statistically significant ($p < 0.05$).

Table 4. Injectability of printing solutions (n=3).

Printing solution	Maximum injection force (N)
PEO15	95.7 ± 5.9
PEO10	43.7 ± 6.2
PEO_THEO	52.9 ± 2.2

Key: THEO = theophylline, PEO = polyethylene oxide.

The injectability test is widely used for determining the critical rheology-related parameters affecting the subcutaneous and intramuscular injection of APIs (Cilurzo et al., 2011). To date, however, this test method has not been used frequently in the evaluation of 3D printing materials, even though the test setup mimics well the syringe-like printing head of a nozzle-based 3D-printing system. Moreover, the test method enables the visual monitoring of the flowing behaviour of a printing solution and the formation or presence of air bubbles in the solution, thus predicting the success of a printing process.

With the aqueous solutions of PEO, the impact of the polymer concentration on the injection force is evident, and this finding is in good agreement with our previous studies on the effects of viscosity on 3D printing. The high molecular weight of PEO can also play an important role in resisting injectability (Meruva and Donovan, 2020). Despite of the advantages of using an injectability test for predicting the materials behaviour in 3D printing, there are some limitations related to this test. Such limitations include the difference in the flow velocity of materials in the injectability test and extrusion-based 3D printing. Therefore, for improving the prediction capacity, it would be important to use the same shear rate levels in an injectability test as in the real extrusion-based 3D printing process.

6.2. Formulation of HME filaments (II)

Finding a suitable carrier polymer for a HME process is crucial since the polymer affects the stability and physicochemical characteristics of the final drug-loaded filaments. We selected PCL as a carrier polymer, since it is extrudable in a HME process alone at 75 °C. The HME filaments fabricated from PCL, however, were soft, somewhat uneven in thickness and not intact enough for handling. In our study, the main reason for adding a secondary excipient (in addition to a carrier polymer) was to improve the overall processability of filaments. This can be achieved by the addition of a suitable plasticizer (Desai et al., 2018). For HME process, the plasticizer of choice should be a solid plasticizer, since liquid plasticizers could extensively decrease the viscosity and solidity of HME mass, and thus impair extrusion and subsequent 3D printing. To date, there are only a few studies in the literature reporting on the use of solid plasticizer(s) in the HME of polymeric filaments (Desai et al., 2018;

Schilling et al., 2007; Wu and Mcginity, 2003). Based on the results of our preliminary tests, a carrier polymer-plasticizer mixture of PCL and ARA was chosen for fabricating the HME filaments loaded with API. In comparison with the other solid plasticizers preliminary tested (citric acid, solid polyethylene glycols), ARA (incorporated with PCL) aided a HME process the most enabling the most uniform filament flow. The addition of ARA in the HME filament composition made the filaments mechanically strong (less brittle), thus improving their handling and further processing.

Table 5 summarizes the composition, extrusion temperature and some key final filament properties of the API-loaded HME filaments. For fabricating the HME filaments, the model API (IND, THEO or IBU) was loaded in the filaments at the concentration levels of 20%, 30% and 40%. The HME temperature was kept as low as possible for each formulation (Table 5). We found that the HME filaments loaded with IND or THEO can be fabricated at all three API concentrations without any limitations. The addition of IBU in the HME filaments, however, resulted in soft filaments with an uneven filament diameter and non-repeatable process. Therefore, the IBU-loaded filaments were excluded from the further studies. The limitations associated with IBU filament formulations could be explained by the significantly lower melting temperature of IBU (80 °C) (Lerdkanchanaporn and Dollimore, 1997) compared to the melting temperatures of approximately 160°C for IND (Tita et al., 2009) and 270 °C for THEO (Shaikh et al., 2019).

6.2.1. Physical appearance of HME filaments (II)

Figure 6 shows the appearance of the API-loaded HME filaments (reference is also made to Table 5). With the THEO-loaded filaments, the surface roughness apparently increased as the concentration of the API in the filaments was increased. The corresponding trend was not observed with the IND-loaded HME filaments. The IND-loaded filaments, however, were found to be more yellowish in colour as the concentration of API was increased.

Table 5. Composition, extrusion temperature and properties of the drug-loaded hot-melt extruded (HME) polycaprolactone (PCL) filaments.

Batch	PCL	ARA	API	API (%) measured	Extrusion temperature	Filament description	⌀ (mm)
IND20	70%	10%	20%	13.3 ± 3.8	100...105°C	Light yellowish uniform filament, slightly rough surface	1.83 ± 0.15
IND30	60%	10%	30%	16.3 ± 4.8	100...105°C	Light yellowish uniform filament, slightly rough surface	-
IND40	50%	10%	40%	33.9 ± 3.4	100...105°C	Light yellowish, slightly rough surface, more brittle	1.78 ± 0.03
THEO20	70%	10%	20%	19.1 ± 4.5	120...125°C	Off-white uniform filament, smooth surface	1.74 ± 0.07
THEO30	60%	10%	30%	29.6 ± 3.4	120...125°C	Off-white uniform filament, somewhat rough surface	-
THEO40	50%	10%	40%	40.0 ± 3.9	120...125°C	Off-white uniform filament, visibly rough surface	1.88 ± 0.03
IBU20	70%	10%	20%	-	75…85°C	Light yellowish, non-uniform, rough surface	-
IBU30	60%	10%	30%	-	-	-	-
IBU40	50%	10%	40%	-	-	-	-

Key: ARA = arabic gum; API = active pharmaceutical ingredient; IBU = ibuprofen; IND = indomethacin; THEO = theophylline; PCL = polycaprolactone.

As seen in Table 5, the average diameter of IND20 and IND40 HME filaments (n = 9) was 1.83 ± 0.15 mm and 1.78 ± 0.03 mm, respectively. The present difference in diameter, however, was not statistically significant. With the THEO-loaded HME filaments, the trend went perhaps surprisingly the other way around: THEO20 filaments had a diameter of 1.74 ± 0.07 mm and THEO40 filaments 1.88 ± 0.03 mm ($p < 0.05$). In both cases, the HME filaments with higher percentage of API had a more uniform filament diameter.

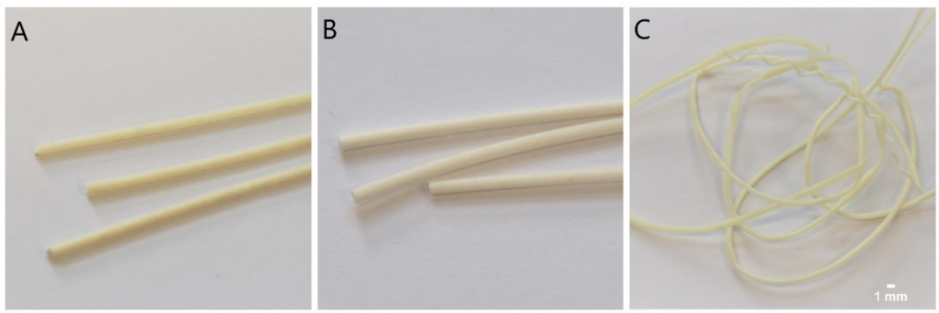

Figure 6. Hot melt extruded (HME) filaments composing of polycaprolactone (PCL), arabic gum (ARA) and 20% of (A) indomethacin (IND), (B) theophylline (THEO), or (C) ibuprofen (IBU).

6.2.2. Homogeneity of HME filaments (II)

The uniformity of HME filaments is one of the key parameters for the further development of successful 3D-printed DDSs (Govender et al., 2020). The concentrations of API in the HME filaments are shown in Table 5. With both THEO- and IND-loaded filaments, the actual API concentration was lower than the corresponding theoretical values. The API-content in THEO-loaded filaments, however, was very close to the theoretical nominal value at all concentrations studied (Table 5).

The variation of API concentration in the API-loaded HME filaments is shown in Figure 7. With the IND-loaded filaments, the concentration of IND was decreased on the course of a HME process. The corresponding trend was not observed with the THEO-loaded HME filaments, but the variation in the API concentration in the different measurement points along the filament was evident. With both APIs, the variation in concentration along the filament appeared to be the smallest with the filaments having the highest concentration of API. The heterogeneity of the filaments in terms of an API concentration could be explained by the inadequate degree of mixing of API and excipients prior to extrusion, or de-mixing during extrusion. As mentioned earlier, the particle size reduction of the components prior to HME could improve the homogeneity of the filaments. Another reason for the inhomogeneity of the

IND-loaded filaments could be the cohesiveness of IND, which has been reported to cause challenges in a HME process (Holländer et al., 2016).

We also found that the homogeneity of the HME filaments loaded with THEO was not as good as expected (reference is also made to Table 5 and Figure 6). There are, however, no reports in the literature for such limitations with the HME filaments loaded with THEO.

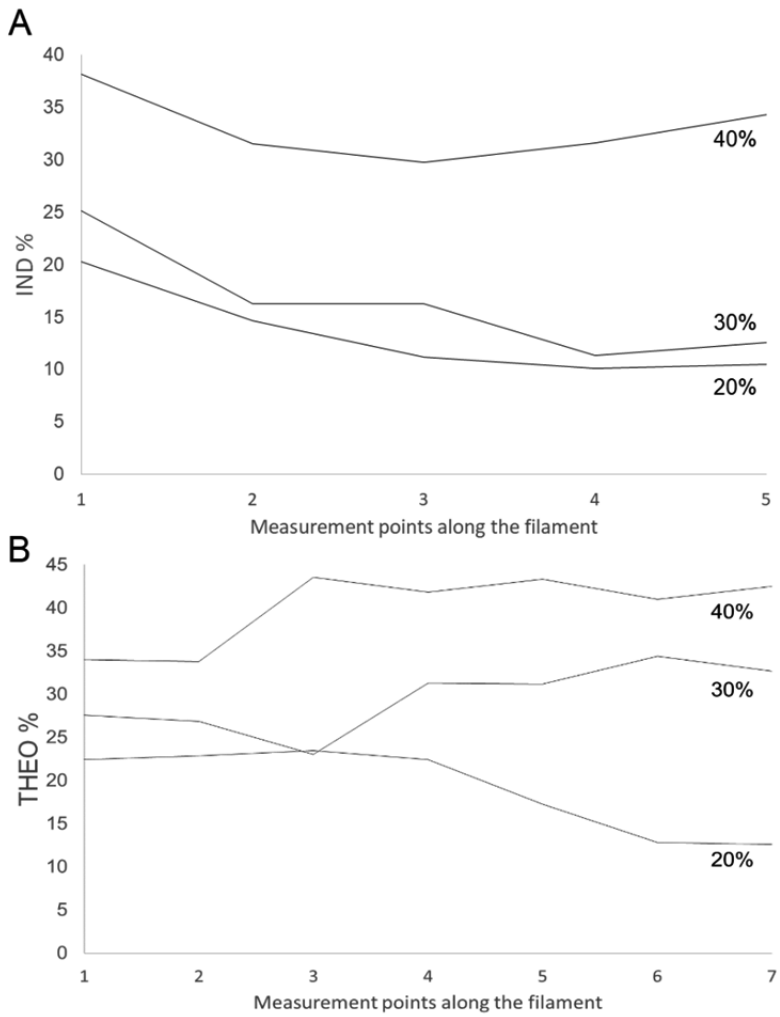

Figure 7. Changes in the concentration (%) of (A) indomethacin (IND) and (B) theophylline (THEO) along the corresponding hot melt extruded (HME) filament.

6.2.3. Mechanical properties of HME filaments (II)

Several recent studies in the literature have focused on describing the importance and evaluation of the mechanical properties of filaments intended for 3D-printing (Aho et al., 2019; Nasereddin et al., 2018). We used an established three-point bending test for investigating the mechanical properties of HME filaments (Figure 8). This test method was considered as the method of choice for characterizing the polymeric filaments in our study, since it provides information about the filament properties relevant to the process behaviour in HME and resistance to flexural strength.

The results of the three-point bending test showed that as the content of API was decreased in both IND and THEO-loaded HME filaments, the mechanical resistance to deformation and elongation of the filaments were enhanced (Figure 8). This could be explained by the higher ratio of polymer (PCL) to API in the powder mixture used for extruding filaments, thus promoting the handling properties of given HME filaments. This phenomenon could be expected, since PCL itself is also shown to have plasticizing characteristics, and it has been also used as a plasticizer (Olewnik-Kruszkowska et al., 2016). Combining materials with such properties with our primary plasticizer, ARA, can result in a synergistic effect.

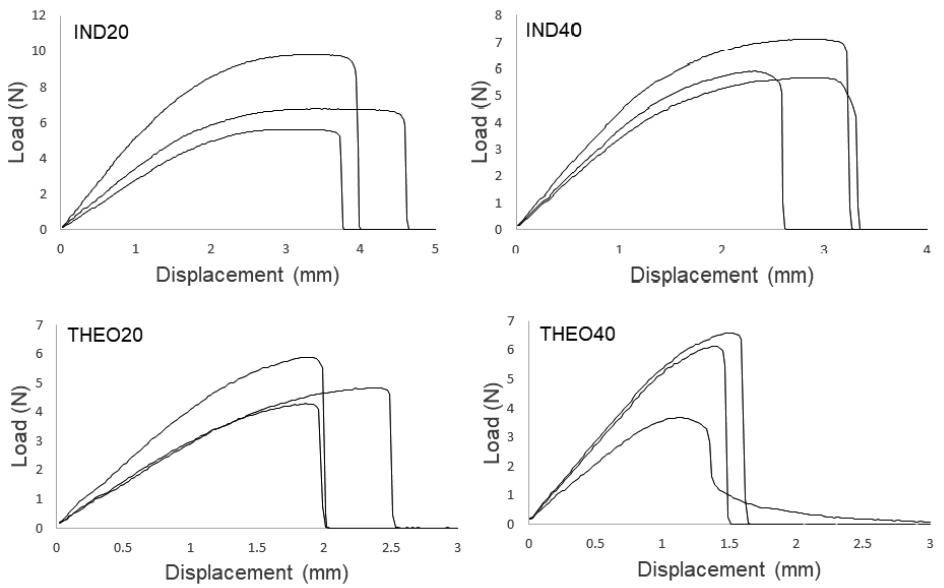

Figure 8. Load-displacement curves of hot-melt extruded (HME) filaments loaded with theophylline (THEO) and indomethacin (IND) at two different drug concentrations (20% and 40%). The filaments were tested with a three-point bending test (n = 3). Each line represents one test sample.

The mechanical strength (load) values for the IND-loaded HME filaments were quite equal in comparison with the corresponding values obtained with the THEO HME filaments (the difference in load values was not statistically significant). With the IND filaments, however, the displacement values for the elongation (at break) were significantly higher than the corresponding values for the THEO filaments. This suggests the auto-plasticization characteristic of IND resulting in enhanced strain behaviour of HME filaments.

The limited elongation (strain values) of THEO filaments suggests that THEO does not support the plasticization and formation of PCL filaments in a HME process. With the THEO filaments, the relatively large variation in the results of a three-point bending test could be explained by the uneven filament diameter observed with the THEO filaments (Table 5).

6.2.4. 3D printing of HME filaments (II)

According to the state-of-the-art literature, the temperature in 3D printing should be set slightly higher than the temperature used in the HME of the polymeric filaments (Kollamaram et al., 2018). Therefore, it is important to select the temperature used in the HME process as low as possible to minimize the potential negative effects on the final product in 3D printing. We found that all HME filaments loaded with a model API were applicable for the 3D printing of tablets with different geometries. The HME filaments loaded with 20% of IND showed very good 3D-printing properties, and the printing of tablets was performed without any drawbacks. With the HME filaments loaded with the highest concentration of IND (40%), the 3D printing was limited due to regular nozzle blockages. With the HME filaments loaded with THEO, the uneven filament diameter made the final 3D printing of tablets somewhat complicated. While printing solid cylindrical-shape tablets or lattice (“honeycomb”) tablets, no technical problems were met. Both types of 3D-printed tablets were successfully generated using the HME filaments of an API.

6.2.5. Solid-state characterisation of HME filaments (II)

The effects of a HME and 3D-printing process on the physical solid state of the APIs (IND, THEO) and key excipients are shown in Figure 9. The XRPD pattern of IND powder showed the characteristic major diffraction peaks for the γ-polymorph (indicated by the tiny arrows in Figure 9A), and this finding is also in line with the literature (Aceves-Hernandez et al., 2009). The HME of IND-loaded filaments resulted in an apparent loss in crystallinity of the API (i.e., blunting of the corresponding XRPD reflections), and after 3D printing it is evident that IND is in an amorphous form (Figure 9A). While there is an enhancement to solubility in amorphous state, the physicochemical behaviour of the API is less predictable (Skrdla et al., 2016). The XRPD pattern of THEO

powder showed the characteristic diffraction peaks of THEO (Figure 9B), previously also described in the literature (Phadnis and Suryanarayanan, 1997). As shown in Figure 9B, these characteristic reflections can be found also in the XRPD diffraction patterns of the PMs and HME filaments of THEO. The latter showing that the solid-state of THEO was preserved during HME.

The thermal behaviour of pure substances, HME filaments and 3D-printed tablets is presented in Figure 10. Figure 10A shows the characteristic melting endotherm for IND (at onset temperature 160 °C) and THEO (270 °C), which are both in good agreement with the literature (Holländer et al., 2016; Karmwar et al., 2011; Shaikh et al., 2019). PCL as a semi-crystalline polymer presented a melting endotherm at onset temperature of approximately 55 °C (Figure 10A).

The DSC thermograms for the HME filaments show the characteristic melting endotherms for both IND and PCL (Figure 10B). It is evident that amorphous IND recrystallizes in the filaments upon heating (as verified also by XRPD). A slight shift of the endothermic peak temperature of PCL (approximately 2.5 °C) was observed with the HME filaments compared to that obtained with pure PCL. This suggests potential interaction (but not necessarily incompatibility) of PCL with IND confirming also the previous results reported in the literature on the interaction between the API and polymer (Kempin et al., 2017). As seen in Figure 10B, the melting peak for IND is more prominent in the DSC thermograms of HME filaments loaded with higher concentration (30% or 40%) of API. In the case of 3D-printed tablets (Figure 10C), the melting endotherm of PCL has been shifted towards lower temperature. The DSC thermogram of 3D-printed tablets with 40% of API presented a small characteristic melting peak of IND indicating that the API is at least partially in a crystalline form.

With the THEO-loaded HME filaments, the melting endotherm of PCL can be seen at 55 °C onset temperature (Figure 10D), and this peak was slightly shifted to lower temperature as the concentration of API in the filaments was decreased. Similar endothermic peak shift (PCL) was observed with the IND filaments, thus indicating potential interaction of PCL with the other components of the HME filaments (APIs, ARA). Moreover, the characteristic melting endotherm of THEO can be seen, thus confirming its crystallinity. Figure 10E shows the DSC thermogram of 3D-printed tablets of THEO. The deformed endothermic peaks for both PCL and THEO suggest the occurrence of some thermal-induced changes in the formulation. Overall, the present DSC thermal profiles are in good agreement with the XRPD results shown in Figure 9.

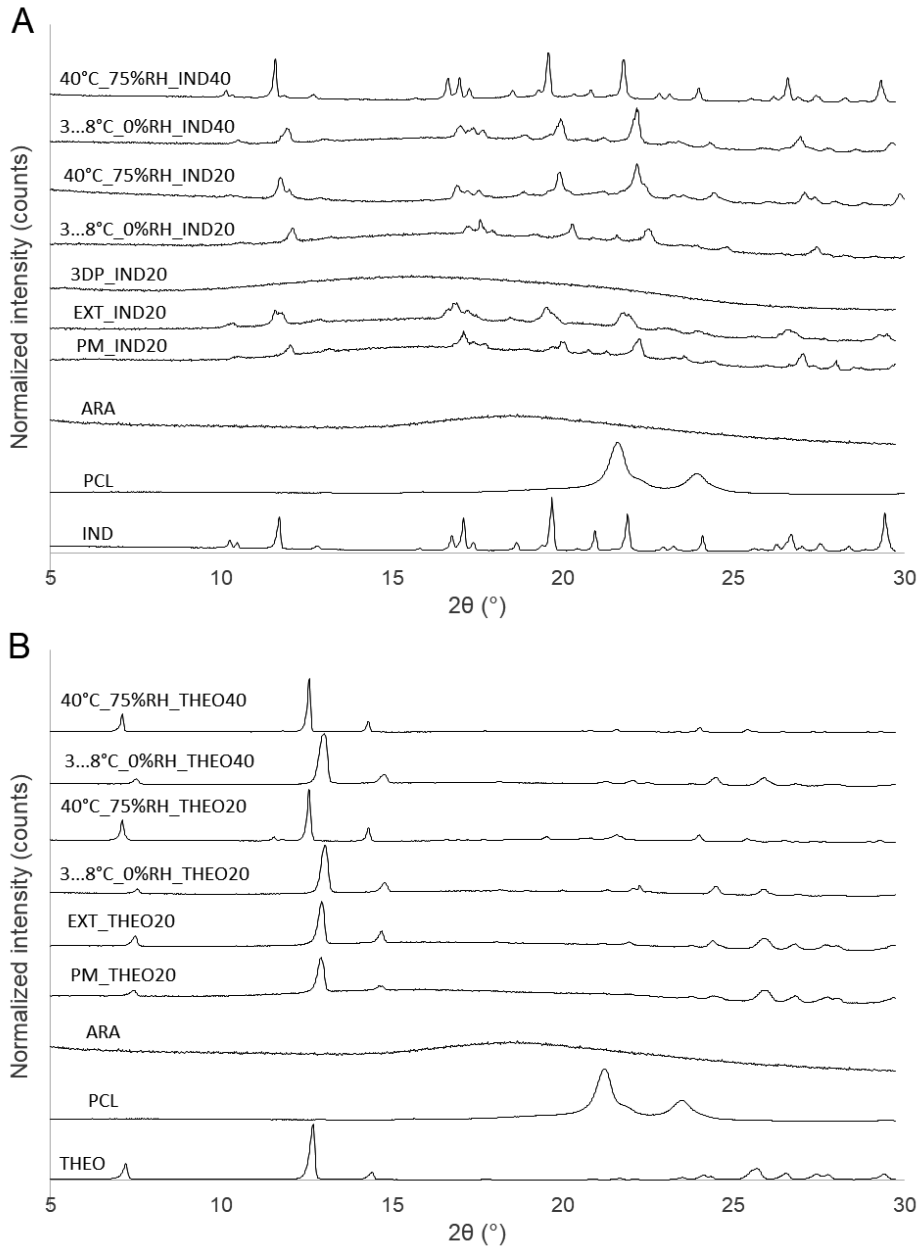

Figure 9. X-ray powder diffraction (XRPD) patterns of model drugs, polycaprolactone (PCL), arabic gum (ARA) as a powder form, and the corresponding XRPD patterns for the physical mixtures (PM), hot-melt extruded (HME, EXT) filaments, 3D-printed tablets (3DP), and the HME filaments after a 3-month storage stability test. Key: (A) Indomethacin (IND) and (B) Theophylline (THEO).

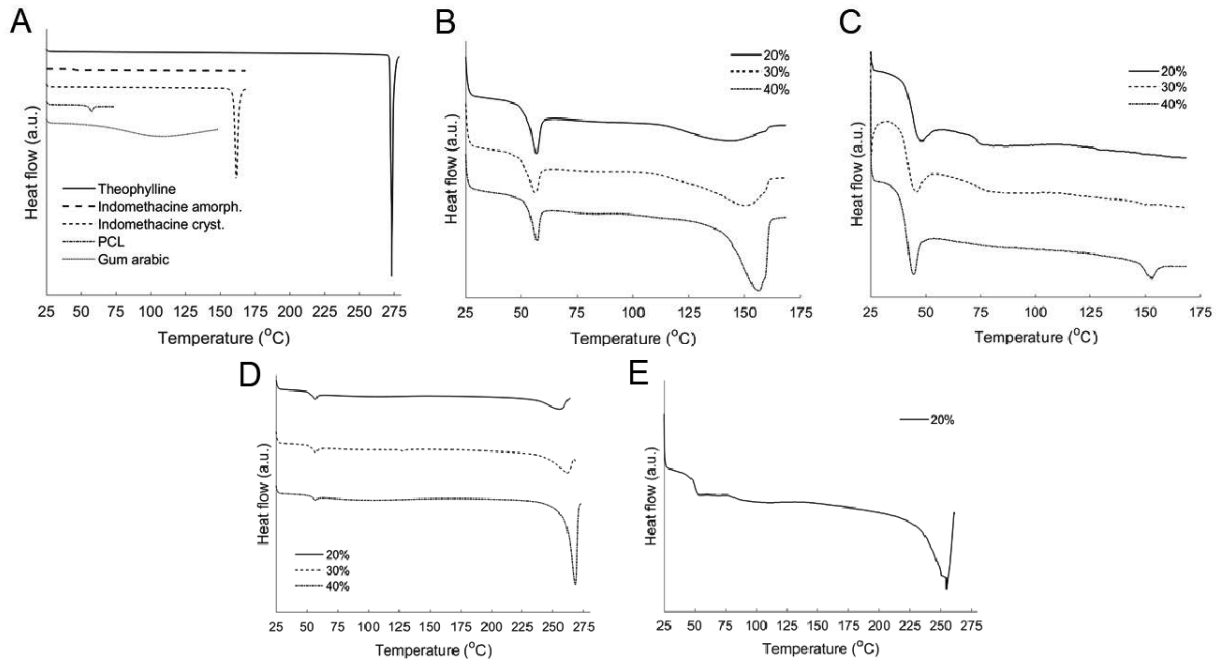

Figure 10. Differential scanning calorimetry (DSC) thermograms (exotherm up) of (A) pure materials, (B) hot-melt extruded (HME) filaments loaded with indomethacin (IND), (C) 3D-printed tablets of indomethacin (IND), (D) HME filaments loaded with theophylline (THEO), and (E) 3D-printed tablets of THEO.

6.2.6. Storage stability (II)

Figure 9 shows the physical stability of the API-loaded HME filaments stored for 3 months at the elevated temperature of 40 °C and 75% RH, or in a refrigerator at 3–8 °C and 0% RH. We found that the HME filaments loaded with IND or THEO changed their appearance and colour from off-white/yellowish to either darker (IND) or lighter (THEO) brownish paste-like slurry when the filaments were stored at 40°C/75% RH for 3 months. In the slurry, there were some fiber-like and crystal structures detectable. The crystal formation can be observed also in the XRPD diffraction patterns of the aged HME filaments presenting the characteristic diffraction peaks for IND and THEO (Figure 9). A slight shift in the diffraction peak positions can be observed, which could be due to the limitations in the sample preparation of the filaments for XRPD. When the IND or THEO-loaded HME filaments were stored in a refrigerator (3-8 °C and 0% RH) for 3 months, no physical solid-state changes were detected in the filaments (Figure 9). The colour of all aged filaments, however, was slightly changed to darker, but the shape and structure of the filaments were virtually the same as observed with the original filaments.

6.3. Influence of the printing parameters on 3D printability

6.3.1. Visual appearance of the 3D printed polymer lattices (I) and tablets (III)

The extrusion-based 3D printing of the model lattices using aqueous PEO gels was found to be possible at all printing parameter levels included in the experimental design (Table 2). The general morphology and printing accuracy of the polymeric lattices, however, varied significantly. As shown in Figure 11, the overall appearance and quality of the printed lattices were improved as the PEO concentration of the gels (and therefore also the gel viscosity) was increased. The two most common defects of the 3D-printed lattices were a dumbbell-shaped lattice and the fusion of separate printed layers, thus indicating unsatisfactory 3D-printing. The quality grades given in the visual inspection session by the independent inspectors (n = 10) to the 3D-printed lattices were in line with the results obtained in the subsequent deeper characterisation of the printed lattices. Calculating the area of printed lattices by image analysis and comparing it with the theoretical area of a designed model enabled us to evaluate the printability of aqueous PEO gels and influence of the key process parameters on the 3D printing.

Two batches of tablets varying with the number of layers were successfully 3D-printed. The physical appearance, weight and water uptake of the 3D-printed multilayered tablets are summarised in Table 6. The weight variation of the tablets was found to increase as the weight of the tablets was increased. This is most likely due to the uneven material deposition onto the tablets because of

an increased printing time of the tablets with a higher number of layers. The printed tablets were white to off-white in color, and occasional lines of a material deposition can be discovered on the top surface of the tablets. The UV-crosslinked tablets were the only preparations in our study having a subtle yellowish tint. No visual deformation was observed on the surface of the UV-crosslinked tablets.

6.3.2. Weight variation of the 3D printed polymeric lattices (I)

Figure 12 shows the effects of the PEO concentration (X1) and printing head speed (X2) on the weight and lattice area of the 3D printed polymeric lattices. The PEO concentration (X1) had a positive effect on the weight of the extrusion-based 3D printed lattices (R^2=0.9995). If higher concentration of PEO (20%) was used in 3D printing, more polymer was deposited during printing, thus resulting in a slight overall increase in the weights of 3D-printed PEO lattices (Figures 12A and 12B). The average weights for the 3D-printed lattices were 31.5 ± 9.7 mg (PEO gel concentration of 10%), 45.0 ± 4.9 mg (15%) and 58.2 ± 7.9 mg (20%), respectively.

In addition to PEO concentration (X1), a printing head speed (X2) (i.e., the movement speed of a printing head on X-Y axis) affected the lattice weight. Since a gel-extrusion speed was kept constant, the printing head speed determines the time to complete the lattice printing and the amount of material deposited during that time. Therefore, as a printing head speed (X2) was decreased (for a longer time to complete printing), a slight increasing trend in lattice weight was observed (Figures 12A and 12B). The printing plate temperature (X3) did not affect the weight of the extrusion-based 3D printed lattices.

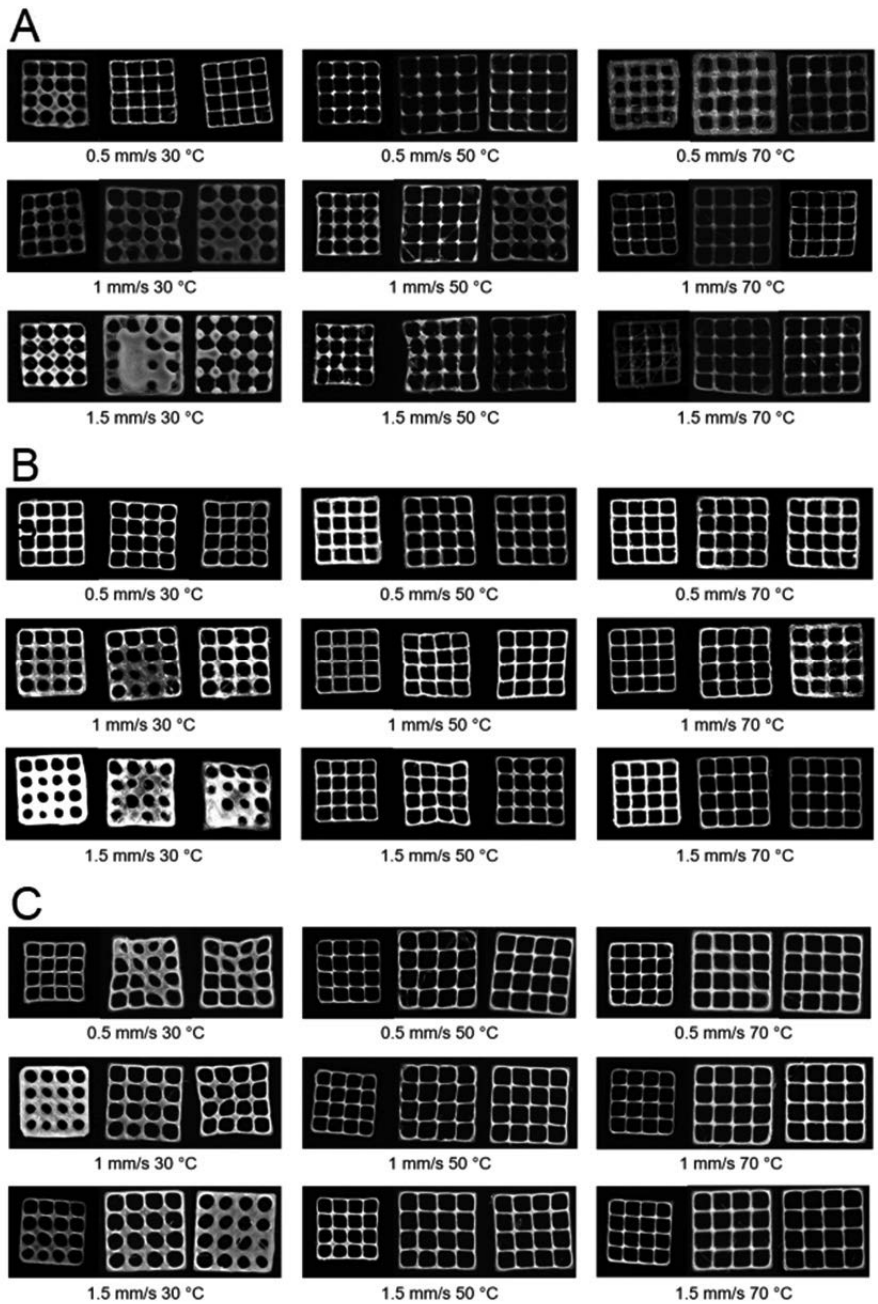

Figure 11. Photographs of the 3D printed polyethylene oxide (PEO) lattices. The photographs A, B and C denote the polymeric lattices printed with 10%, 15% or 20% PEO printing solution, accordingly.

Table 6. Visual appearance, weight, and water uptake of 3D-printed tablets (n=3).

Batch code	Visual appearance	Weight (mg ± SD)			Water uptake (%)
		Post-print	Pre-dissolution	Post-dissolution	
TH	white, dissolves in water	35 ± 5	34 ± 4	N/A	N/A
TH_UV	yellowish, fully gel-like when in water	37 ± 5	35 ± 4	184 ± 4	526%
TK	white, dissolves in water	71 ± 8	71 ± 8	N/A	N/A
TK_UV	yellowish, fully gel-like when in water	63 ± 5	63 ± 5	385 ± 35	611%
TK_gamma	white, dissolves in water	103 ± 4	91 ± 1	N/A	N/A

Key: N/A – non-applicable, TH – thin (tablet), TK – thick (tablet), TH_UV – thin UV-crosslinked 3D-printed tablets, TK_UV – thick UV-crosslinked 3D-printed tablets, TH_gamma – thin gamma-radiation crosslinked 3D-printed tablets.

6.3.3. Surface area of the 3D printed polymeric lattices (I)

According to the literature, extrusion-based (fused deposition) 3D-printing can result in the thermal contraction and shrinkage of the printed objects (Dizon et al., 2018). The effects of a printing head speed (X2) on the area of 3D-printed lattices at different PEO concentrations are shown in Figures 12C and 12D. Increasing the printing head speed (X2) and decreasing the PEO gel concentration (X1) led to larger area of the 3D printed lattices. It is evident that by using a higher printing head speed (X2), the gel material for one layer will be deposited faster, thus shortening the gap time before the next layer is printed. As shown in Figure 5, the PEO gels studied exhibit pseudoplastic behaviour, thus interfering with the gel settling. In addition, if a new layer is printed before the previous gel layer has not dried completely, the mass of the next layer will cause the deformation of the previous layer. This effect was seen with all 3D printing formulations studied here.

The printing plate temperature (X3) had a significant influence on the surface area of the 3D printed lattices ($p < 0.05$). The increase of a printing plate temperature (X3) resulted in a clear decrease of the surface area of the 3D printed lattices (Figure 13). This decrease in a lattice surface area was observed with all PEO gel concentrations (X1) studied but it was especially prominent with a PEO 20% gel concentration (Figure 13). The higher viscosity PEO gels could keep their initial shape on the course of a curing time, while lower viscosity gels exhibited deformation. The higher printing plate temperature enhances the drying of the previous gel layer prior to printing the subsequent layer onto it.

As shown in Figure 14, increasing the printing plate temperature (X3) lead to a clear decrease of the surface area of the 3D printed lattices at the printing head speed (X2) settings higher than 1.0 mm/s. Since the extrusion speed is kept constant, the amount of extruded material per lattice surface area is dependent on a printing head speed (X2) creating visually thinner print lines at higher printing speed levels and thicker print lines at lower printing speed levels. This in turn results in either smaller or larger 3D printed lattice surface areas, respectively. Interestingly, a printing head speed (X2) had a two-fold effect on a lattice surface area: a positive effect as the lowest printing plate temperature (30°C) was used, and a negative effect at the highest printing plate temperature (70°C) used. However, these contradiction effects could not be explained by the amount of the extruded material per a lattice surface area. Further studies are needed to gain understanding of this phenomenon.

Printing head speed had a positive effect on the 3D lattice area at low printing plate temperature levels and negative effect on the present response at high printing plate temperatures (Figure 14). As discussed earlier, when the PEO gel is not exposed to higher temperature, print lines will be deformed by the flow of the material itself and the mass of the next layer. This results in the increase of the print line width. As the drying of the gel material is aided by elevated printing plate temperature, the lines remain thinner. Since the model lattice grid consists of one print line, the width of this line determines the overall lattice area. However, the application of higher temperature in 3D printing may affect the other relevant properties of polymer(s) and/or drug substance(s) incorporated in the DDS (Okwuosa et al., 2016), and hence these effects need to be separately investigated. In the present study, the solid-state properties of the 3D printed lattices were investigated and compared to raw materials.

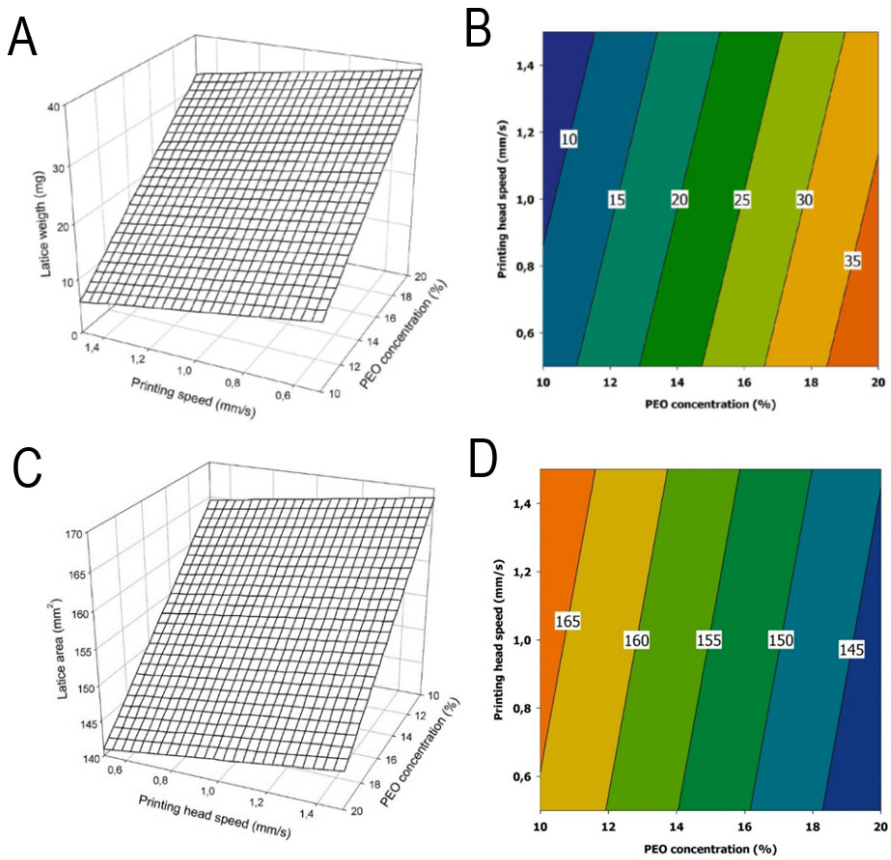

Figure 12. Effects of polyethylene oxide (PEO) concentration (%) and printing head speed (mm/s) on the weight (mg) (A, B) and lattice area (mm^2) (C, D) of the 3D-printed polymeric lattices (n = 3). A surface plot (A, C) and contour plot (B, D) presentation.

6.3.4. Surface area ratio of the 3D printed polymeric lattices (I)

The lattice area measurements of the 3D-printed objects give us information only on the layer formation behaviour of the gel during printing. These measurements, however, do not directly indicate, if the printability of the gel is good or poor. To evaluate the true printability, the actual value of the surface area of the 3D-printed lattice was compared to the theoretical lattice area (160.89 mm^2). As shown previously in Figures 12C and 12D, the use of higher printing head speed resulted in a slightly larger area of the 3D-printed PEO lattices. The lattice area ratio (r_x) (i.e., the ratio of the areas of an experimental and theoretical lattice) was similarly affected by both the printing head speed and PEO gel concentration (Figure 15). As seen in Figure 15, the area of the experimental 3D-printed lattice was the closest to the theoretical value when the

PEO concentration of the gel was 12% and the printing head speed used was 1.0 mm/s.

It was confirmed that 3D printing is a multivariate process, and the accuracy of the printing process is influenced by more than one parameter at a time. The printing plate temperature and printing head speed were the most critical and prevalent process parameters ($p = 0.002$). The present results suggest that the most challenging combination of the process parameters in terms of 3D printability is a high printing head speed (Figure 15A) and low plate temperature (Figure 15B). With the 3D-printed polymeric lattices, the measured area was larger than the theoretical value. Also, instead of a straight-lined grid, dumbbell shaped lattices were formed. Similar material spreading effect in 3D printing (resulting in insufficient printability) has been reported in the literature (Habib et al., 2018; Li et al., 2016; Lille et al., 2018). Heating up the printing plate results in faster drying of the printed PEO gels, thus allowing a faster printing head speed to be used (Figure 15C). The application of a faster printing head speed in turn lead to more precise 3D printing. With some other 3D-printed lattices (especially with those printed with a high PEO gel concentration), the experimental lattice area was smaller than the theoretical value (Figures 15A and 15B). The possible reasons for this phenomenon were discussed already in the previous section.

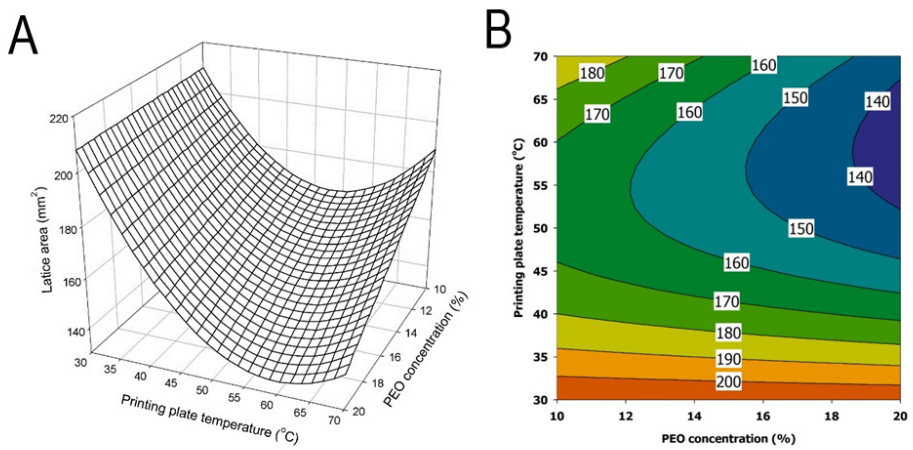

Figure 13. Effects of polyethylene oxide (PEO) concentration (%) and printing plate temperature (°C) on the lattice area (mm^2) of the 3D-printed polymeric lattices (n = 3). A surface plot (A) and contour plot (B) presentation.

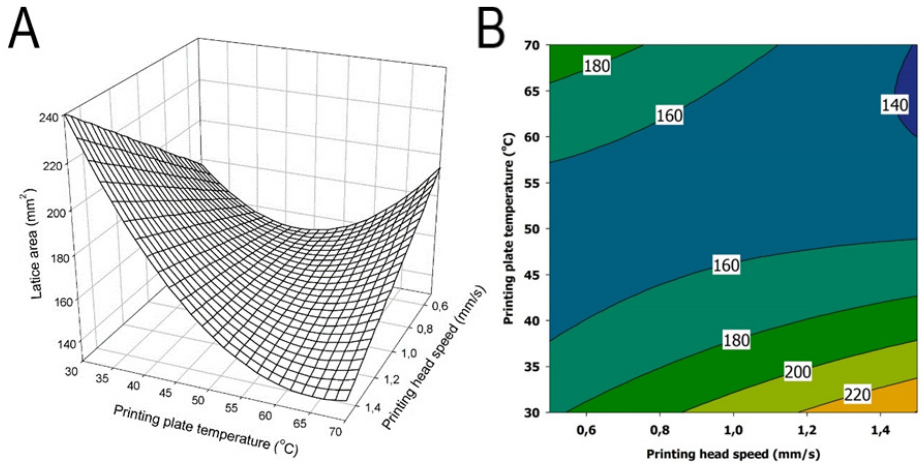

Figure 14. Effects of printing head speed (mm/s) and printing plate temperature (°C) on the lattice area (mm^2) of the 3D printed polymeric lattices (n = 3). A surface plot (A) and contour plot (B) presentation.

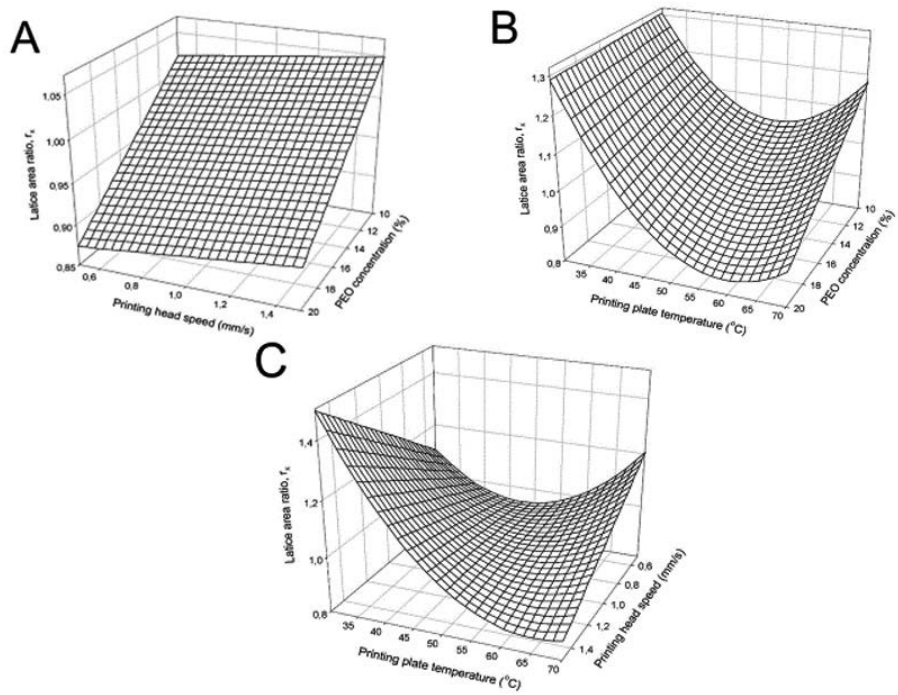

Figure 15. Effects of polyethylene oxide (PEO) concentration (%) (A, B), printing head speed (mm/s) (A, C), printing plate temperature (°C) (B, C) on the lattice area ratio (r_x) of the 3D- printed polymeric lattices (n = 3). Reference is also made to Table 1.

6.4. Solid state characterisation of the printed object

6.4.1. Thermal-induced solid-state changes (I)

To verify whether any unexpected solid-state transformations took place at the utilised printing settings, we also conducted the solid-state analyses for the samples. It is well known that solid state transformations can have a great impact on the final performance and stability of DDSs. In our study, the printing plate temperatures above 70°C were not studied due to the possible melting of PEO. Therefore, the elevated temperatures higher than 70°C are not considered as applicable for the 3D printing process described here.

According to the literature, PEO degrades at elevated temperatures (Crowley et al., 2002). In the present extrusion-based 3D printing, the aqueous PEO gel and printed lattices were exposed to the printing plate temperatures ranging from 30 °C to 70 °C. The printing contact time ranged from 20 min to 60 min. The melting temperature of PEO is approximately 65 °C (Warfield and Hartmann, 1973). In the present study, no visible melting of the carrier material was detected when the PEO gel was printed onto a plate at the temperature of 70 °C for up to 60 min. The possible thermal-induced solid-state changes of PEO in extrusion-based 3D printing were investigated by means of FTIR spectroscopy and XRPD.

Figure 16A shows the FTIR spectra of the 3D printed PEO-based squares. Two significant absorption complexes were displayed between 2960 cm^{-1} and 2890 cm^{-1} and around 1100 cm^{-1} representing methylene stretching and a combination of ether group and methylene group stretching, respectively. The present results are in line with the earlier findings in the literature (Yoshihara et al., 1964). An increase in the intensity of absorption can be seen at approximately 2875 cm^{-1} with the increase of the printing plate temperature.

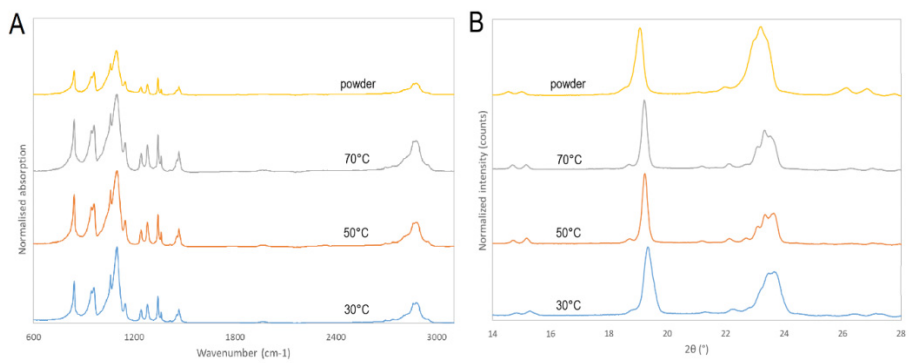

Figure 16. Fourier-transform infrared (FTIR) spectra (A) and X-ray diffraction (XRD) patterns (B) of polyethylene oxide (PEO) polymer and the 3D-printed PEO-based squares printed at different plate temperatures.

Figure 16B presents the XRD patterns of PEO powder and the 3D-printed PEO-based squares printed at different plate temperatures. PEO shows two distinctive diffraction peaks at 2θ = 19° and 23° (Uyar and Besenbacher, 2009). In our study, as the plate temperature was increased, the intensity of the characteristic XRD peak for PEO at approximately 23° was very slightly decreased. We found that the XRD patterns did not show any significant difference in the degree of crystallinity between the 3D-printed PEO lattices prepared with different plate temperatures (Figure 16B).

Figure 17 shows the DSC thermograms of pure substances (THEO and PEO), PMs, and non-crosslinked and UV-crosslinked 3D-printed tablets. According to the literature, the degradation temperature of PEO ranges from 400 °C to 450 °C for a high molecular weight PEO (Jakic et al., 2013; Samad et al., 2013; Wang et al., 2001). The characteristic melting peaks for THEO and PEO are seen at 273 °C and at approximately 70 °C, respectively (Figure 17). With the non-crosslinked tablets, the melting endotherm for PEO can be seen at a slightly lower temperature at 68 °C. Since the temperature will not rise to 400 °C in an extrusion-based 3D printing process, and since we did not observe any solid-state changes (XRD) at the process temperatures used, PEO was considered as a plausible model polymer for these printability studies.

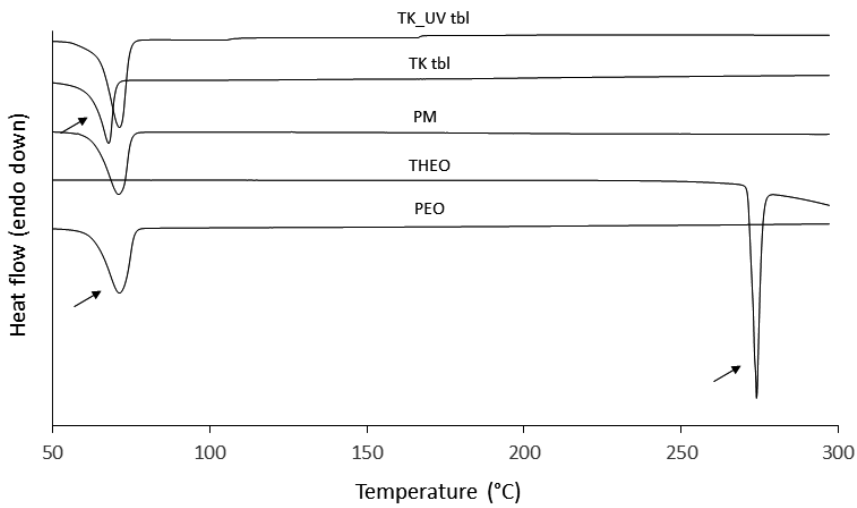

Figure 17. Differential scanning calorimetry (DSC) thermograms of pure substances, physical mixture (PM), and non-crosslinked and UV-crosslinked 3D-printed tablet. Key: THEO = theophylline, PEO = polyethylene oxide, TK = thick.

As seen in Figure 17, no melting endotherm of anhydrous THEO is displayed in the DSC thermograms of the PMs and 3D-printed tablets. This is a well-known effect occurring with API-polymer mixtures where the polymer melts at a lower temperature than the melting temperature of an API. This kind of behaviour and

phenomenon affect also the dissolution of THEO in PEO (Hakkarainen et al., 2019). It is evident that THEO acting as a nucleating agent is able to facilitate the crystallisation of polymer (PEO) (Renterghem et al., 2017). As seen in Figure 17, the glass transition temperature of PEO was not detectable under the present testing conditions by DSC. We assume that no thermal degradation took place during a heating phase as there are no additional peaks seen in the DSC thermograms.

6.4.2. Near-infrared spectroscopy (III)

The importance of a drying step in the extrusion-based 3D printing of semisolid materials has been discussed previously in this dissertation. The water activity of 3D-printed tablets can be very high immediately after printing (El Aita et al., 2019). We compared the water content of the freshly prepared PMs, the PMs stored at high humidity conditions (40 °C/75% RH), and the freshly prepared and aged 3D-printed tablets by using NIR spectroscopy (Figure 18).

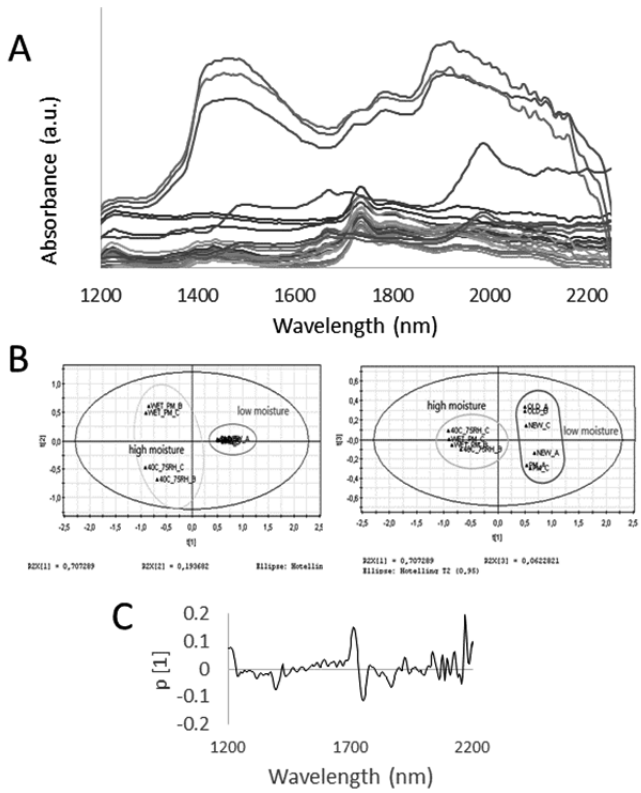

Figure 18. Principal component analysis (PCA) of the water content in the freshly prepared physical mixtures (PMs), the PMs stored at high humidity conditions (40 °C/75% RH), and the freshly prepared and aged 3D-printed tablets. Fig. 18A: The untreated near-infrared (NIR) spectra of samples. Fig. 18B: The scores plot of t1/t2 and t1/t3. Fig. 18C: The loadings of a component 1.

NIR spectroscopy has been widely used for monitoring the drying as it is very sensitive towards H-bonding related to water molecules, and it is easy to correlate the water content with NIR spectral features using modelling. No quantitative spectral analyses were performed, but the interpretation of the raw NIR spectra and PCA was used to qualitatively analyze the data and understand the drying effect. Figure 18B shows the score plots of the PCA displaying two or three distinct groups for the NIR spectra. It was confirmed by the loadings plot that the present groups obtained in the PCA differ from each other based on the water content in the sample (Figure 18C). The NIR spectra of the freshly prepared and stored 3D-printed tablets were grouped together with the NIR spectra of the freshly prepared PMs. The results suggest that the selected drying period for the 3D-printed tablets of the present size and shape is sufficient to remove any excess water.

The PCA model revealed that the largest differences between the samples were due to the presence of water. Hence, the first principal component (PC1) can be used to explain the water content in the samples, and it represented 70.1% of the spectral variation. As the PC1 loadings at the selected wavelengths were plotted, we found that the major differences in the variables occur at approximately 1200 nm, 1700 nm, 1750 nm, and 2170 nm. These differences can be associated with water absorption, since the bands at 1200 nm and 1700 nm correspond to the first and second overtone of the C-H stretching, and the band at 2200 nm corresponds to O-H stretch (Clevers et al., 2008; Giangiacomo, 2006).

We observed also in our preliminary tests (data not shown) that the time required for the weight stabilization was longer with the thicker 3D-printed tablets than that with the corresponding thinner tablets. Therefore, the water content (NIR spectra) of the 3D-printed tablets needs to be evaluated (collected) over the time-period long enough to ensure the drying of such tablet preparations.

6.4.3. Crosslinking efficacy

FTIR spectroscopy was used to evaluate possible molecular interactions during the 3D-printing process and to confirm the crosslinking of PEO. Figure 19 shows the FTIR spectra of pure materials, PMs, and non-crosslinked 3D-printed tablets. PEO has characteristic peaks at 840 cm^{-1} (relates to bonds of CH_2), 1093 cm^{-1} (shows triplet C-O-C stretching (Noor et al., 2011)) and 2875 cm^{-1} (relates to C-H methylene stretching and shows semi-crystalline phase of PEO) (Jurkin and Pucić, 2012). All the above-mentioned peaks are also seen in Figure 19 for the PM and non-crosslinked 3D printed tablets at very similar intensity. The peaks for HBP were not detected in the above-mentioned spectra. The specific absorption bands at 1658 cm^{-1} (related to C-O stretching for carbonyl group (Nokhodchi et al., 2009)) and at 3118 cm^{-1} (N–H stretching (Lin et al., 2013)) are characteristic for THEO. The barely visible absorption band at 1658 cm^{-1} can be seen in the FTIR spectra of PM and non-crosslinked 3D-

printed tablets, being more intense in the latter. The phenomenon of lower intensity of the 1658 cm^{-1} peak has been also reported in previous studies (Hakkarainen et al., 2019). We found that similar behaviour also applied for non-crosslinked tablets. Another characteristic peak for THEO is hardly seen at 3118 cm^{-1} in the FTIR-spectrum of the PM, but this peak is detectable in the FTIR-spectrum of the non-crosslinked tablets.

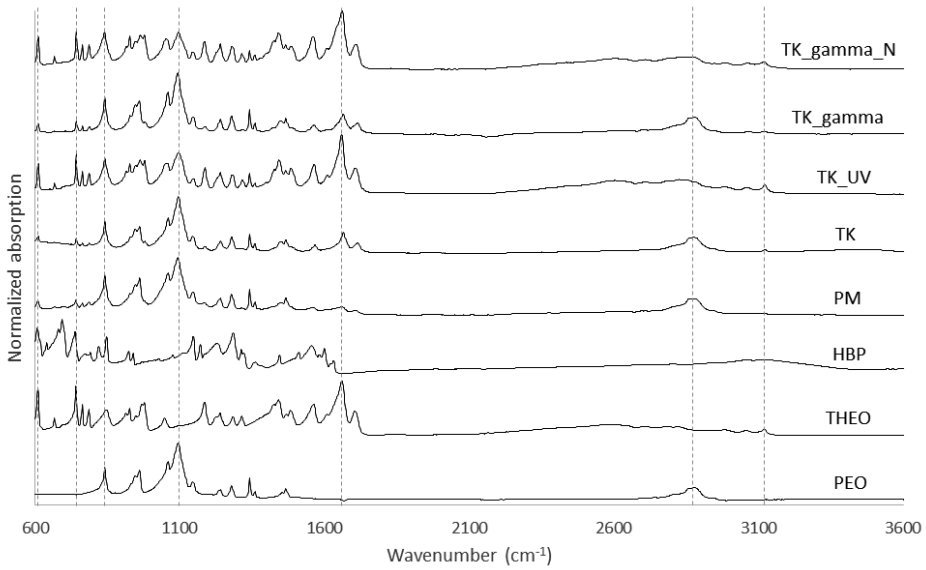

Figure 19. Fourier-transform infrared (FTIR) spectra of pure substances, physical mixture (PM) and 3D-printed non-crosslinked tablets, and non-crosslinked, UV- and gamma-radiated crosslinked 3D-printed tablets. Key: THEO = theophylline, PEO = polyethylene oxide, HBP = 4-hydroxybenzophenone, TK = thick, N = nitrogen. Dotted lines show the characteristic peaks of PEO and THEO.

The effects of the two radiation-based crosslinking treatments on the solid-state properties of 3D-printed tablets were also investigated. As seen in Figure 19, the non-irradiated and gamma-radiated tablets presented the characteristic peaks for PEO at 1093 cm^{-1} and at 2875 cm^{-1} in the FTIR-spectrum. The 3D-printed tablets irradiated by UV and gamma-radiation in a nitrogen environment showed very low-intensity peaks at 2875 cm^{-1} and 1093 cm^{-1} in the FTIR spectra (the characteristic peaks of PEO were only slightly observed). This peak disappearance at 2875 cm^{-1} suggests molecular interactions by homolytic scission of C-H bonds (especially, at the presence of nitrogen) as a crosslinking effect (Hennink and Nostrum, 2002; Teixeira et al., 2013). The characteristic high-intensity absorption peaks for THEO at 1658 cm^{-1}, 609 cm^{-1} and 742 cm^{-1} are clearly seen in the FTIR spectra of the 3D-printed tablets radiated with UV

and gamma-radiation in nitrogen environment (Figure 19). This suggests the presence of API in a free state in these tablets. The present characteristic peaks for THEO are much less-intense (or absent) in the FTIR spectra of the gamma-radiated (without nitrogen) and non-crosslinked tablets. We found that the presence of HBP as a photo-initiator and the use of both UV- and gamma-radiation treatments (only in a nitrogen environment) result in successful cross-linking. In the literature, the use of nitrogen environment and/or antioxidants has been shown to benefit a crosslinking process and to prevent the chemical degradation of the polymer when gamma-radiation is used (Crowley et al., 2002; Jurkin and Pucić, 2012).

6.5. Drug release behaviour *in vitro* (II, III)

The 3D-printed tablets fabricated from the API-loaded HME filaments presented a sustained drug release behaviour *in vitro* (Figure 20). The drug release of the 3D-printed tablets (cylinder-shape) loaded with IND was negligible (i.e., practically no drug was released within 24 hours; data not shown). With the 3D-printed tablets (cylinder-shape) loaded with THEO, the amount of API released within 24 hours was somewhat higher, but the overall drug release was still very low (less than 5% from the theoretical drug load 48.9 ± 3.7 mg). According to the literature, the PCL-based DDSs exhibited a prolonged drug release (Lao et al., 2008). The dissolution results obtained in our study suggest that the present active-loaded 3D-printed tablets based on PCL are more applicable for implant drug-delivery applications than for oral administration. To accelerate the drug release, we made further 3D printing experiments with the HME filaments loaded with the model APIs.

We changed the geometry and texture of the 3D-printed tablets from cylindrical to “honeycomb” (theoretical API loading 48.3 ± 5.2 mg) and found a significant increase in the amount of drug released compared to that obtained with conventional-shaped tablets (Figure 20). The weight of the novel “designed” tablets was kept as much as possible the same as with the conventional-shaped tablets (assuming that the amount of API in both tablets would be then identical as well). The drug release of the “honeycomb”-patterned 3D-printed tablets loaded with THEO was approximately 12% within 24 hours, while the drug release of the cylinder-shaped tablets was only 2% within the same time-period. Much larger outer surface area of the “honeycomb”-structured tablets greatly enhances the drug release from the 3D-printed tablets.

The positive effect of the increased surface area on the drug release behaviour has been reported also in the literature (Goyanes et al., 2015b). As the size, shape and texture of 3D-printed DDSs are easily modified, this could open a true option for the patient-specific formulation of drug products and tailoring the drug release in accordance with patient needs in the future.

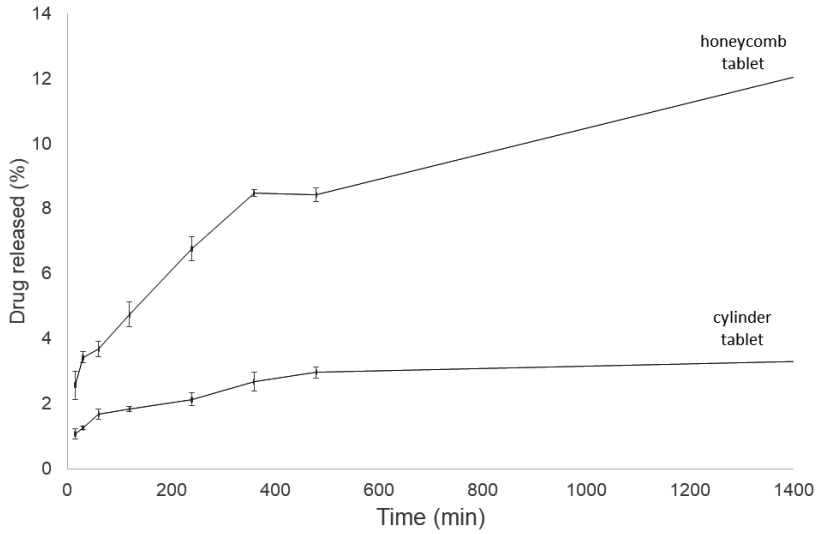

Figure 20. Drug release profiles of the 3D-printed theophylline (THEO) tablets with different geometry and texture (n = 3). The amount of THEO in the tablet was 20% of the total tablet weight.

Figure 21 shows the influence of the number of printing layers and crosslinking on the drug release behaviour of the micro-extrusion-based 3D-printed THEO tablets. The dissolution results were calculated as the drug release of an average-weighed tablet of the batch and considering the weights of the individual tablets selected in the dissolution test (Table 6). As seen in Figure 21, the UV-crosslinked thin 3D-printed tablets (TH, tablet height, h = 2 mm) presented an immediate-release dissolution pattern and the drug (THEO) was released approximately within 30 minutes (Figure 21A). With the non-crosslinked and UV-crosslinked thick tablets (TK, h = 5 mm), however, the amount of THEO released within 30 minutes (and within subsequent 60 min) was only about 50% of the theoretical amount of drug (Figure 21A). Both thin and thick UV-crosslinked tablets exhibited an identical immediate-release behaviour *in vitro*.

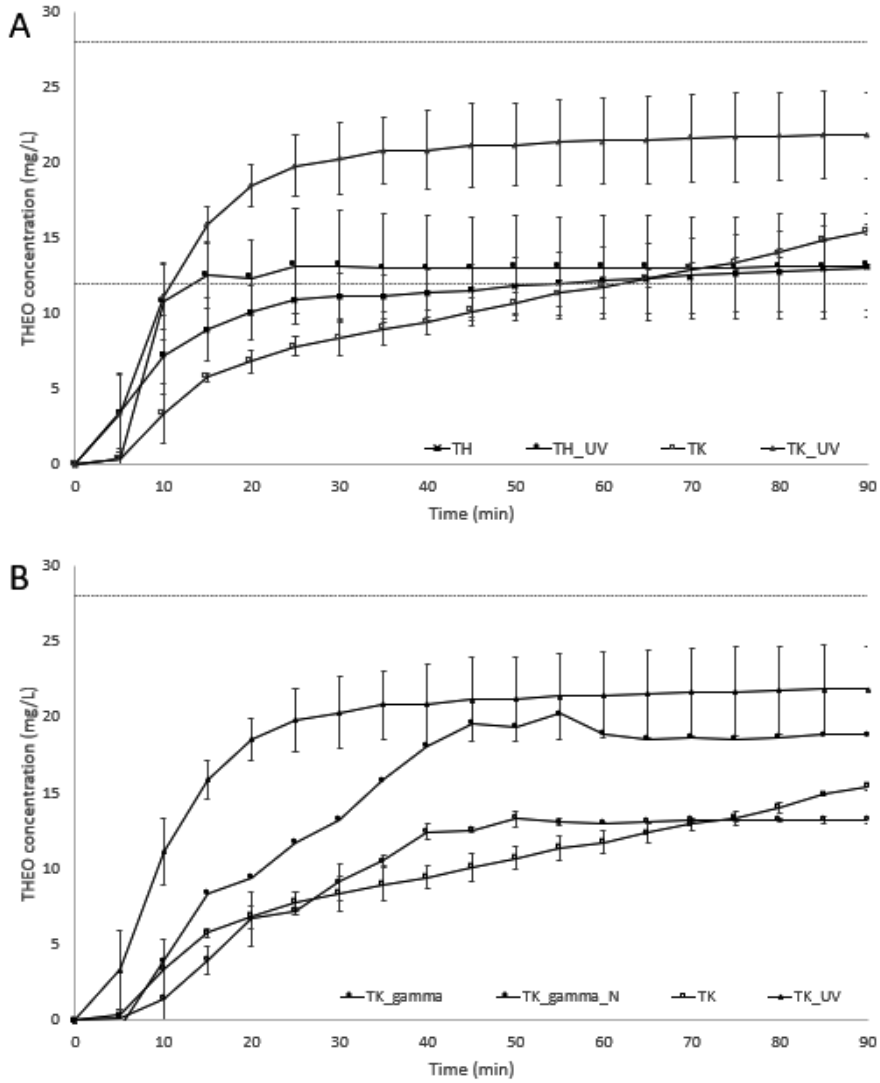

Figure 21. The in-vitro theophylline (THEO) release of 3D-printed tablets. (A) The dissolution of untreated and UV-crosslinked 3D-printed tablets (thin tablets TH_UV and thick tablets TK_UV). (B) The dissolution of UV-crosslinked (TK_UV) and gamma-radiated (TK_gamma and TK_gamma_N) 3D-printed tablets. Standard deviations (n=3, TK_gamma_N n=1) and horizontal dashed lines for theoretical nominal concentrations are shown in both figures A and B.

The non-crosslinked thick 3D-printed tablets presented a prolonged drug-release pattern *in vitro* with the release of approximately 60% of the theoretical amount of drug within 90 minutes. Based on the visual inspection, the non-crosslinked thin and thick tablets were all completely dissolved by the end of

the dissolution test. Our results are in agreement with those reported by Pietrzak et al. (2015). They found that the dissolution of Eudragit RL-based 3D-printed tablets presented a prolonged THEO release behaviour as the volume of the tablets (i.e., the number of printing layers) was increased (Pietrzak et al., 2015). Since the drug release of 3D-printed tablets is dependent on a carrier polymer, this is important to be considered in adjusting ("tailoring") the individualised API dose and release pattern for the patients via the volume changes of 3D printed tablets.

Figure 22 shows the photographs of the 3D-printed THEO tablets before, within and after a dissolution test *in vitro*. Based on the *visual* inspection, the UV-crosslinked 3D-printed tablets presented an insoluble residue in the dissolution vessel after completing the dissolution test *in vitro* (90 min). We also found that the water uptake of such TH_UV and TK_UV tablets on the course of a dissolution test was on average 526% and 611%, respectively (Table 6). The increase in weight, however, shows us only swelling, and it does not consider the potential weight changes caused by the dissolution/erosion of THEO or PEO. TK_UV tablets were enlarged in size, but the shape of the tablets did not change (Figure 22A). When the tablets were dried, a characteristic crisscross pattern (surface texture) caused by the deposited material can be seen (Figure 22B). Interestingly, when a solvent cast UV-crosslinked PEO films of equivalent diameter and thickness were dissolved in distilled water for same time as the 3D-printed tablets, the films lost their structure and shape (Figures 22C and 22D). Further studies on the importance of material deposition itinerary are needed to give a deeper insight into this phenomenon.

The crosslinked extrusion-based 3D-printed tablets are the multilayer-structured systems with interlayer spaces. The importance of the porosity of PEO hot-melt extrudates in drug release has been discussed in the literature (Cantin et al., 2021). The porosity and subsequent drug release of traditional compressed tablets are dependent on the compression force, while the extrusion-based 3D-printed ones are composed of the deposited layers of semisolid material, which enables larger interlayer spaces. Crosslinking such 3D-printed tablets results in a loose tablet structure enabling the API to release and dissolve faster. With the non-crosslinked 3D-printed tablets, a viscous gel-layer is formed around the tablet, thus prolonging the drug release (THEO) from the tablet.

The gamma-irradiated TK (thick) tablets presented a slow drug-release pattern like that obtained with the non-crosslinked TK tablets (Figure 21B). The TK 3D-printed tablets kept in a nitrogen environment during gamma irradiation exhibited faster drug release like that observed with the UV-crosslinked TK tablets. The present two sets of 3D-printed tablets showed also the similar FTIR spectra (Figure 19). Nonetheless, the gamma-radiated 3D-printed tablets did not have any residue left to be weighed after a dissolution test.

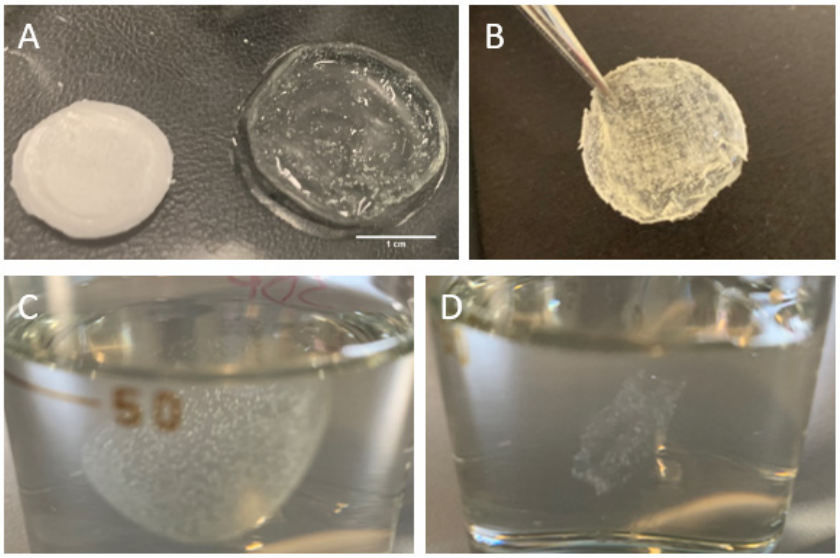

Figure 22. Photographs of the 3D-printed tablets before, within and after a dissolution test in vitro. (A) Comparison of a thick UV-crosslinked (TK_UV) 3D-printed tablet before and after a dissolution test in vitro (scale bar equal to 1 cm); (B) The UV-crosslinked 3D-printed tablet (TK_UV) dried after a dissolution test in vitro; (C) The UV-crosslinked 3D-printed tablet after the exposition of 2 hours to distilled water; (D) The UV-crosslinked solvent-cast free film after the exposition of 2 hours to distilled water.

7. SUMMARY AND CONCLUSIONS

The present dissertation provides further insight into the applicability of micro-extrusion based and HME-integrated FDM 3D printing methods in pharmaceutics. The printed formulations were developed for either method allowing the successful use of established polymeric excipients in pharmaceutics without any organic solvents.

From the results obtained here we can conclude, that

(1) Polyethylene oxide (PEO) and polycaprolactone (PCL) are feasible carrier polymers to be applied in a micro-extrusion-based 3D printing and fused deposition modelling (FDM) 3D printing, respectively. Indomethacin (IND) combined with PCL as a carrier polymer and arabic gum (ARA) as an external plasticizer enables the preparation of hot melt extruded (HME) filaments intended for FDM 3D printing. Theophylline (THEO) can be used in both PCL- and PEO-based formulations and with both 3D-printing technologies.

(2) Printing solution viscosity, printing head speed, printing plate temperature, solid-state properties and crosslinking efficacy are important material and process parameters in 3D printing affecting the final properties and behaviour of printed drug delivery systems (DDS). Cylindrical model tablets with varying number of layers were designed and successfully fabricated in a micro-extrusion-based 3D printing process. Both full and honeycomb latticed cylindrical model tablets were used for FDM 3D printing.

(3) The accuracy of a micro-extrusion-based 3D printing process (3D printability) is influenced by more than one parameter at a time, and the combination of printing plate temperature and printing head speed is the most prevalent. For optimizing 3D printing, the printing solution consisting of 1.2 g of PEO in 10 ml of distilled water and the printing head speed set at 1.0 mm/s were selected for micro-extrusion-based 3D printing.

(4) The HME filaments with the active pharmaceutical ingredient (API) concentrations of 20%, 30% and 40% (w/w) were prepared. Both IND and THEO loaded HME filaments showed some surface roughness and were more resistant to mechanical forces at lower API concentrations. The experimental API load was lower than theoretical API concentration, and the distribution of API was not homogeneous through the filament. After being stored for 3 months in 40°C/75% RH both filaments had turned brown and soft, losing their integrity. The IND filaments were printed at 175°C with the printing plate heated to 40°C. The corresponding temperature levels used with the THEO filaments were 190°C and 40°C, respectively.

(5) The *in vitro* drug release from the PCL-based full cylindrical FDM tablets followed a sustained-release pattern. Practically no IND and less than 5% of THEO was released in 24 hours. The dissolution rate increased when the tablet geometry was changed to honeycomb structure. The honeycomb-structured lattices released approximately 12% of the API (THEO) within

24 hours. The PEO-based micro-extruded tablets presented slower drug release (THEO) with thicker tablets (more layers) compared to that obtained with the corresponding thinner tablets. With the thick (TK) tablets, UV-crosslinking and gamma-radiation in nitrogen environment resulted in faster drug release compared to that obtained with the corresponding non-radiated 3D-printed tablets.

REFERENCES

Aceves-Hernandez, J.M., Nicolas-Vazquez, I., Aceves, F.J., Hinojosa-Torres, J., Paz, M., Castano, V.M., 2009. Indomethacin polymorphs: Experimental and conformational analysis. J. Pharm. Sci. 98, 2448–2463.

Ahmed, Z., 2020. Practicing precision medicine with intelligently integrative clinical and multi- omics data analysis. Hum. Genomics 35.

Aho, J., Boetker, J.P., Baldursdottir, S., Rantanen, J., 2015. Rheology as a tool for evaluation of melt processability of innovative dosage forms. Int. J. Pharm. https://doi.org/10.1016/j.ijpharm.2015.02.009

Aho, J., Bøtker, J.P., Genina, N., Edinger, M., Arnfast, L., 2019. Roadmap to 3D-Printed Oral Pharmaceutical Dosage Forms: Feedstock Filament Properties and Characterization for Fused Deposition Modeling. J. Pharm. Sci. 108, 26–35. https://doi.org/10.1016/j.xphs.2018.11.012

Andrews, D., Salunke, S., Cram, A., Bennett, J., Ives, R.S., Basit, A.W., Tuleu, C., 2021. Bitter-blockers as a taste masking strategy: A systematic review towards their utility in pharmaceuticals. Eur. J. Pharm. Biopharm. 158, 35–51. https://doi.org/10.1016/j.ejpb.2020.10.017

Antman, E.M., Loscalzo, J., 2016. Precision medicine in cardiology. Nat. Rev. Cardiol. 13. https://doi.org/10.1038/nrcardio.2016.101

Ashley, E.A., 2016. Towards precision medicine. Nat. Rev. Genet. 17. https://doi.org/10.1038/nrg.2016.86

Awad, A., Tren, S.J., Gaisford, S., Basit, A.W., 2018. 3D printed medicines: A new branch of digital healthcare. Int. J. Pharm. 548, 586–596. https://doi.org/10.1016/j.ijpharm.2018.07.024

Azad, M.A., Olawuni, D., Kimbell, G., Badruddoza, A.Z., Hossain, S., Sultana, T., 2020. Polymers for Extrusion-Based 3D Printing of Pharmaceuticals: A Holistic Materials – Process Perspective. Pharmaceutics 12, 124.

Baumgartner, A., Drame, K., Geutjens, S., Airaksinen, M., 2020. Does the Polypill Improve Patient Adherence Compared to Its Individual Formulations ? A Systematic Review. Pharmaceutics 12, 90.

Beck, R.C.R., Chaves, P.S., Goyanes, A., Vukosavljevic, B., Buanz, A., Windbergs, M., Basit, A.W., Gaisford, S., 2017. 3D printed tablets loaded with polymeric nanocapsules: An innovative approach to produce customized drug delivery systems. Int. J. Pharm. 528, 268–279. https://doi.org/10.1016/j.ijpharm.2017.05.074

Beer, N., Hegger, I., Kaae, S., Bruin, M.L. De, Genina, N., Alves, T.L., Hoebert, J., Kälvemark Sporrong, S., 2021. Scenarios for 3D printing of personalized medicines – A case study. Explor. Res. Clin. Soc. Pharm. https://doi.org/10.1016/j.rcsop.2021.100073

Binson, G., Beuzit, K., Migeot, V., Marco, L., Troussier, B., Venisse, N., Dupuis, A., 2019. Preparation and Physicochemical Stability of Liquid Oral Dosage Forms Free of Potentially Harmful Excipient Designed for Pediatric Patients. Pharmaceutics 11, 190.

Brown, S.-A., 2016. Patient Similarity: Emerging Concepts in Systems and Precision Medicine. Front. Physiol. 7, 561. https://doi.org/10.3389/fphys.2016.00561

Buckley, L.A., Salunke, S., Thompson, K., Baer, G., Fegley, D., Turner, M.A., 2018. Challenges and strategies to facilitate formulation development of pediatric drug products: Safety qualification of excipients. Int. J. Pharm. 536, 563–569. https://doi.org/10.1016/j.ijpharm.2017.07.042

Cailleaux, S., Sanchez-ballester, N.M., Gueche, Y.A., Bataille, B., Soulairol, I., 2021. Fused Deposition Modeling (FDM), the new asset for the production of tailored medicines. J. Control. Release 330, 821–841. https://doi.org/10.1016/j.jconrel.2020.10.056

Cantin, O., Siepmann, F., Willart, J.F., Danede, F., Siepmann, J., Karrout, Y., 2021. PEO hot melt extrudates for controlled drug delivery: Importance of the type of drug and loading. J. Drug Deliv. Sci. Technol. 61, 102238. https://doi.org/10.1016/j.jddst.2020.102238

Cerda, J.R., Arifi, T., Ayyoubi, S., Knief, P., Ballesteros, M.P., Keeble, W., Barbu, E., Healy, A.M., Lalatsa, A., Serrano, D.R., 2020. Personalised 3D Printed Medicines: Optimising Material Properties for Successful Passive Diffusion Loading of Filaments for Fused Deposition Modelling of Solid Dosage Forms. Pharmaceutics 12, 345.

Chang, C.C., Boland, E.D., Williams, S.K., Hoying, J.B., Blvd, E.M.A., 2013. Direct-write Bioprintin Three-Dimensonal Biohybrid Systems for Future Regenerative Therapies. J. Biomed. Mater. Res. B Appl. Biomater. 98, 160–170. https://doi.org/10.1002/jbm.b.31831.Direct-write

Chen, R., Snyder, M., 2013. Promise of personalized omics to precision medicine. WIREs Syst. Biol. Med. 5, 73–82. https://doi.org/10.1002/wsbm.1198

Chia, H.N., Wu, B.M., 2015. Recent advances in 3D printing of biomaterials. J. Biol. Eng. 9, 4. https://doi.org/10.1186/s13036-015-0001-4

Choong, Y.Y.C., Tan, H.W., Patel, D.C., Choong, W.T.N., Chen, C.-H., Low, H.Y., Tan, M.J., Patel, C.D., Chua, C.K., 2020. The global rise of 3D printing during the COVID-19 pandemic. Nat. Rev. Mater. 5, 637–639. https://doi.org/10.1038/s41578-020-00234-3

Chung, J.H.Y., Naficy, S., Yue, Z., Kapsa, R.M., Quigley, A.F., Moulton, S.E., Wallace, G.G.; J., Wallace, G.G., 2013. Bio-ink properties and printability for extrusion printing living cells, Journal of Biomaterials Science: Polymer Edition.

Cilurzo, F., Selmin, F., Minghetti, P., Adami, M., Bertoni, E., Lauria, S., Montanari, L., 2011. Injectability Evaluation: An Open Issue. AAPS PharmSciTech 12, 604–609. https://doi.org/10.1208/s12249-011-9625-y

Clevers, J.G.P.W., Kooistra, L., Schaepman, M.E., 2008. Using spectral information from the NIR water absorption features for the retrieval of canopy water content. Int. J. Appl. Earth Obs. Geoinf. 10, 388–397. https://doi.org/10.1016/j.jag.2008.03.003

Compton, B.G., Lewis, J.A., 2014. 3D-printing of lightweight cellular composites. Adv. Mater. 26, 5930–5935. https://doi.org/10.1002/adma.201401804

Conrad, K., Shoenfeld, Y., Fritzler, M.J., 2020. Precision health: A pragmatic approach to understanding and addressing key factors in autoimmune diseases. Autoimmun. Rev. 19, 102508. https://doi.org/10.1016/j.autrev.2020.102508

Cox, J.L., Koepsell, S.A., 2020. 3D-Printing to Address COVID-19 Testing Supply Shortages. Lab. Med. 51, 45–46. https://doi.org/10.1093/labmed/lmaa031

Crowley, M.M., Zhang, F., Koleng, J.J., McGinity, J.W., 2002. Stability of polyethylene oxide in matrix tablets prepared by hot-melt extrusion. Biomaterials 23, 4241–4248. https://doi.org/10.1016/S0142-9612(02)00187-4

Curti, C., Kirby, D.J., Russell, C.A., 2020. Current formulation approaches in design and development of solid oral dosage forms through three – dimensional printing. Prog. Addit. Manuf. 5, 111–123. https://doi.org/10.1007/s40964-020-00127-5

Daly, R., Harrington, T.S., Martin, G.D., Hutchings, I.M., 2015. Inkjet printing for pharmaceutics – A review of research and manufacturing. Int. J. Pharm. 494, 554–567. https://doi.org/10.1016/j.ijpharm.2015.03.017

Desai, D., Sandhu, H., Shah, N., Malick, W., Zia, H., Phuapradit, W., Ram, S., Vaka, K., 2018. Selection of Solid-State Plasticizers as Processing Aids for Hot-Melt Extrusion. J. Pharm. Sci. 107, 372–379. https://doi.org/10.1016/j.xphs.2017.09.004

Dizon, J.R.C., Espera, A.H., Chen, Q., Advincula, R.C., 2018. Mechanical characterization of 3D-printed polymers. Addit. Manuf. 20, 44–67. https://doi.org/10.1016/J.ADDMA.2017.12.002

du Plessis, A., Yadroitsev, I., Yadroitsava, I., Le Roux, S.G., 2018. X-Ray Microcomputed Tomography in Additive Manufacturing: A Review of the Current Technology and Applications. 3D Print. Addit. Manuf. 5, 227–247. https://doi.org/10.1089/3dp.2018.0060

Dumpa, N.R., Bandari, S., Repka, M.A., 2020. Novel Gastroretentive Floating Pulsatile Drug Delivery System Produced via Hot-Melt Extrusion and Fused Deposition Modeling 3D Printing. Pharmaceutics 12, 52.

Ebagninin, K.W., Benchabane, A., Bekkour, K., 2009. Rheological characterization of poly(ethylene oxide) solutions of different molecular weights. J. Colloid Interface Sci. 336, 360–367. https://doi.org/10.1016/j.jcis.2009.03.014

El Aita, I., Breitkreutz, J., Quodbach, J., 2019. On-demand manufacturing of immediate release levetiracetam tablets using pressure-assisted microsyringe printing. Eur. J. Pharm. Biopharm. 134, 29–36. https://doi.org/10.1016/j.ejpb.2018.11.008

El Aita, I., Rahman, J., Breitkreutz, J., Quodbach, J., 2020. 3D-Printing with precise layer-wise dose adjustments for paediatric use via pressure-assisted microsyringe printing. Eur. J. Pharm. Biopharm. 157, 59–65. https://doi.org/10.1016/j.ejpb.2020.09.012

Elbadawi, M., Nikjoo, D., Gustafsson, T., Gaisford, S., Basit, A.W., 2021. Pressure-assisted microsyringe 3D printing of oral films based on pullulan and hydroxypropyl methylcellulose. Int. J. Pharm. 595, 120197.

Faes, M., Valkenaers, H., Vogeler, F., Vleugels, J., Ferraris, E., 2015. Extrusion-based 3D printing of ceramic components. Procedia CIRP 28, 76–81. https://doi.org/10.1016/j.procir.2015.04.028

Falconer, J.R., Steadman, K.J., 2017. Extemporaneously compounded medicines. Aust. Prescr. 40, 5–8.

Fanous, M., Gold, S., Muller, S., Hirsch, S., Ogorka, J., 2020. Simplification of fused deposition modeling 3D-printing paradigm: Feasibility of 1-step direct powder printing for immediate release dosage form production. Int. J. Pharm. 578, 119124. https://doi.org/10.1016/j.ijpharm.2020.119124

FDA, 2020. Table of Pharmacogenetic Associations [WWW Document]. URL https://www.fda.gov/medical-devices/precision-medicine/table-pharmacogenetic-associations (accessed 3.5.21).

Fina, F., Goyanes, A., Madla, C.M., Awad, A., Trenfield, S.J., Kuek, J.M., Patel, P., Gaisford, S., Basit, A.W., 2018a. 3D printing of drug-loaded gyroid lattices using selective laser sintering. Int. J. Pharm. 547, 44–52. https://doi.org/10.1016/j.ijpharm.2018.05.044

Fina, F., Madla, C.M., Goyanes, A., Zhang, J., Gaisford, S., Basit, A.W., 2018b. Fabricating 3D printed orally disintegrating printlets using selective laser sintering. Int. J. Pharm. 541, 101–107. https://doi.org/10.1016/j.ijpharm.2018.02.015

Florence, A.T., Lee, V.H.L., 2011. Personalised medicines: More tailored drugs, more tailored delivery. Int. J. Pharm. 415, 29–33. https://doi.org/10.1016/j.ijpharm.2011.04.047

Forough, A.S., Lau, E.T.L., Steadman, K.J., Cichero, J.A.Y., Kyle, G.J., 2018. A spoonful of sugar helps the medicine go down? A review of strategies for making pills easier to swallow. Patient Prefer. Adherence 12, 1337–1346.

Fu, J., Yu, X., Jin, Y., 2018. 3D printing of vaginal rings with personalized shapes for controlled release of progesterone. Int. J. Pharm. 539, 75–82. https://doi.org/10.1016/j.ijpharm.2018.01.036

Fubini, G., 1907. Sugli integrali multipli. Accad. dei Lincei, Rend. V. Ser. (5) 16, 608–614.

Galande, A.D., Khurana, N.A., Mutalik, S., 2020. Pediatric dosage forms – challenges and recent developments: A critical review. J. Appl. Pharm. Sci. 10, 155–166. https://doi.org/10.7324/JAPS.2020.10718

Gambhir, S.S., Ge, T.J., Vermesh, O., Spitler, R., 2018. Toward achieving precision health. Sci. Transl. Med. 10.

Gao, T., Gillispie, G.J., Copus, J.S., Asari, A.K.P.R., Seol, Y.-J., Atala, A., Yoo, J.J., Lee, S.J.J., 2018. Optimization of gelatin-alginate composite bioink printability using rheological parameters: a systematic approach. Biofabrication 10. https://doi.org/10.1088/1758-5090/aacdc7

Garay, J.P., Gray, J.W., 2012. Omics and therapy - A basis for precision medicine. Mol. Oncol. 6, 128–139. https://doi.org/10.1016/j.molonc.2012.02.009

Garcia, J., Yang, Z., Mongrain, R., Leask, R.L., Lachapelle, K., 2018. 3D printing materials and their use in medical education: a review of current technology and trends for the future. BMJ Simul. Technol. Enhanc. Learn. 4, 27–40. https://doi.org/10.1136/bmjstel-2017-000234

Giacomelli, R., Afeltra, A., Bartoloni, E., Berardicurti, O., Bombardieri, M., Bortoluzzi, A., Carubbi, F., Caso, F., Cervera, R., Ciccia, F., Cipriani, P., Coloma-baz, E., Conti, F., Costa, L., Angelo, S.D., Distler, O., Feist, E., Foulquier, N., Gabini, M., Gerber, V., Gerli, R., Daniela, R., Guggino, G., Hoxha, A., Iagnocco, A., Jordan, S., Kahaleh, B., Lauper, K., Liakouli, V., Lubrano, E., Margiotta, D., Naty, S., Navarini, L., Perosa, F., Perricone, C., Perricone, R., Prete, M., Pers, J., Pitzalis, C., Priori, R., Rivellese, F., Ruffatti, A., Ruscitti, P., Scarpa, R., Shoenfeld, Y., Triolo, G., 2021. The growing role of precision medicine for the treatment of autoimmune diseases ; results of a systematic review of literature and Experts ' Consensus. Autoimmun. Rev. 20. https://doi.org/10.1016/j.autrev.2020.102738

Giangiacomo, R., 2006. Study of water – sugar interactions at increasing sugar concentration by NIR spectroscopy. Food Chem. 96, 371–379. https://doi.org/10.1016/j.foodchem.2005.02.051

Giri, B.R., Song, E.S., Kwon, J., Lee, J., Park, J., 2020. Fabrication of Intragastric Floating, Controlled Release 3D Printed Theophylline Tablets Using Hot-Melt Extrusion and Fused Deposition Modeling. Pharmaceutics 12, 77.

Gladman, A.S., Matsumoto, E.A., Nuzzo, R.G., Mahadevan, L., Lewis, J.A., 2016. Biomimetic 4D printing. Nat. Mater. 15. https://doi.org/10.1038/NMAT4544

Govender, R., Abrahmsen-Alami, S., Folestad, S., Larsson, A., 2020. High Content Solid Dispersions for Dose Window Extension: A Basis for Design Flexibility in Fused Deposition Modelling. Pharm. Res. 37, 9.

Goyanes, A., Allahham, N., Trenfield, S.J., Stoyanov, E., Gaisford, S., Basit, A.W., 2019. Direct powder extrusion 3D printing: Fabrication of drug products using a

novel single-step process. Int. J. Pharm. 567. https://doi.org/10.1016/j.ijpharm.2019.118471
Goyanes, A., Buanz, A.B.M., Hatton, G.B., Gaisford, S., Basit, A.W., 2015a. 3D printing of modified-release aminosalicylate (4-ASA and 5-ASA) tablets. Eur. J. Pharm. Biopharm. 89, 157–162. https://doi.org/10.1016/j.ejpb.2014.12.003
Goyanes, A., Det-amornrat, U., Wang, J., Basit, A.W., Gaisford, S., 2016. 3D scanning and 3D printing as innovative technologies for fabricating personalized topical drug delivery systems. J. Control. Release 234, 41–48. https://doi.org/10.1016/j.jconrel.2016.05.034
Goyanes, A., Robles, P., Buanz, A., Basit, A.W., Gaisford, S., 2015b. Effect of geometry on drug release from 3D printed tablets. Int. J. Pharm. 494, 657–663. https://doi.org/10.1016/j.ijpharm.2015.04.069
Gray, I.D., Kross, A.R., Hlthed, G., Renfrew, M.E., 2019. Precision Medicine in Lifestyle Medicine: The Way of the Future ? Am. J. Lifestyle Med. 14, 169–186. https://doi.org/10.1177/1559827619834527
Grießmann, K., Breitkreutz, J., Schubert-Zsilavecz, M., Abdel-Tawab, M., 2007. Dosing accuracy of measuring devices provided with antibiotic oral suspensions. Paediatr. Perinat. Drug Ther. 8. https://doi.org/10.1185/146300907X178950
Groll, J., Boland, T., Blunk, T., Burdick, J.A., Cho, D.-W., Dalton, P.D., Derby, B., Forgacs, G., Li, Q., Mironov, V.A., Moroni, L., Nakamura, M., Shu, W., Takeuchi, S., Vozzi, G., Woodfield, T.B.F., Xu, T., Yoo, J.J., Malda, J., 2016. Biofabrication: reappraising the definition of an evolving field. Biofabrication 8, 013001.
Guerra, A.J., Ciurana, J., 2018. 3D-printed bioabsordable polycaprolactone stent: The effect of process parameters on its physical features. Mater. Des. 137, 430–437. https://doi.org/10.1016/j.matdes.2017.10.045
Habib, A., Sathish, V., Mallik, S., Khoda, B., 2018. 3D printability of alginate-carboxymethyl cellulose hydrogel. Materials (Basel). 11. https://doi.org/10.3390/ma11030454
Hakkarainen, E., Kõrkjas, A., Laidmäe, I., Lust, A., Semjonov, K., Kogermann, K., Nieminen, H.J., Salmi, A., Korhonen, O., Haeggström, E., Heinämäki, J., 2019. Comparison of Traditional and Ultrasound-Enhanced Electrospinning in Fabricating Nanofibrous Drug Delivery Systems. Pharmaceutics 11, 495.
Haleem, A., Javaid, M., 2019. 3D scanning applications in medical field: A literature-based review. Clin. Epidemiol. Glob. Heal. 7, 199–210. https://doi.org/10.1016/j.cegh.2018.05.006
Hamamoto, R., Suvarna, K., Yamada, M., Kobayashi, K., Shinkai, N., Miyake, M., Takahashi, M., Jinnai, S., Shimoyama, R., Sakai, A., Takasawa, K., Bolatkan, A., Shozu, K., Dozen, A., Machino, H., Takahashi, S., Asada, K., Komatsu, M., Sese, J., Kaneko, S., 2020. Application of Artificial Intelligence Technology in Oncology: Towards the Establishment of Precision Medicine. Cancers (Basel). 12, 3532.
Han, Y.L., Hu, J., Genin, G.M., Lu, T.J., Xu, F., 2014. BioPen: direct writing of functional materials at the point of care. Sci. Rep. 4, 4872. https://doi.org/10.1038/srep04872
Haywood, A., Glass, B.D., 2013. Liquid Dosage Forms Extemporaneously Prepared from Commercially Available Products – Considering New Evidence on Stability. J. Pharm. Pharm. Sci. 16, 441–455.
He, Y., Yang, F., Zhao, H., Gao, Q., Xia, B., Fu, J., 2016. Research on the printability of hydrogels in 3D bioprinting. Sci. Rep. 6, 29977. https://doi.org/10.1038/srep29977

Hekler, E., Tiro, J.A., Hunter, C.M., Nebeker, C., 2020. Precision Health: The Role of the Social and Behavioral Sciences in Advancing the Vision. Ann. Behav. Med. 54, 805–826. https://doi.org/10.1093/abm/kaaa018

Hennink, W.E., Nostrum, C.F. Van, 2002. Novel crosslinking methods to design hydrogels. Adv. Drug Deliv. Rev. 54, 13–36. https://doi.org/10.1016/j.addr.2012.09.009

Herzberger, J., Niederer, K., Pohlit, H., Seiwert, J., Worm, M., Wurm, F.R., Frey, H., 2015. Polymerization of Ethylene Oxide, Propylene Oxide, and Other Alkylene Oxides: Synthesis, Novel Polymer Architectures, and Bioconjugation. https://doi.org/10.1021/acs.chemrev.5b00441

Ho, D., Quake, S.R., Mccabe, E.R.B., Chng, W.J., Chow, E.K., Ding, X., Gelb, B.D., Ginsburg, G.S., Hassenstab, J., Ho, C., 2019. Enabling Technologies for Personalized and Precision Medicine. Trends Biotechnol. 38, 497–518. https://doi.org/10.1016/j.tibtech.2019.12.021

Holländer, J., Genina, N., Jukarainen, H., Khajeheian, M., Rosling, A., Mäkilä, E., Sandler, N., 2016. Three-Dimensional Printed PCL-Based Implantable Prototypes of Medical Devices for Controlled Drug Delivery. J. Pharm. Sci. 105, 2665–2676. https://doi.org/10.1016/j.xphs.2015.12.012

Huang, S.H., Liu, P., Mokasdar, A., 2013. Additive manufacturing and its societal impact: a literature review. Int. J. Adv. Manuf. Technol. 67, 1191–1203. https://doi.org/10.1007/s00170-012-4558-5

Hull, C.W., 1986. Apparatus for Production of Three-dimensional Objects by Stereolithography. 4575330.

Hulsen, T., Jamuar, S.S., Moody, A.R., Karnes, J.H., Varga, O., Hedensted, S., Spreafico, R., Hafler, D.A., Mckinney, E.F., 2019. From Big Data to Precision Medicine. Front. Med. 6, 39. https://doi.org/10.3389/fmed.2019.00034

Hung, K.C., Tseng, C.S., Hsu, S.H., 2014. Synthesis and 3D Printing of biodegradable polyurethane elastomer by a water-based process for cartilage tissue engineering applications. Adv. Healthc. Mater. 3, 1578–1587. https://doi.org/10.1002/adhm.201400018

Huri, E., Mourad, S., Bhide, A., Digesu, G.A., 2020. 3D modeling and 3D printing in functional urology: the future perspective. Int. Urogynecol. J. 31, 1977–1978.

ISO/ASTM 52900:2015 Standard Terminology for Additive Manufacturing – General Principles – Terminology, 2015.

Isreb, A., Baj, K., Wojsz, M., Isreb, M., Peak, M., 2019. 3D printed oral theophylline doses with innovative ‘ radiator-like ’ design: Impact of polyethylene oxide (PEO) molecular weight. Int. J. Pharm. 564, 98–105. https://doi.org/10.1016/j.ijpharm.2019.04.017

Jakic, M., Stipanelov, N., Klaric, I., 2013. Thermal degradation of poly (vinyl chloride)/ poly (ethylene oxide) blends: Thermogravimetric analysis. Polym. Degrad. Stab. 98, 1738–1743. https://doi.org/10.1016/j.polymdegradstab.2013.05.024

Jamróz, W., Szafraniec, J., Kurek, M., Jachowicz, R., 2018. 3D Printing in Pharmaceutical and Medical Applications – Recent Achievements and Challenges. Pharm. Res. 35, 176. https://doi.org/10.1007/s11095-018-2454-x

Jeong, I., Bychkov, D., Searson, P.C., 2019. Wearable Devices for Precision Medicine and Health State Monitoring. IEEE Trans. Biomed. Eng. 66, 1242–1258.

Joshi, S., Rawat, K., Karunakaran, C., Rajamohan, V., Tom, A., Koziol, K., Kumar, V., Balan, A.S.S., 2020. 4D printing of materials for the future: Opportunities and

challenges. Appl. Mater. Today 18, 100490. https://doi.org/10.1016/j.apmt.2019.100490
Joshi, S.C., 2011. Sol-Gel Behavior of Hydroxypropyl Methylcellulose (HPMC) in Ionic Media Including Drug Release. Materials (Basel). 4, 1861–1905. https://doi.org/10.3390/ma4101861
Jurkin, T., Pucić, I., 2012. Poly (ethylene oxide) irradiated in the solid state, melt and aqueous solution — a DSC and WAXD study. Radiat. Phys. Chem. 81, 1303–1308. https://doi.org/10.1016/j.radphyschem.2011.12.021
Kadushin, R., 2011. Bearina IUD Concept [WWW Document]. URL https://www.ronen-kadushin.com/bearina-iud-concept (accessed 3.6.21).
Karmwar, P., Graeser, K., Gordon, K.C., Strachan, C.J., Rades, T., 2011. Investigation of properties and recrystallisation behaviour of amorphous indomethacin samples prepared by different methods. Int. J. Pharm. 417, 94–100. https://doi.org/10.1016/j.ijpharm.2010.12.019
Kempin, W., Domsta, V., Grathoff, G., Brecht, I., Semmling, B., Tillmann, S., Weitschies, W., Seidlitz, A., 2018. Immediate Release 3D-Printed Tablets Produced Via Fused Deposition Modeling of a Thermo-Sensitive Drug. Pharm. Res. 35.
Kempin, W., Franz, C., Koster, L., Schneider, F., Bogdahn, M., Weitschies, W., Seidlitz, A., 2017. Assessment of different polymers and drug loads for fused deposition modeling of drug loaded implants. Eur. J. Pharm. Biopharm. 115, 84–93. https://doi.org/10.1016/j.ejpb.2017.02.014
Khaled, Shaban A., Burley, J.C., Alexander, M.R., Yang, J., Roberts, C.J., 2015. 3D printing of tablets containing multiple drugs with defined release profiles. Int. J. Pharm. 494, 643–650. https://doi.org/10.1016/j.ijpharm.2015.07.067
Khaled, Shaban A, Burley, J.C., Alexander, M.R., Yang, J., Roberts, C.J., 2015. 3D printing of five-in-one dose combination polypill with defined immediate and sustained release profiles. J. Control. Release 217, 308–314. https://doi.org/10.1016/j.jconrel.2015.09.028
Khoury, M.J., Iademarco, M.F., Riley, W.T., Sciences, P., Service, P.H., Corps, C., Precision, T., Initiative, M., 2016. Precision Public Health for the Era of Precision Medicine. Am. J. Prev. Med. 50, 398–401. https://doi.org/10.1016/j.amepre.2015.08.031.Precision
Kolesky, D.B., Truby, R.L., Gladman, A.S., Busbee, T.A., Homan, K.A., Lewis, J.A., 2014. 3D bioprinting of vascularized, heterogeneous cell-laden tissue constructs. Adv. Mater. 26, 3124–3130. https://doi.org/10.1002/adma.201305506
Kollamaram, G., Croker, D.M., Walker, G.M., Goyanes, A., Basit, A.W., Gaisford, S., 2018. Low temperature fused deposition modeling (FDM) 3D printing of thermolabile drugs. Int. J. Pharm. 545, 144–152. https://doi.org/10.1016/j.ijpharm.2018.04.055
Kyle, S., Jessop, Z.M., Al-Sabah, A., Whitaker, I.S., 2017. 'Printability'' of Candidate Biomaterials for Extrusion Based 3D Printing: State-of-the-Art.' Adv. Healthc. Mater. 6, 1–16. https://doi.org/10.1002/adhm.201700264
Kyobula, M., Adedeji, A., Alexander, M.R., Saleh, E., Wildman, R., Ashcroft, I., Gellert, P.R., Roberts, C.J., 2017a. 3D inkjet printing of tablets exploiting bespoke complex geometries for controlled and tuneable drug release. J. Control. Release 261, 207–215. https://doi.org/10.1016/j.jconrel.2017.06.025
Kyobula, M., Adedeji, A., Alexander, M.R., Saleh, E., Wildman, R., Ashcroft, I., Gellert, P.R., Roberts, C.J., 2017b. 3D inkjet printing of tablets exploiting bespoke

complex geometries for controlled and tuneable drug release. J. Control. Release 261, 207–215. https://doi.org/10.1016/j.jconrel.2017.06.025
Landsteiner, K., Levine, P., 1927. A New Agglutinable Factor Differentiating Individual Human Bloods. Proc. Soc. Exp. Biol. Med. 24, 600–602.
Lanno, G.-M., Ramos, C., Preem, L., Putriņš, M., Laidmäe, I., Tenson, T., Kogermann, K., 2020. Antibacterial Porous Electrospun Fibers as Skin Scaffolds for Wound Healing Applications. ACS Omega 5, 30011–30022. https://doi.org/10.1021/acsomega.0c04402
Lao, L.L., Venkatraman, S.S., Peppas, N.A., 2008. Modeling of drug release from biodegradable polymer blends. Eur. J. Pharm. Biopharm. 70, 796–803. https://doi.org/10.1016/j.ejpb.2008.05.024
Lee, J.M., Sing, S.L., Zhou, M., Yeong, W.Y., 2018. 3D bioprinting processes: A perspective on classification and terminology. Int. J. Bioprinting 4, 1–10.
Lee, M. Van Der, Kriek, M., Guchelaar, H., 2020. Technologies for Pharmacogenomics: A Review. Genes (Basel). 11, 1456.
Lerdkanchanaporn, S., Dollimore, D., 1997. A Thermal Analysis Study of Ibuprofen. J. Therm. Anal. 49, 879–886.
Li, H., Liu, S., Lin, L., 2016. Rheological study on 3D printability of alginate hydrogel and effect of graphene oxide. Int. J. Bioprinting 2, 10–12. https://doi.org/10.18063/IJB.2016.02.007
Li, X., Warner, J.L., Petty, H.R., Carter, A., Warner, J.L., 2020. A Review of Precision Oncology Knowledgebases for Determining the Clinical Actionability of Genetic Variants. Front. Cell Dev. Biol. 8, 1–8. https://doi.org/10.3389/fcell.2020.00048
Lille, M., Nurmela, A., Nordlund, E., Metsä-Kortelainen, S., Sozer, N., 2018. Applicability of protein and fiber-rich food materials in extrusion-based 3D printing. J. Food Eng. 220, 20–27. https://doi.org/10.1016/j.jfoodeng.2017.04.034
Lin, A.Y., Yarholar, L.M., 2020. Plastic Surgery Innovation with 3D Printing for Craniomaxillofacial Operations. Mo. Med. 117.
Lin, H., Hsu, P., Lin, S., 2013. Theophylline e citric acid co-crystals easily induced by DSC e FTIR microspectroscopy or different storage conditions. Asian J. Pharm. Sci. 8, 19–27. https://doi.org/10.1016/j.ajps.2013.07.003
Lin, L., Fang, Y., Liao, Y., Chen, G., Gao, C., Zhu, P., 2019. 3D Printing and Digital Processing Techniques in Dentistry: A Review of Literature. Adv. Eng. Mater. 21, 1801013. https://doi.org/10.1002/adem.201801013
Liu, Z., Zhang, M., Bhandari, B., Wang, Y., 2017. 3D printing: Printing precision and application in food sector. Trends Food Sci. Technol. 69, 83–94. https://doi.org/10.1016/j.tifs.2017.08.018
Long, N.P., Nghi, T.D., Kang, Y.P., Anh, N.H., Kim, H.M., Park, S.K., Kwon, S.W., 2018. Toward a Standardized Strategy of Clinical Metabolomics for the Advancement of Precision Medicine. Metabolites 10, 50.
Luo, H., Meyer-Szary, J., Wang, Z., Sabiniewicz, R., Liu, Y., 2017. Three-dimensional printing in cardiology: Current applications and future challenges. Cardiol. J. 24, 436–444. https://doi.org/10.5603/CJ.a2017.0056
Lynch, T., Price, A., 2007. The Effect of Cytochrome P450 Metabolism on Drug Response, Interactions, and Adverse Effects. Am. Fam. Physician 76.
Melocchi, A., Briatico-Vangosa, F., Uboldi, M., Parietti, F., Turchi, M., Zeppelin, D. Von, Maroni, A., Zema, L., Gazzaniga, A., Zidan, A., 2021. Quality considerations on the pharmaceutical applications of fused deposition modeling 3D printing. Int. J. Pharm. 592, 119901. https://doi.org/10.1016/j.ijpharm.2020.119901

Melocchi, A., Parietti, F., Maroni, A., Foppoli, A., Gazzaniga, A., Zema, L., 2016. Hot-melt extruded filaments based on pharmaceutical grade polymers for 3D printing by fused deposition modeling. Int. J. Pharm. 509, 255–263. https://doi.org/10.1016/j.ijpharm.2016.05.036

Melocchi, A., Uboldi, M., Cerea, M., Foppoli, A., Maroni, A., Moutaharrik, S., Palugan, L., Zema, L., Gazzaniga, A., 2020a. A Graphical Review on the Escalation of Fused Deposition Modeling (FDM) 3D Printing in the Pharmaceutical Field. J. Pharm. Sci. 109, 2943–2957. https://doi.org/10.1016/j.xphs.2020.07.011

Melocchi, A., Uboldi, M., Maroni, A., Foppoli, A., Palugan, L., Zema, L., Gazzaniga, A., 2020b. 3D printing by fused deposition modeling of single- and multi-compartment hollow systems for oral delivery – A review. Int. J. Pharm. 579, 119155. https://doi.org/10.1016/j.ijpharm.2020.119155

Meruva, S., Donovan, M.D., 2020. Polyethylene Oxide (PEO) Molecular Weight Effects on Abuse-Deterrent Properties of Matrix Tablets. AAPS PharmSciTech 21, 28. https://doi.org/10.1208/s12249-019-1565-y

Mills, P.A.S., Mills, D.K., 2020. Reduced Supply in the Organ Donor Market and How 3D Printing Can Address This Shortage: A Critical Inquiry into the Collateral E ff ects of Driverless Cars. Appl. Sci. 10, 6400.

Mistry, P., Batchelor, H., 2017. Methodology Used to Assess Acceptability of Oral Pediatric Medicines: A Systematic Literature Search and Narrative Review. Pediatr. Drugs 19, 223–233. https://doi.org/10.1007/s40272-017-0223-7

Momeni, F., N, S.M.M.H., Liu, X., Ni, J., 2017. A review of 4D printing. Mater. Des. 122, 42–79. https://doi.org/10.1016/j.matdes.2017.02.068

Moroni, L., Boland, T., Burdick, J.A., Maria, C. De, Derby, B., Forgacs, G., Groll, J., Li, Q., Malda, J., Mironov, V.A., Mota, C., Nakamura, M., Shu, W., Takeuchi, S., Wood, T.B.F., Xu, T., 2018. Biofabrication: A Guide to Technology and Terminology. Trends Biotechnol. 36, 384–402. https://doi.org/10.1016/j.tibtech.2017.10.015

Munoz-Abraham, A.S., Rodriguez-Davalos, M.I., Bertacco, A., Wengerter, B., Geibel, J.P., Mulligan, D.C., 2016. 3D Printing of Organs for Transplantation: Where Are We and Where Are We Heading ? Curr. Transplantantion Reports 3, 93–99. https://doi.org/10.1007/s40472-016-0089-6

Murphy, G.A., Leeke, M.J., Jenkins, S.H., 2012. A Comparison of the use of FTIR spectroscopy with DSC in the characterisation of melting and crystallisation in polycaprolactone. J. Therm. Anal. Calorim. 107, 669–674. https://doi.org/10.1007/s10973-011-1771-7

Mutie, P.M., Giordano, G.N., Franks, P.W., 2017. Lifestyle precision medicine: the next generation in type 2 diabetes prevention? BMC Med. 15, 171. https://doi.org/10.1186/s12916-017-0938-x

Muwaffak, Z., Goyanes, A., Clark, V., Basit, A.W., Hilton, S.T., Gaisford, S., 2017. Patient-speci fi c 3D scanned and 3D printed antimicrobial polycaprolactone wound dressings. Int. J. Pharm. 527, 161–170. https://doi.org/10.1016/j.ijpharm.2017.04.077

Nasereddin, J.M., Wellner, N., Alhijjaj, M., Belton, P., Qi, S., 2018. Development of a Simple Mechanical Screening Method for Predicting the Feedability of a Pharmaceutical FDM 3D Printing Filament. Pharm. Res. 35, 151.

National Research Council, 2011. Toward Precision Medicine: Building a Knowledge Network for Biomedical Research and a New Taxonomy of Disease. The National Academies Press, Washington, DC. https://doi.org/10.17226/13284

Nellis, G., Metsvaht, T., Varendi, H., Lass, J., Duncan, J., 2016. Product Substitution as a Way Forward in Avoiding Potentially Harmful Excipients in Neonates. Pediatr. Drugs 18, 221–230. https://doi.org/10.1007/s40272-016-0173-5

Ning, L., Yang, B., Mohabatpour, F., Betancourt, N., 2020. Process-induced cell damage: pneumatic versus screw-driven bioprinting Process-induced cell damage: pneumatic versus screw-driven bioprinting. Biofabrication 12, 025011.

Nokhodchi, A., Okwudarue, O.N., Valizadeh, H., Momin, M.N., 2009. Cogrinding as a Tool to Produce Sustained Release Behavior for Theophylline Particles Containing Magnesium Stearate. AAPS PharmSciTech 10. https://doi.org/10.1208/s12249-009-9326-y

Noor, S.A.M., Ahmad, A., Talib, I.A., Rahman, M.Y.A., 2011. Effect of ZnO nanoparticles filler concentration on the properties of PEO-ENR50-LiCF 3 SO 3 solid polymeric electrolyte. Ionics (Kiel). 451–456. https://doi.org/10.1007/s11581-011-0534-6

Norman, J., Madurawe, R.D., Moore, C.M. V, Khan, M.A., Khairuzzaman, A., 2016. A new chapter in pharmaceutical manufacturing: 3D-printed drug products ☆, ☆☆.

Ojarinta, R., Heikkinen, A.T., Sievänen, E., Laitinen, R., 2017. Dissolution behavior of co-amorphous amino acid-indomethacin mixtures: The ability of amino acids to stabilize the supersaturated state of indomethacin. Eur. J. Pharm. Biopharm. 112, 85–95. https://doi.org/10.1016/j.ejpb.2016.11.023

Okwuosa, T.C., Stefaniak, D., Arafat, B., Isreb, A., Wan, K.W., Albed Alhnan, M., 2016. Article A Lower Temperature FDM 3D Printing for the Manufacture of Patient – Specific Immediate Release Tablets. Pharm. Res. 33, 2704–2712.

Oladapo, B.I., Ismail, S.O., Afolalu, T.D., Olawade, D.B., 2021. Review on 3D printing: Fight against COVID-19. Mater. Chem. Phys. 258, 123943. https://doi.org/10.1016/j.matchemphys.2020.123943

Olewnik-Kruszkowska, E., Kasperska, P., Koter, I., 2016. Effect of poly (ε-caprolactone) as plasticizer on the properties of composites based on polylactide during hydrolytic degradation. React. Funct. Polym. 103, 99–107. https://doi.org/10.1016/j.reactfunctpolym.2016.03.026

Olivier, M., Asmis, R., Hawkins, G.A., Howard, T.D., Cox, L.A., 2019. The Need for Multi-Omics Biomarker Signatures in Precision Medicine. Int. J. Mol. Sci. 20, 4781.

Oropallo, W., Piegl, L.A., 2016. Ten challenges in 3D printing. Eng. Comput. 32, 135–148. https://doi.org/10.1007/s00366-015-0407-0

Ouyang, L., Yao, R., Zhao, Y., Sun, W., 2016. Effect of bioink properties on printability and cell viability for 3D bioplotting of embryonic stem cells. Biofabrication 8.

Ozbolat, I.T., Hospodiuk, M., 2016. Current advances and future perspectives in extrusion-based bioprinting. Biomaterials. https://doi.org/10.1016/j.biomaterials.2015.10.076

Parikh, N., Sharma, P., 2018. Three-Dimensional Printing in Urology: History, Current Applications, and Future Directions. Urology 121, 3–10. https://doi.org/10.1016/j.urology.2018.08.004

Parimbelli, E., Marini, S., Sacchi, L., Bellazzi, R., 2018. Patient similarity for precision medicine: A systematic review. J. Biomed. Inform. 83, 87–96. https://doi.org/10.1016/j.jbi.2018.06.001

Patil, H., Tiwari, R. V, Repka, M.A., 2016. Hot-Melt Extrusion: from Theory to Application in Pharmaceutical Formulation. AAPS PharmSciTech 17, 20–42. https://doi.org/10.1208/s12249-015-0360-7

Paul, G.M., Rezaienia, A., Wen, P., Condoor, S., Parkar, N., King, W., Korakianitis, T., 2018. Medical Applications for 3D Printing: Recent Developments. Mo. Med. 115, 75–81.

Paxton, N., Smolan, W., Böck, T., Melchels, F., Groll, J., Jungst, T., 2017. Proposal to assess printability of bioinks for extrusion-based bioprinting and evaluation of rheological properties governing bioprintability. Biofabrication 9, 044107. https://doi.org/10.1088/1758-5090/aa8dd8

Phadnis, N. V., Suryanarayanan, R., 1997. Polymorphism in Anhydrous Theophylline - Implications on the Dissolution Rate of Theophylline Tablets. J. Pharm. Sci. 86, 1256–1263.

Pietrzak, K., Isreb, A., Alhnan, M.A., 2015. A flexible-dose dispenser for immediate and extended release 3D printed tablets. Eur. J. Pharm. Biopharm. 96, 380–387. https://doi.org/10.1016/j.ejpb.2015.07.027

Piyush, Kumar, Raman, Kumar, Ranvijay, 2020. 3D printing of food materials: A state of art review and future applications. Mater. Today Proc. 33, 1463–1467. https://doi.org/10.1016/j.matpr.2020.02.005

Postiglione, G., Natale, G., Griffini, G., Levi, M., Turri, S., 2015. Conductive 3D microstructures by direct 3D printing of polymer/carbon nanotube nanocomposites via liquid deposition modeling. Compos. Part A Appl. Sci. Manuf. 76, 110–114. https://doi.org/10.1016/j.compositesa.2015.05.014

Preem, L., Mahmoudzadeh, M., Putrinš, M., Meos, A., Laidmäe, I., Romann, T., Aruväli, J., Härmas, R., Koivuniemi, A., Bunker, A., Tenson, T., Kogermann, K., 2017. Interactions between Chloramphenicol, Carrier Polymers, and Bacteria − Implications for Designing Electrospun Drug Delivery Systems Countering Wound Infection. Mol. Pharm. 14, 4417–4430. https://doi.org/10.1021/acs.molpharmaceut.7b00524

Prendergast, M.E., Burdick, J.A., 2020. Recent Advances in Enabling Technologies in 3D Printing for Precision Medicine. Adv. Mater. 32, 1902516. https://doi.org/10.1002/adma.201902516

Pugliese, L., Marconi, S., Negrello, E., Mauri, V., Peri, A., Gallo, V., Auricchio, F., Pietrabissa, A., 2018. The clinical use of 3D printing in surgery. Updates Surg. 70, 381–388. https://doi.org/10.1007/s13304-018-0586-5

Ramanath, H.S., Chua, C.K., Leong, K.F., Shah, K.D., 2008. Melt flow behaviour of poly-e-caprolactone in fused deposition modelling. J. Mater. Sci. Mater. Med. 19, 2541–2550. https://doi.org/10.1007/s10856-007-3203-6

Ramos, C., Lanno, G.-M., Laidmäe, I., Meos, A., Härmas, R., Kogermann, K., 2021. High humidity electrospinning of porous fibers for tuning the release of drug delivery systems. Int. J. Polym. Mater. Polym. Biomater. 70, 880–892. https://doi.org/ 10.1080/00914037.2020.1765361

Ranmal, S., Tuleu, C., 2013. Demonstrating Evidence of Acceptability: The “Catch-22” of Pediatric Formulation Development. Clin. Pharmacol. Ther. 94, 582–584. https://doi.org/10.1038/clpt.2013.154

Rayna, T., Striukova, L., 2016. Technological Forecasting & Social Change From rapid prototyping to home fabrication: How 3D printing is changing business model innovation. Technol. Forecast. Soc. Chang. 102, 214–224. https://doi.org/10.1016/j.techfore.2015.07.023

Renterghem, J. Van, Vervaet, C., Beer, T. De, 2017. Rheological Characterization of Molten Polymer-Drug Dispersions as a Predictive Tool for Pharmaceutical Hot-Melt

Extrusion Processability. Pharm. Res. 34, 2312–2321. https://doi.org/10.1007/s11095-017-2239-7
Robles-Martinez, P., Xu, X., Trenfield, S.J., Awad, A., Goyanes, A., Telford, R., Basit, A.W., Gaisford, S., 2019. 3D Printing of a Multi-Layered Polypill Containing Six Drugs Using a Novel Stereolithographic Method. Pharmaceutics 11, 274.
Rocha, C.R., Torrado Perez, A.R., Roberson, D.A., Shemelya, C.M., Macdonald, E., Wicker, R.B., 2014. Novel ABS-based binary and ternary polymer blends for material extrusion 3D printing. J. Mater. Res. 29, 1859–1866. https://doi.org/10.1557/jmr.2014.158
Ross, J.S., Slodkowska, E.A., Symmans, W.F., Pusztal, L., Ravdin, P.M., Hortobagyi, G.N., 2009. The HER-2 Receptor and Breast Cancer: Ten Years of Targeted Anti–HER-2 Therapy and Personalized Medicine. Oncologist 14, 320–368. https://doi.org/10.1634/theoncologist.2008-0230
Sadia, M., Arafat, B., Ahmed, W., Forbes, R.T., Alhnan, M.A., 2018. Channelled tablets: An innovative approach to accelerating drug release from 3D printed tablets. J. Control. Release 269, 355–363. https://doi.org/10.1016/j.jconrel.2017.11.022
Samad, Y.A., Asghar, A., Hashaikeh, R., 2013. Electrospun cellulose / PEO fi ber mats as a solid polymer electrolytes for Li ion batteries. Renew. Energy 56, 90–95. https://doi.org/10.1016/j.renene.2012.09.015
Schiele, J.T., Quinzler, R., Klimm, H.-D., 2013. Difficulties swallowing solid oral dosage forms in a general practice population: prevalence, causes, and relationship to dosage forms. Eur. J. Clin. Pharmacol. 69, 937–948. https://doi.org/10. 1007/s00228-012-1417-0
Schilling, S.U., Shah, N.H., Malick, A.W., Infeld, M.H., Mcginity, J.W., 2007. Citric acid as a solid-state plasticizer for Eudragit RS PO. J. Pharm. Pharmacol. 59, 1493–1500. https://doi.org/10.1211/jpp.59.11.0005
Shaikh, R., Walker, G.M., Croker, D.M., 2019. Continuous, simultaneous cocrystallization and formulation of Theophylline and 4-Aminobenzoic acid pharmaceutical cocrystals using twin screw melt granulation. Eur. J. Pharm. Sci. 137, 104981. https://doi.org/10.1016/j.ejps.2019.104981
Siepmann, F., Brun, V. Le, Siepmann, J., 2006. Drugs acting as plasticizers in polymeric systems: A quantitative treatment. J. Control. Release 115, 298–306. https://doi.org/10.1016/j.jconrel.2006.08.016
Simões, M.F., Pinto, R.M.A., Simões, S., 2019. Hot-melt extrusion in the pharmaceutical industry: toward filing a new drug application. Drug Discov. Today 24, 1749–1768. https://doi.org/10.1016/j.drudis.2019.05.013
Skrdla, P.J., Floyd, P.D., Dell'ocro, P.C., 2016. Practical Estimation of Amorphous Solubility Enhancement Using Thermoanalytical Data: Determination of the Amorphous / Crystalline Solubility Ratio for Pure Indomethacin and Felodipine. J. Pharm. Sci. 105, 2625–2630. https://doi.org/10.1016/j.xphs.2016.03.036
Sreekala, P., Suresh, M., Priyadarsini, S.L., 2020. Proceedings 3D organ printing: Review on operational challenges and constraints. Mater. Today Proc. 33, 4703–4707. https://doi.org/10.1016/j.matpr.2020.08.349
Stegemann, S., Gosch, M., Breitkreutz, J., 2012. Swallowing dysfunction and dysphagia is an unrecognized challenge for oral drug therapy. Int. J. Pharm. 430, 197–206. https://doi.org/10.1016/j.ijpharm.2012.04.022
Tahara, K., 2020. Pharmaceutical formulation and manufacturing using particle / powder technology for personalized medicines q. Adv. Powder Technol. 31, 387–392. https://doi.org/10.1016/j.apt.2019.10.031

Tan, D.K., Maniruzzaman, M., Nokhodchi, A., 2018. Advanced Pharmaceutical Applications of Hot-Melt Extrusion Coupled with Fused Deposition Modelling (FDM) 3D Printing for Personalised Drug Delivery. Pharmaceutics 10. https://doi.org/10.3390/pharmaceutics10040203

Tarfaoui, M., Nachtane, M., Goda, I., Qureshi, Y., Benyahia, H., 2020. 3D Printing to Support the Shortage in Personal Protective Equipment Caused by COVID-19 Pandemic. Materials (Basel). 13, 3339.

Teixeira, R.S.P., Correa, R.J., Belvino, A., Nascimento, R.S. V, 2013. UV Irradiation-Induced Crosslinking of Aqueous Solution of Poly (ethylene oxide) with Benzophenone as Initiator. J. Appl. Polym. Sci. 130, 2458–2467. https://doi.org/10.1002/app.39381

Ternik, R., Liu, F., Bartlett, J.A., Mei, Y., Cheng, D., Tan, T., Dixit, T., Wang, S., Galella, E.A., Gao, Z., Klein, S., 2018. Assessment of swallowability and palatability of oral dosage forms in children: Report from an M-CERSI pediatric formulation workshop. Int. J. Pharm. 536, 570–581. https://doi.org/10.1016/j. ijpharm. 2017.08.088

Thiry, J., Krier, F., Evrard, B., 2015. A review of pharmaceutical extrusion: Critical process parameters and scaling-up. Int. J. Pharm. 479, 227–240. https://doi.org/10.1016/j.ijpharm.2014.12.036

Tian, Y., Orlu, M., Woerdenbag, H.J., Scarpa, M., Kottke, D., Sjöholm, E., Öblom, H., Sandler, N., Wouter, L.J., Frijlink, H.W., Breitkreutz, J., Visser, J.C., Tian, Y., Orlu, M., Woerdenbag, H.J., Scarpa, M., Frijlink, W., Breitkreutz, J., Visser, J.C., 2019. Expert Opinion on Drug Delivery Oromucosal films: from patient centricity to production by printing techniques. Expert Opin. Drug Deliv. 16, 981–993. https://doi. org/10.1080/17425247.2019.1652595

Tita, B., Fulias, A., Rusu, G., Tita, D., 2009. Thermal Behaviour of Indomethacin - Active Substance and Tablets Kinetic Study Under Non-Isothermal Conditions. Rev. Chim.

Trenfield, S.J., Awad, A., Goyanes, A., Gaisford, S., Basit, A.W., 2018. 3D Printing Pharmaceuticals: Drug Development to Frontline Care. Trends Pharmacol. Sci. 1–12. https://doi.org/10.1016/j.tips.2018.02.006

Trusheim, M.R., Berndt, E.R., Douglas, F.L., 2007. Stratified medicine: strategic and economic implications of combining drugs and clinical biomarkers. Nat. Rev. Drug Discov. 6, 287–293.

Trusheim, M.R., Burgess, B., Hu, S.X., Long, T., Averbuch, S.D., Flynn, A.A., Lieftucht, A., Mazumder, A., Milloy, J., Shaw, P.M., Swank, D., Wang, J., Berndt, E.R., Goodsaid, F., Palmer, M.C., 2011. Quantifying factors for the success of stratified medicine. Nat. Rev. Drug Discov. 10, 817–833. https://doi.org/10.1038/nrd3557

Uyar, T., Besenbacher, F., 2009. Electrospinning of cyclodextrin functionalized polyethylene oxide (PEO) nanofibers. Eur. Polym. J. 45, 1032–1037. https://doi.org/10.1016/j.eurpolymj.2008.12.024

Vasarhelyi, L., Konya, Z., Kukovecz, A., Vajtai, R., 2020. Microcomputed tomography-based characterization of advanced materials: a review. Mater. Today Adv. 8, 100084. https://doi.org/10.1016/j.mtadv.2020.100084

Vo, A.Q., Zhang, J., Nyavanandi, D., Bandari, S., Repka, M.A., 2020. Hot melt extrusion paired fused deposition modeling 3D printing to develop hydroxypropyl cellulose based fl oating tablets of cinnarizine. Carbohydr. Polym. 246, 116519. https://doi.org/10.1016/j.carbpol.2020.116519

Voon, S.L., An, J., Wong, G., Zhang, Y., Chua, C.K., 2019. 3D food printing: a categorised review of inks and their development. Virtual Phys. Prototyp. 14, 203–218. https://doi.org/10.1080/17452759.2019.1603508

Vukicevic, M., Mosadegh, B., Min, J.K., Little, S.H., 2017. Cardiac 3D Printing and its Future Directions. JACC Cardiovasc. Imaging 10. https://doi.org/10.1016/j.jcmg.2016.12.001

Walsh, J., Ranmal, S.R., Ernest, T.B., Liu, F., 2018. Patient acceptability, safety and access: A balancing act for selecting age-appropriate oral dosage forms for paediatric and geriatric populations. Int. J. Pharm. 536, 547–562. https://doi.org/10.1016/j.ijpharm.2017.07.017

Wang, F., Ma, C.M., Wu, W., 2001. Thermal degradation of polyethylene oxide blended with novolac type phenolic resin. J. Mater. Sci. 36, 943–947.

Wang, G.S., Reynolds, K.M., Banner, W., Bond, G.R., Kauffman, R.E., Palmer, R.B., Paul, I.M., Rapp-olsson, M., Green, J.L., Dart, R.C., 2020. Medication Errors From Over-the-Counter Cough and Cold Medications in Children. Acad. Pediatr. 20, 327–332. https://doi.org/10.1016/j.acap.2019.09.006

Warfield, R.W., Hartmann, B., 1973. Melting and freezing behavior of polyethylene oxide. J. Appl. Phys. 44, 708–714. https://doi.org/10.1063/1.1662248

Whenham, N., Hondt, V.D., Piccart, M.J., 2008. HER2-Positive Breast Cancer: From Trastuzumab to Innovatory Anti-HER2 Strategies. Clin. Breast Cancer 8, 38–49. https://doi.org/10.3816/CBC.2008.n.002

Williams, T.A., Wolf, M.S., Parker, R.M., Sanders, L.M., Bailey, S., Mendelsohn, A.L., Dreyer, B.P., Velazquez, J.J., Yin, H.S., 2019. Parent Dosing Tool Use, Beliefs, and Access: A Health Literacy Perspective. J. Pediatr. 215, 244-251.e1. https://doi.org/10.1016/j.jpeds.2019.08.017

Willis, A., Speicher, J., Cooper, D.B., 2007. Rapid prototyping 3D objects from scanned measurement data. Image Vis. Comput. 25, 1174–1184. https://doi.org/10.1016/j.imavis.2006.06.011

Wu, C., Mcginity, J.W., 2003. Influence of methylparaben as a solid-state plasticizer on the physicochemical properties of Eudragit w RS PO hot-melt extrudates. Eur. J. Pharm. Biopharm. 56, 95–100. https://doi.org/10.1016/S0939-6411(03)00035-3

Yan, Q., Dong, H., Su, J., Han, J., Song, B., Wei, Q., Shi, Y., 2018. A Review of 3D Printing Technology for Medical Applications. Engineering 4, 729–742. https://doi.org/10.1016/J.ENG.2018.07.021

Yang, F., Zhang, M., Bhandari, B., Liu, Y., 2018. Investigation on lemon juice gel as food material for 3D printing and optimization of printing parameters. LWT - Food Sci. Technol. 87, 67–76. https://doi.org/10.1016/j.lwt.2017.08.054

Yin, H.S., Parker, R.M., Sanders, L.M., Dreyer, B.P., Mendelsohn, A.L., Bailey, S., Patel, D.A., Jimenez, J.J., Kim, K.-Y.A., Jacobson, K., Hedlund, L., Smith, M.C.J., Harris, L.M., McFadden, T., Wolf, M.S., 2016. Liquid Medication Errors and Dosing Tools: A Randomized Controlled Experiment. Pediatrics 138.

Yoo, J.J., Meng, J., Oberpenning, F., Atala, A., 1998. Bladder augmentation using allogenic bladder submucosa seeded with cells. Urology 51.

Yoshihara, T., Tadokoro, H., Murahashi, S., 1964. Normal vibrations of the polymer molecules of helical conformation. IV. Polyethylene oxide and polyethylene-d4oxide. J. Chem. Phys. 41, 2902–2911. https://doi.org/10.1063/1.1726373

Yu, D.G., Zhu, L., Branford-white, C.J., Yang, X.L., 2008. Three-Dimensional Printing in Pharmaceutics: Promises and Problems 97, 3666–3690. https://doi.org/10.1002/jps

Zanger, U.M., Schwab, M., 2013. Cytochrome P450 enzymes in drug metabolism: Regulation of gene expression, enzyme activities, and impact of genetic variation. Pharmacol. Ther. 138, 103–141. https://doi.org/10.1016/j.pharmthera.2012.12.007

Zhang, B., Cristescu, R., Chrisey, D.B., Narayan, R.J., 2020. Solvent-based Extrusion 3D Printing for the Fabrication of Tissue Engineering Scaffolds. Int. J. Bioprinting 6, 28–42. https://doi.org/10.18063/ijb.v6i1.211

Zhang, L., Mao, S., 2017. Application of quality by design in the current drug development. Asian J. Pharm. Sci. 12, 1–8. https://doi.org/10.1016/j.ajps.2016.07.006

Zhou, L., Fu, J., He, Y., 2020. A Review of 3D Printing Technologies for Soft Polymer Materials. Adv. Funct. Mater. 30, 2000187. https://doi.org/10.1002/adfm.202000187

SUMMARY IN ESTONIAN

3D printimine farmaatsias – tee uudsete ravimkandursüsteemideni

Sissejuhatus

Personaal- ehk täppismeditsiini võtete abil soovitakse haigusseisundeid ennetada, diagnoosida ja ravida viisi(de)l, mis saavutaks parima terapeutilise vastuse konkreetsel patsiendil või patsiendigrupil. Siia alla kuuluvad muuhulgas diagnostikavahendite parendamine bioloogiliste markerite kasutamisega, farmakogeneetika meetmed ja ka ravivastuse patsiendikesksem hindamine. Nende teadmiste kasutamine sobivaima raviaine, annuse ja ravimvormi valimisel aitab kaasa optimaalse ravitulemuse saavutamisele. Kusjuures, seda mitte ainult väga spetsiifiliste ja harvaesinevate haiguste, vaid ka tavapärasemate patsiendipopulatsioonide, nagu lapsed ja eakad, puhul.

Ameerika Ühendriikide Toidu- ja Ravimiamet (FDA) on avaldanud nimekirja rohkem kui viiekümnest raviainest, mille puhul geneetilised eripärad võivad muuta patsiendile vajalikku annust. Enamus neist on seotud tsütokroom P450 ensüümidega, kuna viimased vastutavad ligi 75% kliinilises praktikas olevate raviainete biotransformatsiooni eest. Traditsioonilised ravimvormid raviaine organismi viimiseks on aja jooksul arenenud keerulisteks raviainet modifitseeritult ja/või sihtmärgistatult vabastavateks ravimkandursüsteemideks. Farmakogeneetilise info ja uudsete ravimkandursüsteemide kombineerimisel on võimalik luua personaliseeritum ravi. Parema ravitulemuse saavutamiseks kasutatav teine strateegia võiks olla mitme raviaine ühte kandursüsteemi koondamine. Sellisel viisil saab vähendada patsiendi poolt võetavate ravimite hulka ning sellega omakorda parandada ravisoostumust. Mitut erinevat raviainet sisaldavad kombinatsioonravimid on näiteks kõrgvererõhutõve raviks juba apteekides müügil, kuid jällegi vaid teatud keskmistes annusekombinatsioonides. Samm õiges suunas on tehtud, kuid pikk tee on veel minna. Ravimitööstuses kasutatavad tootmistehnoloogiad, näiteks tableteerimine, on usaldusväärsed, laialdaselt uuritud ja odavad, kuid ei ole mõeldud väikesemahuliste personaliseeritud ravimite partiide loomiseks. Uute paindlikumate tootmismeetodite kasutuselevõtt on seetõttu farmaatsiateadlaste üks eesmärk.

Üheks lahenduseks eelmainitud probleemidele võib olla kolmemõõtmeline (3D) printimine. Tegu on kihtlisandustehnoloogiaga ehk varasemalt raalprojekteeritud (CAD) mudeli loomine toimub kiht kihi haaval. Sõltuvalt kasutatavatest materjalidest ja kihi lisamise viisist, jaguneb 3D printimine veel erinevateks meetoditeks. Meetodi valik aga omakorda võib seada kasutatavatele materjalidele lisatingimusi, näiteks sobilikud reoloogilised omadused ja vastupidavus kõrgele temperatuurile. 3D printimine sai alguse 1980ndatel, kuid oma laialdase populaarsuse on see meetod kogunud viimasel aastakümnel, jõudes kasutusele nii näiteks elektroonikas, autotööstuses, toiduainetööstuses, kunstivaldkonnas kui ka meditsiinis.

ISO/ASTM 52900:2015 standardi alusel jaotatakse 3D printimismeetodid seitsmesse gruppi: sideainejoa sadestamine, suunatud energiavooga mõjutamine, materjali ekstrusioon, materjali sadestamine, pulbrikihi fusioon, kihtide lamineerimine ja VAT-fotopolümerisatsioon. Selles töös kasutatakse materjali ekstrusioonil põhinevat kahte 3D printimistehnoloogiat: mikroekstrusioon ja sulatatud sadestusega modelleerimine.

Mikroekstrusioonil põhinev 3D printimine kasutab printimismaterjalina viskoosseid lahuseid või pooltahkeid materjale. Süstla-laadne printimispea liigub seatud kiirusega mööda kindlat trajektoori printimisplaadi kohal. Liikumise jooksul surutakse printimispeast kontrollitud jõul välja materjal, mis sadestub printimisplaadile ning seal kuivab. Kuivanud materjalile on võimalik peale printida järgmine kiht. Nii printimisplaati kui -pead on võimalik protsessi kiirendamiseks kuumutada.

Sulatatud sadestamisega modelleerimine kasutab materjalina varasemalt valmistatud filamente. Filamendid valmistatakse enamasti kuumsulatusekstrusioonil. Saadud filament söödetakse printimispeasse, kus see sulatatakse. Sulatatud materjal sadestatakse printimispeast etteantud kiirusel ja trajektooril printimisplaadile. Jahtunud ja tahkunud materjalile on võimalik printida järgmine kiht.

Viimastel aastatel on 3D printimistehnoloogiad jõudnud ka meditsiinivaldkonda. Kirjandusest leiab põhjalikke ülevaateid nende kasutamisest nt kardioloogias, hambaravis, plastilises kirurgias, bioprintimisel. Ravimitööstuses nähakse 3D printimises võimalikku abimeest personaliseeritud ravimite tootmisel. Aastal 2015 sai FDA poolt müügiloa esimene 3D prinditud ravim Spritam®.

Töö eesmärgid

Doktoritöö üldine eesmärk oli saavutada parem arusaam ekstrusioonil põhinevate 3D printimistehnoloogiate kasutatavusest ja olulistest protsessiparameetritest tahkete suukaudsete ravimvormide tootmisel.

Eesmärgi saavutamiseks seati tööle viis spetsiifilisemat ülesannet:

(1) leida mikroekstrusioonil põhinevale ja sulatatud sadestusega modelleerimise 3D printimismeetoditele sobilikud kandurpolümeerid ja raviained,
(2) uurida sulatatud sadestusega modelleerimisel ja mikroekstrusioonil põhinevate 3D printimismeetodite olulisi materjalidest ja protsessitingimustest tulenevaid parameetreid,
(3) uurida printimispea kiiruse ja printimisplaadi temperatuuri mõju vesipõhise polümeerlahuse 3D prinditavusele,
(4) uurida raviaine valiku mõju kuumsulatusekstrusioonil loodud filamentide toodetavusele, mehaanilistele omadustele, homogeensusele ja 3D prinditavusele,
(5) hinnata tableti geomeetria ja järeltöötluse mõju raviaine vabanemisele 3D prinditud tablettidest.

Materjalid ja meetodid

Töös kasutati polüetüleenoksiidi (PEO) vesilahuseid printimislahustena mikroekstrusioonil põhineval 3D printimisel. Ristsidumisel kasutati fotoinitsiaatorina 4-hüdroksübensofenooni (HBP). Sulatatud materjali sadestamisel põhineval 3D printimisel kasutati polükaprolaktoonil (PCL) põhinevaid kuumsulatusekstrusioonil (HME) valmistatud filamente. Plastifikaatorina filamentides kasutati araabiakummit (ARA). Mudelraviainetena olid kasutusel indometatsiin (IND), teofülliin (THEO) ja ibuprofeen (IBU).

Printimislahused (10%, 15% ja 20%) valmistati vastavalt 1 g, 1,5 g või 2 g PEO lahustamisel 10 ml destilleeritud vees. THEO lisamisel printimislahusesse lahustati raviaine kuumutamisel enne polümeeri lisamist. Ristseotud proovide puhul lisati HBP lahusesse vahetult enne printimist.

Töös kasutatud füüsikalised segud valmistati käsitsi uhmri ja nuia abil, geomeetrilise lahjendamise meetodil. HME filamentide valmistamiseks valmistati segud vastavalt 20%, 30% ja 40% IND, THEO või IBU sisaldusega. Plastifikaatori kogus oli igas segus 10%, PCL kogus muutus sõltuvalt raviaine osakaalust. Filamentide ekstrusioon viidi läbi iga segu jaoks sobivaima kiiruse ja temperatuuri juures.

Printimislahuste reoloogilisi omadusi kirjeldati viskoossuse ja süstitavuse määramise abil. Tahke faasi uuringud viidi läbi kasutades Fourier teisendusega infrapunaspektroskoopiat (FTIR), lähiinfrapunaspektroskoopiat (NIR), diferentsiaalset skaneerivat kalorimeetriat (DSC) ja (pulber)röntgendifraktomeetriat (XR(P)D). Filamendi mehhaanilisi omadusi mõõdeti kolme-punkti murdetesti abil, homogeensust kõrgefektiivse vedelikkromatograafia abil.

Töö tarbeks valmistati mudelsüsteemid kasutades nii mikroekstrusioonil kui sulatatud sadestusega modelleerimisel põhinevaid 3D printimismeetodeid. Mikroekstrusioonil prinditi PEO-põhised THEO sisaldusega silindrikujulised tabletid, mis erinesid üksteisest kihtide arvu (tableti paksuse) ja ristsidumismeetodite poolest. Sulatatud sadestusega modelleerimisel loodi PCL-põhised silindrikujulised täidetud või meekärjestruktuuriga mudeltabletid, raviainena IND või THEO.

3D-prinditavust hinnati ruudukujuliste PEO võrestike piltanalüüsil. Eksperimentaalselt saadud mudelvõrestike pindala võrreldi arvutusliku teoreetilise pindalaga. Modelleerimisel arvestati PEO kontsentratsiooni, printimispea liikumise kiiruse ja printimisplaadi temperatuuri mõju printimise korrektsusele.

Raviaine vabanemist mikroekstrusioonil ja FDM printimisel saadud tablettidest uuriti farmakopöa dissolutsioonitesti abil.

Materjali kuivamise hindamiseks pooltahke printimislahuse mikroekstrusioonil viidi läbi peakomponentanalüüs. Printimisparameetrite mõju 3D-prinditavusele hinnati regressioonanalüüsil. Gruppide omavaheliseks võrdluseks kasutati sobivaid t-teste. Tulemused on väljendatud keskmise väärtuse ja standardhälbena, kui pole märgitud teisiti.

Tulemused ja arutelu

3D prinditavuse hindamiseks kasutatud PEO10, PEO15 ja PEO20 lahused käitusid pseudoplastiliselt. Uuritud lahuste viskoossus jäi nihkekiirusel 10 s^{-1} vahemikku 24,4 ± 1,1 Pa·s kuni 186,7 ± 6,8 Pa·s (I).

Meile teadaolevalt esmakordselt printimislahuse iseloomustamiseks kasutatud süstitavuse test oli hästi rakendatav. Kasutatava raviainega printimislahuse PEO_THEO maksimaalne surumisjõud süstimiseks oli 52,9 ± 2,2 N (III).

Kandursüsteemi kombinatsioon PCL ja ARA (10%) võimaldas valmistada kuumsulatusekstrusioonil edukalt 20%, 30% ja 40% (m/m) IND või THEO sisaldusega filamente. IND filamendid olid kergelt kollakad, ühtlase läbimõõdu ja kergelt kareda pealispinnaga. THEO filamendid olid naturaalvalged ja ühtlase läbimõõduga, raviaine sisalduse kasvamisel muutus pealispind nähtavalt karedamaks. Mõlema raviainega filamendid olid 3D-prinditavad. Filamentides sisaldus teoreetilisest vähem raviainet ning see oli jaotunud ebaühtlaselt, viidates ühekruvilise ekstrusioonisüsteemi miinustele. Filamentide mehaaniline tugevus oli mõlema raviaine korral suurem väiksema raviaine sisalduse juures. Filamentide säilitamisel 40°C/75% RH juures kolme kuu jooksul muutus filamentide värv pruunikaks ning nende struktuur kadus täielikult (II).

PEO mikroekstrusioonil 3D prinditavuse hindamine oli mudelvõrestike piltanalüüsil edukas. Suurema kontsentratsiooniga PEO printimislahust kasutades ladestus printimisplaadile rohkem polümeerset materjali ning kuivamisel saadi sama printimisdisaini kasutades suurema kaalutisega objektid. Rohkem materjali deponeeriti ka madalama printimispea liikumise kiiruse korral. Prinditud võrestike pindala oli suurem (ehk materjal oli rohkem laiali valgunud) võrestikel, mille puhul kasutati kiiremat printimispea liikumise kiirust ja madalamat PEO kontsentratsiooni. Printimisplaadi kuumutamine aitas kaasa prinditud objekti kuivamisele ning väiksema pindala saavutamisele.

Analüüside käigus ei tuvastatud tehnoloogiliselt olulisi probleeme komponentide tahke faasi käitumises.

PEO-põhiste tablettide ristsidumine õnnestus UV-kiirguse ja lämmastiku keskkonnas läbi viidud gamma-kiiritamise abil. Edukas ristsidumine kiirendas THEO vabanemist tablettidest. Nii ristseotud kui ristsidumata tablettide puhul aeglustus raviaine vabanemine paksemate (rohkemate kihtidega) tablettide puhul.

PCL-põhistest tablettidest ei vabanenud IND peaaegu üldse. 24 tunni jooksul vabanes silindrikujulistest täidetud tablettidest vähem kui 5% THEO. Tableti geomeetria muutmisel meekärjestruktuuriks suurenes raviaine vabanemiskiirus ja 24 tunni jooksul vabanes ligi 12% THEO.

Järeldused ja kokkuvõte

Doktoritöös saadud tulemustest võib järeldada, et

(1) Polüetüleenoksiid (PEO) on sobilik kandjapolümeer mikroekstrusioonil, ja polükaprolaktoon (PCL) sulatatud sadestamisega modelleerimisel (FDM) põhinevatel 3D printimismeetoditel. Indometatsiini (IND) saab kasutada kombinatsioonis PCL ja kummiaraabikuga (ARA) kuumsulatusekstrusioonil filamentide valmistamiseks. Teofülliin (THEO) on kasutatav raviaine nii PCL- kui PEO-põhistes formulatsioonides.

(2) Printimisprotsessil on olulised materjali ja meetodi omadused nagu näiteks printimislahuse viskoossus, tahke faasi muutused, ning ristsidumine. Mikroekstrusioonil 3D printimiseks disainiti erineva kihtide arvuga silindrilised mudeltabletid. FDM printimisel kasutati lisaks täidetud silindrilistele tablettidele ka meekärjestruktuuriga mudeltablette.

(3) Mikroekstrusioonil põhineva 3D printimise täpsus (3D prinditavus) sõltub mitme parameetri koosmõjudest. Neist olulisim on printimisplaadi temperatuuri ja printimispea liikumise kiiruse kombinatsioon. PEO printimiseks on optimaalne kasutada printimislahust 1,2 g PEO lahustatuna 10 ml destilleeritud vees printimiskiirusel 1,0 mm/s.

(4) 20%, 30% ja 40% (m/m) kuumsulatusekstrusioonil filamendid valmistati nii IND kui THEO sisaldusega. Mõlemat tüüpi filamentide puhul oli märgatav pinnakaredus, ning suurem vastupanu mehaanilistele jõududele raviaine madalama sisalduse korral. Raviaine eksperimentaalne sisaldus filamentides oli teoreetilisest madalam ja jaotus ebaühtlane. Kolme kuu jooksul 40°C/75% RH tingimustes muutusid filamendid pruuniks ning kaotasid oma struktuuri. IND-filamendid olid prinditavad 175°C juures 40°C printimisplaadiga; THEO-filamendid vastavalt 190°C ja 40°C.

(5) Raviaine *in vitro* vabanemine PCL-põhistest täidetud tablettidest oli marginaalne. 24 h jooksul vabanes peaaegu olematu kogus IND ja vähem kui 5% THEO kogusest. Raviaine vabanemiskiirus suurenes meekärjestruktuuriga tablettide korral – 24 h jooksul vabanes umbes 12% THEO kogusest. PEO-põhistest tablettidest vabanes THEO aeglasemalt rohkemate kihtidega (paksemate) tablettide puhul. UV-ristseotud ja lämmastiku keskkonnas gamma-kiiritatud tablettidest vabanes raviaine kiiremini kui ristsidumata tablettidest.

ACKNOWLEDGEMENTS

The experiments for this work were carried out during the years 2016–2020 mainly in the Institute of Pharmacy, Faculty of Medicine, University of Tartu, Estonia. This work has been part of the Estonian Research Council projects PUT1088, PRG726, and IUT-34-18. Nordic POP (patient-oriented products), a Nordic University Hub project #85352 funded by NordForsk is acknowledged for providing the funds for a mobility action between University of Tartu and University of Eastern Finland. Doctoral School of Clinical Medicine, supported by the European Union, European Regional Development Fund (University of Tartu ASTRA project PER ASPERA) and Estonian Academical Society of Pharmacy are thanked for additional funding for presenting the results of this thesis.

My deepest gratitude goes to my supervisors, associate professor Ivo Laidmäe, associate professor Karin Kogermann, and professor Jyrki Heinämäki for their patience, feedback, and guidance. Implementing a novel technology is never easy, and every one of them played a crucial part in helping me successfully through it.

Professor Ursel Soomets from the Institute of Biomedicine and Translational Medicine, University of Tartu and dr Tarmo Tamm from the Institute of Technology, University of Tartu are thanked for thoroughly reviewing and providing their expertise and perspective in improving the quality of my dissertation.

I am thankful for professor Thomas De Beer from Ghent University, Belgium accepting the invitation to be the opponent for my dissertation commence. I enjoyed the fruitful and inspiring discussion.

I would kindly like to acknowledge

- Dr Gunnar Nurk from the Institute of Chemistry, University of Tartu for providing the facilities and helping with the rheology measurements; professor Kalle Kirsimäe and dr Jaan Aruväli from the Department of Geology, University of Tartu for providing the facilities and conducting the XRPD measurements.
- Dr Osmo Antikainen from the Division of Pharmaceutical Chemistry and Technology, University of Helsinki for modelling the results for 3D printability evaluation.
- Dr Tuomas Ervasti for our fruitful collaboration over hot-melt extrusion and 3D printing during the Nordic POP mobility action in Tartu; him and our co-authors MSc Jemina Vesala, dr Riikka Laitinen, professor Ossi Korhonen and professor Jarkko Ketolainen from the School of Pharmacy, University of Eastern Finland for conducting the solid state analysis of extruded filaments and in vitro drug release studies for FDM printed tablets, and providing their experience in data analysis and discussion.
- Professor Anne Juppo from the Division of Pharmaceutical Chemistry and Technology, University of Helsinki for providing her experience in data analysis and discussion.

- Dr Urve Paaver for giving me the opportunity to challenge myself in the field of teaching, and all those spontaneous conversations over the office door.
- Dr Andres Lust and MSc Georg-Marten Lanno for sharing the office space over the years and providing an occasional well-needed help and distraction from writing or lab work. My warmest gratitude goes to my fellow "PhD babies" Kairi Tiirik, Kaisa Põhako, Arle Kõrkjas and Georg Lanno.
- Dr Mirja Palo from Åbo Akademi University for all the help and answers to my printing-related questions and worries. I am thoroughly glad for being offered the possibility to continue and expand her PhD project work to University of Tartu.

I am thankful for the supervising experience and their help in the lab work for Pharmacy MSc students Dagmar Seera, Maria Malk and Kristjan Olado, Science and Technology BSc student Richard Erelt, and Industrial Pharmacy MSc student Hele Anderspuk.

I would like to thank all my fellow former and current PhD students and all other colleagues at the Institute of Pharmacy, who I got to share these years working with. Last, but not least I am forever grateful for my closest friends and family, who kept me going throughout my decade in the University.

PUBLICATIONS

CURRICULUM VITAE

Name	Laura Viidik
Date of birth	March 28th, 1992
Address	Nooruse Str 1, Tartu 50411
Phone	+372 737 5292
E-mail	laura.viidik@gmail.com

Education

2016–…	University of Tartu, PhD studies in Pharmacy
2011–2016	University of Tartu, MSc in Pharmacy
1999–2011	Tallinn Laagna Secondary School

Professional employment

11.2021–…	Estonian Ministry of Social Affairs, Advisor
01.2021–06.2021	University of Tartu, Institute of Pharmacy, Junior Lecturer in Pharmaceutical Technology
02.2018–12.2020	University of Tartu, Institute of Pharmacy, Assistant in Pharmaceutical Technology
01.2019–12.2019	University of Tartu, Institute of Pharmacy, Junior Research Fellow in Pharmaceutical Sciences
06.2016–10.2017	Raja Apteek OÜ, pharmacist

Fields of research

T410	Pharmaceuticals and related technologies
B740	Pharmacological sciences, pharmacognosy, pharmacy, toxicology
T390	Polymer technology, biopolymers

Honours and awards

2015	Anniversary of the Faculty of Medicine, best student poster award

Research projects

2020–2021	Participation in project LMVFA20209: The suitability of fish and shellfish materials for electrospinning of fibrous wound scaffolds
2017–2019	Participation in project PUT1088: Design and Development of Multicomponent Antibacterial Nanofibrous Dressings for Advanced Wound Care
2016–2020	Participation in project IUT34-18: Multifunctional nanomedicines – design and quality assessment

ELULOOKIRJELDUS

Nimi	Laura Viidik
Sünniaeg	28. märts 1992
Aadress	Nooruse 1, Tartu 50411
Telefon	+372 737 5292
E-mail	laura.viidik@gmail.com

Haridustee

2016–…	Tartu Ülikool, farmaatsia doktorantuur
2011–2016	Tartu Ülikooli proviisoriõpe, *MSc*
1999–2011	Tallinna Laagna Gümnaasium

Töökäik

11.2021–…	Sotsiaalministeerium, nõunik
01.2021–06.2021	Tartu Ülikooli farmaatsia instituudi farmatseutilise tehnoloogia nooremlektor
02.2018–12.2020	Tartu Ülikooli farmaatsia instituudi farmatseutilise tehnoloogia assistent
01.2019–12.2019	Tartu Ülikooli farmaatsia instituudi farmatseutilise tehnoloogia nooremteadur
06.2016–10.2017	Raja Apteek OÜ, proviisor

Teadustöö põhisuunad

T410	Farmaatsiatooted ja nende tehnoloogiad
B740	Farmakoloogia, farmakognoosia, farmaatsia, toksikoloogia
T390	Polümeeride tehnoloogia, biopolümeerid

Teaduspreemiad ja tunnustused

2015	Arstiteaduskonna päevad, parim üliõpilaste stendiettekanne

Teadusprojektid

2020–2021	projekti täitja teadus ja- arendusprojektis koostöös Eesti Maaülikooliga (hange 217903) „Uurimus kala- ja koorik-loomajääkidest valmistatud algmaterjali sobivuse kohta elektrospinnitud fiibriliste haavakatete valmistamiseks„
2017–2019	projekti täitja PUT1088 projektis „Haavaravis kasutatavate mitmeosaliste antibakteriaalsete nanofiiberkatete disain ja valmistamine“
2016–2020	projekti täitja IUT34-18 projektis „Multifunktsionaalsete nanomeditsiiniliste süsteemide väljatöötamine ja kvaliteedi hindamine”

DISSERTATIONES MEDICINAE UNIVERSITATIS TARTUENSIS

1. **Heidi-Ingrid Maaroos**. The natural course of gastric ulcer in connection with chronic gastritis and *Helicobacter pylori*. Tartu, 1991.
2. **Mihkel Zilmer**. Na-pump in normal and tumorous brain tissues: Structural, functional and tumorigenesis aspects. Tartu, 1991.
3. **Eero Vasar**. Role of cholecystokinin receptors in the regulation of behaviour and in the action of haloperidol and diazepam. Tartu, 1992.
4. **Tiina Talvik**. Hypoxic-ischaemic brain damage in neonates (clinical, biochemical and brain computed tomographical investigation). Tartu, 1992.
5. **Ants Peetsalu**. Vagotomy in duodenal ulcer disease: A study of gastric acidity, serum pepsinogen I, gastric mucosal histology and *Helicobacter pylori*. Tartu, 1992.
6. **Marika Mikelsaar**. Evaluation of the gastrointestinal microbial ecosystem in health and disease. Tartu, 1992.
7. **Hele Everaus**. Immuno-hormonal interactions in chronic lymphocytic leukaemia and multiple myeloma. Tartu, 1993.
8. **Ruth Mikelsaar**. Etiological factors of diseases in genetically consulted children and newborn screening: dissertation for the commencement of the degree of doctor of medical sciences. Tartu, 1993.
9. **Agu Tamm**. On metabolic action of intestinal microflora: clinical aspects. Tartu, 1993.
10. **Katrin Gross**. Multiple sclerosis in South-Estonia (epidemiological and computed tomographical investigations). Tartu, 1993.
11. **Oivi Uibo**. Childhood coeliac disease in Estonia: occurrence, screening, diagnosis and clinical characterization. Tartu, 1994.
12. **Viiu Tuulik**. The functional disorders of central nervous system of chemistry workers. Tartu, 1994.
13. **Margus Viigimaa**. Primary haemostasis, antiaggregative and anticoagulant treatment of acute myocardial infarction. Tartu, 1994.
14. **Rein Kolk**. Atrial versus ventricular pacing in patients with sick sinus syndrome. Tartu, 1994.
15. **Toomas Podar**. Incidence of childhood onset type 1 diabetes mellitus in Estonia. Tartu, 1994.
16. **Kiira Subi**. The laboratory surveillance of the acute respiratory viral infections in Estonia. Tartu, 1995.
17. **Irja Lutsar**. Infections of the central nervous system in children (epidemiologic, diagnostic and therapeutic aspects, long term outcome). Tartu, 1995.
18. **Aavo Lang**. The role of dopamine, 5-hydroxytryptamine, sigma and NMDA receptors in the action of antipsychotic drugs. Tartu, 1995.
19. **Andrus Arak**. Factors influencing the survival of patients after radical surgery for gastric cancer. Tartu, 1996.

20. **Tõnis Karki**. Quantitative composition of the human lactoflora and method for its examination. Tartu, 1996.
21. **Reet Mändar**. Vaginal microflora during pregnancy and its transmission to newborn. Tartu, 1996.
22. **Triin Remmel**. Primary biliary cirrhosis in Estonia: epidemiology, clinical characterization and prognostication of the course of the disease. Tartu, 1996.
23. **Toomas Kivastik**. Mechanisms of drug addiction: focus on positive reinforcing properties of morphine. Tartu, 1996.
24. **Paavo Pokk**. Stress due to sleep deprivation: focus on $GABA_A$ receptor-chloride ionophore complex. Tartu, 1996.
25. **Kristina Allikmets**. Renin system activity in essential hypertension. Associations with atherothrombogenic cardiovascular risk factors and with the efficacy of calcium antagonist treatment. Tartu, 1996.
26. **Triin Parik**. Oxidative stress in essential hypertension: Associations with metabolic disturbances and the effects of calcium antagonist treatment. Tartu, 1996.
27. **Svetlana Päi**. Factors promoting heterogeneity of the course of rheumatoid arthritis. Tartu, 1997.
28. **Maarike Sallo**. Studies on habitual physical activity and aerobic fitness in 4 to 10 years old children. Tartu, 1997.
29. **Paul Naaber**. *Clostridium difficile* infection and intestinal microbial ecology. Tartu, 1997.
30. **Rein Pähkla**. Studies in pinoline pharmacology. Tartu, 1997.
31. **Andrus Juhan Voitk**. Outpatient laparoscopic cholecystectomy. Tartu, 1997.
32. **Joel Starkopf**. Oxidative stress and ischaemia-reperfusion of the heart. Tartu, 1997.
33. **Janika Kõrv**. Incidence, case-fatality and outcome of stroke. Tartu, 1998.
34. **Ülla Linnamägi**. Changes in local cerebral blood flow and lipid peroxidation following lead exposure in experiment. Tartu, 1998.
35. **Ave Minajeva**. Sarcoplasmic reticulum function: comparison of atrial and ventricular myocardium. Tartu, 1998.
36. **Oleg Milenin**. Reconstruction of cervical part of esophagus by revascularised ileal autografts in dogs. A new complex multistage method. Tartu, 1998.
37. **Sergei Pakriev**. Prevalence of depression, harmful use of alcohol and alcohol dependence among rural population in Udmurtia. Tartu, 1998.
38. **Allen Kaasik**. Thyroid hormone control over β-adrenergic signalling system in rat atria. Tartu, 1998.
39. **Vallo Matto**. Pharmacological studies on anxiogenic and antiaggressive properties of antidepressants. Tartu, 1998.
40. **Maire Vasar**. Allergic diseases and bronchial hyperreactivity in Estonian children in relation to environmental influences. Tartu, 1998.
41. **Kaja Julge**. Humoral immune responses to allergens in early childhood. Tartu, 1998.

42. **Heli Grünberg**. The cardiovascular risk of Estonian schoolchildren. A cross-sectional study of 9-, 12- and 15-year-old children. Tartu, 1998.
43. **Epp Sepp**. Formation of intestinal microbial ecosystem in children. Tartu, 1998.
44. **Mai Ots**. Characteristics of the progression of human and experimental glomerulopathies. Tartu, 1998.
45. **Tiina Ristimäe**. Heart rate variability in patients with coronary artery disease. Tartu, 1998.
46. **Leho Kõiv**. Reaction of the sympatho-adrenal and hypothalamo-pituitary-adrenocortical system in the acute stage of head injury. Tartu, 1998.
47. **Bela Adojaan**. Immune and genetic factors of childhood onset IDDM in Estonia. An epidemiological study. Tartu, 1999.
48. **Jakov Shlik**. Psychophysiological effects of cholecystokinin in humans. Tartu, 1999.
49. **Kai Kisand**. Autoantibodies against dehydrogenases of α-ketoacids. Tartu, 1999.
50. **Toomas Marandi**. Drug treatment of depression in Estonia. Tartu, 1999.
51. **Ants Kask**. Behavioural studies on neuropeptide Y. Tartu, 1999.
52. **Ello-Rahel Karelson**. Modulation of adenylate cyclase activity in the rat hippocampus by neuropeptide galanin and its chimeric analogs. Tartu, 1999.
53. **Tanel Laisaar**. Treatment of pleural empyema — special reference to intrapleural therapy with streptokinase and surgical treatment modalities. Tartu, 1999.
54. **Eve Pihl**. Cardiovascular risk factors in middle-aged former athletes. Tartu, 1999.
55. **Katrin Õunap**. Phenylketonuria in Estonia: incidence, newborn screening, diagnosis, clinical characterization and genotype/phenotype correlation. Tartu, 1999.
56. **Siiri Kõljalg**. *Acinetobacter* – an important nosocomial pathogen. Tartu, 1999.
57. **Helle Karro**. Reproductive health and pregnancy outcome in Estonia: association with different factors. Tartu, 1999.
58. **Heili Varendi**. Behavioral effects observed in human newborns during exposure to naturally occurring odors. Tartu, 1999.
59. **Anneli Beilmann**. Epidemiology of epilepsy in children and adolescents in Estonia. Prevalence, incidence, and clinical characteristics. Tartu, 1999.
60. **Vallo Volke**. Pharmacological and biochemical studies on nitric oxide in the regulation of behaviour. Tartu, 1999.
61. **Pilvi Ilves**. Hypoxic-ischaemic encephalopathy in asphyxiated term infants. A prospective clinical, biochemical, ultrasonographical study. Tartu, 1999.
62. **Anti Kalda**. Oxygen-glucose deprivation-induced neuronal death and its pharmacological prevention in cerebellar granule cells. Tartu, 1999.
63. **Eve-Irene Lepist**. Oral peptide prodrugs – studies on stability and absorption. Tartu, 2000.

64. **Jana Kivastik**. Lung function in Estonian schoolchildren: relationship with anthropometric indices and respiratory symptomas, reference values for dynamic spirometry. Tartu, 2000.
65. **Karin Kull**. Inflammatory bowel disease: an immunogenetic study. Tartu, 2000.
66. **Kaire Innos**. Epidemiological resources in Estonia: data sources, their quality and feasibility of cohort studies. Tartu, 2000.
67. **Tamara Vorobjova**. Immune response to *Helicobacter pylori* and its association with dynamics of chronic gastritis and epithelial cell turnover in antrum and corpus. Tartu, 2001.
68. **Ruth Kalda**. Structure and outcome of family practice quality in the changing health care system of Estonia. Tartu, 2001.
69. **Annika Krüüner**. *Mycobacterium tuberculosis* – spread and drug resistance in Estonia. Tartu, 2001.
70. **Marlit Veldi**. Obstructive Sleep Apnoea: Computerized Endopharyngeal Myotonometry of the Soft Palate and Lingual Musculature. Tartu, 2001.
71. **Anneli Uusküla**. Epidemiology of sexually transmitted diseases in Estonia in 1990–2000. Tartu, 2001.
72. **Ade Kallas**. Characterization of antibodies to coagulation factor VIII. Tartu, 2002.
73. **Heidi Annuk**. Selection of medicinal plants and intestinal lactobacilli as antimicrobil components for functional foods. Tartu, 2002.
74. **Aet Lukmann**. Early rehabilitation of patients with ischaemic heart disease after surgical revascularization of the myocardium: assessment of health-related quality of life, cardiopulmonary reserve and oxidative stress. A clinical study. Tartu, 2002.
75. **Maigi Eisen**. Pathogenesis of Contact Dermatitis: participation of Oxidative Stress. A clinical – biochemical study. Tartu, 2002.
76. **Piret Hussar**. Histology of the post-traumatic bone repair in rats. Elaboration and use of a new standardized experimental model – bicortical perforation of tibia compared to internal fracture and resection osteotomy. Tartu, 2002.
77. **Tõnu Rätsep**. Aneurysmal subarachnoid haemorrhage: Noninvasive monitoring of cerebral haemodynamics. Tartu, 2002.
78. **Marju Herodes**. Quality of life of people with epilepsy in Estonia. Tartu, 2003.
79. **Katre Maasalu**. Changes in bone quality due to age and genetic disorders and their clinical expressions in Estonia. Tartu, 2003.
80. **Toomas Sillakivi**. Perforated peptic ulcer in Estonia: epidemiology, risk factors and relations with *Helicobacter pylori*. Tartu, 2003.
81. **Leena Puksa**. Late responses in motor nerve conduction studies. F and A waves in normal subjects and patients with neuropathies. Tartu, 2003.
82. **Krista Lõivukene**. *Helicobacter pylori* in gastric microbial ecology and its antimicrobial susceptibility pattern. Tartu, 2003.

83. **Helgi Kolk**. Dyspepsia and *Helicobacter pylori* infection: the diagnostic value of symptoms, treatment and follow-up of patients referred for upper gastrointestinal endoscopy by family physicians. Tartu, 2003.
84. **Helena Soomer**. Validation of identification and age estimation methods in forensic odontology. Tartu, 2003.
85. **Kersti Oselin**. Studies on the human MDR1, MRP1, and MRP2 ABC transporters: functional relevance of the genetic polymorphisms in the *MDR1* and *MRP1* gene. Tartu, 2003.
86. **Jaan Soplepmann**. Peptic ulcer haemorrhage in Estonia: epidemiology, prognostic factors, treatment and outcome. Tartu, 2003.
87. **Margot Peetsalu**. Long-term follow-up after vagotomy in duodenal ulcer disease: recurrent ulcer, changes in the function, morphology and *Helicobacter pylori* colonisation of the gastric mucosa. Tartu, 2003.
88. **Kersti Klaamas**. Humoral immune response to *Helicobacter pylori* a study of host-dependent and microbial factors. Tartu, 2003.
89. **Pille Taba**. Epidemiology of Parkinson's disease in Tartu, Estonia. Prevalence, incidence, clinical characteristics, and pharmacoepidemiology. Tartu, 2003.
90. **Alar Veraksitš**. Characterization of behavioural and biochemical phenotype of cholecystokinin-2 receptor deficient mice: changes in the function of the dopamine and endopioidergic system. Tartu, 2003.
91. **Ingrid Kalev**. CC-chemokine receptor 5 (CCR5) gene polymorphism in Estonians and in patients with Type I and Type II diabetes mellitus. Tartu, 2003.
92. **Lumme Kadaja**. Molecular approach to the regulation of mitochondrial function in oxidative muscle cells. Tartu, 2003.
93. **Aive Liigant**. Epidemiology of primary central nervous system tumours in Estonia from 1986 to 1996. Clinical characteristics, incidence, survival and prognostic factors. Tartu, 2004.
94. **Andres, Kulla**. Molecular characteristics of mesenchymal stroma in human astrocytic gliomas. Tartu, 2004.
95. **Mari Järvelaid**. Health damaging risk behaviours in adolescence. Tartu, 2004.
96. **Ülle Pechter**. Progression prevention strategies in chronic renal failure and hypertension. An experimental and clinical study. Tartu, 2004.
97. **Gunnar Tasa**. Polymorphic glutathione S-transferases – biology and role in modifying genetic susceptibility to senile cataract and primary open angle glaucoma. Tartu, 2004.
98. **Tuuli Käämbre**. Intracellular energetic unit: structural and functional aspects. Tartu, 2004.
99. **Vitali Vassiljev**. Influence of nitric oxide syntase inhibitors on the effects of ethanol after acute and chronic ethanol administration and withdrawal. Tartu, 2004.

100. **Aune Rehema**. Assessment of nonhaem ferrous iron and glutathione redox ratio as markers of pathogeneticity of oxidative stress in different clinical groups. Tartu, 2004.
101. **Evelin Seppet**. Interaction of mitochondria and ATPases in oxidative muscle cells in normal and pathological conditions. Tartu, 2004.
102. **Eduard Maron**. Serotonin function in panic disorder: from clinical experiments to brain imaging and genetics. Tartu, 2004.
103. **Marje Oona**. *Helicobacter pylori* infection in children: epidemiological and therapeutic aspects. Tartu, 2004.
104. **Kersti Kokk**. Regulation of active and passive molecular transport in the testis. Tartu, 2005.
105. **Vladimir Järv**. Cross-sectional imaging for pretreatment evaluation and follow-up of pelvic malignant tumours. Tartu, 2005.
106. **Andre Õun**. Epidemiology of adult epilepsy in Tartu, Estonia. Incidence, prevalence and medical treatment. Tartu, 2005.
107. **Piibe Muda**. Homocysteine and hypertension: associations between homocysteine and essential hypertension in treated and untreated hypertensive patients with and without coronary artery disease. Tartu, 2005.
108. **Külli Kingo**. The interleukin-10 family cytokines gene polymorphisms in plaque psoriasis. Tartu, 2005.
109. **Mati Merila**. Anatomy and clinical relevance of the glenohumeral joint capsule and ligaments. Tartu, 2005.
110. **Epp Songisepp**. Evaluation of technological and functional properties of the new probiotic *Lactobacillus fermentum* ME-3. Tartu, 2005.
111. **Tiia Ainla**. Acute myocardial infarction in Estonia: clinical characteristics, management and outcome. Tartu, 2005.
112. **Andres Sell**. Determining the minimum local anaesthetic requirements for hip replacement surgery under spinal anaesthesia – a study employing a spinal catheter. Tartu, 2005.
113. **Tiia Tamme**. Epidemiology of odontogenic tumours in Estonia. Pathogenesis and clinical behaviour of ameloblastoma. Tartu, 2005.
114. **Triine Annus**. Allergy in Estonian schoolchildren: time trends and characteristics. Tartu, 2005.
115. **Tiia Voor**. Microorganisms in infancy and development of allergy: comparison of Estonian and Swedish children. Tartu, 2005.
116. **Priit Kasenõmm**. Indicators for tonsillectomy in adults with recurrent tonsillitis – clinical, microbiological and pathomorphological investigations. Tartu, 2005.
117. **Eva Zusinaite**. Hepatitis C virus: genotype identification and interactions between viral proteases. Tartu, 2005.
118. **Piret Kõll**. Oral lactoflora in chronic periodontitis and periodontal health. Tartu, 2006.
119. **Tiina Stelmach**. Epidemiology of cerebral palsy and unfavourable neurodevelopmental outcome in child population of Tartu city and county, Estonia Prevalence, clinical features and risk factors. Tartu, 2006.

120. **Katrin Pudersell**. Tropane alkaloid production and riboflavine excretion in the field and tissue cultures of henbane (*Hyoscyamus niger* L.). Tartu, 2006.
121. **Külli Jaako**. Studies on the role of neurogenesis in brain plasticity. Tartu, 2006.
122. **Aare Märtson**. Lower limb lengthening: experimental studies of bone regeneration and long-term clinical results. Tartu, 2006.
123. **Heli Tähepõld**. Patient consultation in family medicine. Tartu, 2006.
124. **Stanislav Liskmann**. Peri-implant disease: pathogenesis, diagnosis and treatment in view of both inflammation and oxidative stress profiling. Tartu, 2006.
125. **Ruth Rudissaar**. Neuropharmacology of atypical antipsychotics and an animal model of psychosis. Tartu, 2006.
126. **Helena Andreson**. Diversity of *Helicobacter pylori* genotypes in Estonian patients with chronic inflammatory gastric diseases. Tartu, 2006.
127. **Katrin Pruus**. Mechanism of action of antidepressants: aspects of serotoninergic system and its interaction with glutamate. Tartu, 2006.
128. **Priit Põder**. Clinical and experimental investigation: relationship of ischaemia/reperfusion injury with oxidative stress in abdominal aortic aneurysm repair and in extracranial brain artery endarterectomy and possibilities of protection against ischaemia using a glutathione analogue in a rat model of global brain ischaemia. Tartu, 2006.
129. **Marika Tammaru**. Patient-reported outcome measurement in rheumatoid arthritis. Tartu, 2006.
130. **Tiia Reimand**. Down syndrome in Estonia. Tartu, 2006.
131. **Diva Eensoo**. Risk-taking in traffic and Markers of Risk-Taking Behaviour in Schoolchildren and Car Drivers. Tartu, 2007.
132. **Riina Vibo**. The third stroke registry in Tartu, Estonia from 2001 to 2003: incidence, case-fatality, risk factors and long-term outcome. Tartu, 2007.
133. **Chris Pruunsild**. Juvenile idiopathic arthritis in children in Estonia. Tartu, 2007.
134. **Eve Õiglane-Šlik**. Angelman and Prader-Willi syndromes in Estonia. Tartu, 2007.
135. **Kadri Haller**. Antibodies to follicle stimulating hormone. Significance in female infertility. Tartu, 2007.
136. **Pille Ööpik**. Management of depression in family medicine. Tartu, 2007.
137. **Jaak Kals**. Endothelial function and arterial stiffness in patients with atherosclerosis and in healthy subjects. Tartu, 2007.
138. **Priit Kampus**. Impact of inflammation, oxidative stress and age on arterial stiffness and carotid artery intima-media thickness. Tartu, 2007.
139. **Margus Punab**. Male fertility and its risk factors in Estonia. Tartu, 2007.
140. **Alar Toom**. Heterotopic ossification after total hip arthroplasty: clinical and pathogenetic investigation. Tartu, 2007.

141. **Lea Pehme**. Epidemiology of tuberculosis in Estonia 1991–2003 with special regard to extrapulmonary tuberculosis and delay in diagnosis of pulmonary tuberculosis. Tartu, 2007.
142. **Juri Karjagin**. The pharmacokinetics of metronidazole and meropenem in septic shock. Tartu, 2007.
143. **Inga Talvik**. Inflicted traumatic brain injury shaken baby syndrome in Estonia – epidemiology and outcome. Tartu, 2007.
144. **Tarvo Rajasalu**. Autoimmune diabetes: an immunological study of type 1 diabetes in humans and in a model of experimental diabetes (in RIP-B7.1 mice). Tartu, 2007.
145. **Inga Karu**. Ischaemia-reperfusion injury of the heart during coronary surgery: a clinical study investigating the effect of hyperoxia. Tartu, 2007.
146. **Peeter Padrik**. Renal cell carcinoma: Changes in natural history and treatment of metastatic disease. Tartu, 2007.
147. **Neve Vendt**. Iron deficiency and iron deficiency anaemia in infants aged 9 to 12 months in Estonia. Tartu, 2008.
148. **Lenne-Triin Heidmets**. The effects of neurotoxins on brain plasticity: focus on neural Cell Adhesion Molecule. Tartu, 2008.
149. **Paul Korrovits**. Asymptomatic inflammatory prostatitis: prevalence, etiological factors, diagnostic tools. Tartu, 2008.
150. **Annika Reintam**. Gastrointestinal failure in intensive care patients. Tartu, 2008.
151. **Kristiina Roots**. Cationic regulation of Na-pump in the normal, Alzheimer's and CCK_2 receptor-deficient brain. Tartu, 2008.
152. **Helen Puusepp**. The genetic causes of mental retardation in Estonia: fragile X syndrome and creatine transporter defect. Tartu, 2009.
153. **Kristiina Rull**. Human chorionic gonadotropin beta genes and recurrent miscarriage: expression and variation study. Tartu, 2009.
154. **Margus Eimre**. Organization of energy transfer and feedback regulation in oxidative muscle cells. Tartu, 2009.
155. **Maire Link**. Transcription factors FoxP3 and AIRE: autoantibody associations. Tartu, 2009.
156. **Kai Haldre**. Sexual health and behaviour of young women in Estonia. Tartu, 2009.
157. **Kaur Liivak**. Classical form of congenital adrenal hyperplasia due to 21-hydroxylase deficiency in Estonia: incidence, genotype and phenotype with special attention to short-term growth and 24-hour blood pressure. Tartu, 2009.
158. **Kersti Ehrlich**. Antioxidative glutathione analogues (UPF peptides) – molecular design, structure-activity relationships and testing the protective properties. Tartu, 2009.
159. **Anneli Rätsep**. Type 2 diabetes care in family medicine. Tartu, 2009.
160. **Silver Türk**. Etiopathogenetic aspects of chronic prostatitis: role of mycoplasmas, coryneform bacteria and oxidative stress. Tartu, 2009.

161. **Kaire Heilman**. Risk markers for cardiovascular disease and low bone mineral density in children with type 1 diabetes. Tartu, 2009.
162. **Kristi Rüütel**. HIV-epidemic in Estonia: injecting drug use and quality of life of people living with HIV. Tartu, 2009.
163. **Triin Eller**. Immune markers in major depression and in antidepressive treatment. Tartu, 2009.
164. **Siim Suutre**. The role of TGF-β isoforms and osteoprogenitor cells in the pathogenesis of heterotopic ossification. An experimental and clinical study of hip arthroplasty. Tartu, 2010.
165. **Kai Kliiman**. Highly drug-resistant tuberculosis in Estonia: Risk factors and predictors of poor treatment outcome. Tartu, 2010.
166. **Inga Villa**. Cardiovascular health-related nutrition, physical activity and fitness in Estonia. Tartu, 2010.
167. **Tõnis Org**. Molecular function of the first PHD finger domain of Autoimmune Regulator protein. Tartu, 2010.
168. **Tuuli Metsvaht**. Optimal antibacterial therapy of neonates at risk of early onset sepsis. Tartu, 2010.
169. **Jaanus Kahu**. Kidney transplantation: Studies on donor risk factors and mycophenolate mofetil. Tartu, 2010.
170. **Koit Reimand**. Autoimmunity in reproductive failure: A study on associated autoantibodies and autoantigens. Tartu, 2010.
171. **Mart Kull**. Impact of vitamin D and hypolactasia on bone mineral density: a population based study in Estonia. Tartu, 2010.
172. **Rael Laugesaar**. Stroke in children – epidemiology and risk factors. Tartu, 2010.
173. **Mark Braschinsky**. Epidemiology and quality of life issues of hereditary spastic paraplegia in Estonia and implemention of genetic analysis in everyday neurologic practice. Tartu, 2010.
174. **Kadri Suija**. Major depression in family medicine: associated factors, recurrence and possible intervention. Tartu, 2010.
175. **Jarno Habicht**. Health care utilisation in Estonia: socioeconomic determinants and financial burden of out-of-pocket payments. Tartu, 2010.
176. **Kristi Abram**. The prevalence and risk factors of rosacea. Subjective disease perception of rosacea patients. Tartu, 2010.
177. **Malle Kuum**. Mitochondrial and endoplasmic reticulum cation fluxes: Novel roles in cellular physiology. Tartu, 2010.
178. **Rita Teek**. The genetic causes of early onset hearing loss in Estonian children. Tartu, 2010.
179. **Daisy Volmer**. The development of community pharmacy services in Estonia – public and professional perceptions 1993–2006. Tartu, 2010.
180. **Jelena Lissitsina**. Cytogenetic causes in male infertility. Tartu, 2011.
181. **Delia Lepik**. Comparison of gunshot injuries caused from Tokarev, Makarov and Glock 19 pistols at different firing distances. Tartu, 2011.
182. **Ene-Renate Pähkla**. Factors related to the efficiency of treatment of advanced periodontitis. Tartu, 2011.

183. **Maarja Krass**. L-Arginine pathways and antidepressant action. Tartu, 2011.
184. **Taavi Lai**. Population health measures to support evidence-based health policy in Estonia. Tartu, 2011.
185. **Tiit Salum**. Similarity and difference of temperature-dependence of the brain sodium pump in normal, different neuropathological, and aberrant conditions and its possible reasons. Tartu, 2011.
186. **Tõnu Vooder**. Molecular differences and similarities between histological subtypes of non-small cell lung cancer. Tartu, 2011.
187. **Jelena Štšepetova**. The characterisation of intestinal lactic acid bacteria using bacteriological, biochemical and molecular approaches. Tartu, 2011.
188. **Radko Avi**. Natural polymorphisms and transmitted drug resistance in Estonian HIV-1 CRF06_cpx and its recombinant viruses. Tartu, 2011, 116 p.
189. **Edward Laane**. Multiparameter flow cytometry in haematological malignancies. Tartu, 2011, 152 p.
190. **Triin Jagomägi**. A study of the genetic etiology of nonsyndromic cleft lip and palate. Tartu, 2011, 158 p.
191. **Ivo Laidmäe**. Fibrin glue of fish (*Salmo salar*) origin: immunological study and development of new pharmaceutical preparation. Tartu, 2012, 150 p.
192. **Ülle Parm**. Early mucosal colonisation and its role in prediction of invasive infection in neonates at risk of early onset sepsis. Tartu, 2012, 168 p.
193. **Kaupo Teesalu**. Autoantibodies against desmin and transglutaminase 2 in celiac disease: diagnostic and functional significance. Tartu, 2012, 142 p.
194. **Maksim Zagura**. Biochemical, functional and structural profiling of arterial damage in atherosclerosis. Tartu, 2012, 162 p.
195. **Vivian Kont**. Autoimmune regulator: characterization of thymic gene regulation and promoter methylation. Tartu, 2012, 134 p.
196. **Pirje Hütt**. Functional properties, persistence, safety and efficacy of potential probiotic lactobacilli. Tartu, 2012, 246 p.
197. **Innar Tõru**. Serotonergic modulation of CCK-4- induced panic. Tartu, 2012, 132 p.
198. **Sigrid Vorobjov**. Drug use, related risk behaviour and harm reduction interventions utilization among injecting drug users in Estonia: implications for drug policy. Tartu, 2012, 120 p.
199. **Martin Serg**. Therapeutic aspects of central haemodynamics, arterial stiffness and oxidative stress in hypertension. Tartu, 2012, 156 p.
200. **Jaanika Kumm**. Molecular markers of articular tissues in early knee osteoarthritis: a population-based longitudinal study in middle-aged subjects. Tartu, 2012, 159 p.
201. **Kertu Rünkorg**. Functional changes of dopamine, endopioid and endocannabinoid systems in CCK2 receptor deficient mice. Tartu, 2012, 125 p.
202. **Mai Blöndal**. Changes in the baseline characteristics, management and outcomes of acute myocardial infarction in Estonia. Tartu, 2012, 127 p.

203. **Jana Lass**. Epidemiological and clinical aspects of medicines use in children in Estonia. Tartu, 2012, 170 p.
204. **Kai Truusalu**. Probiotic lactobacilli in experimental persistent *Salmonella* infection. Tartu, 2013, 139 p.
205. **Oksana Jagur**. Temporomandibular joint diagnostic imaging in relation to pain and bone characteristics. Long-term results of arthroscopic treatment. Tartu, 2013, 126 p.
206. **Katrin Sikk**. Manganese-ephedrone intoxication – pathogenesis of neurological damage and clinical symptomatology. Tartu, 2013, 125 p.
207. **Kai Blöndal**. Tuberculosis in Estonia with special emphasis on drug-resistant tuberculosis: Notification rate, disease recurrence and mortality. Tartu, 2013, 151 p.
208. **Marju Puurand**. Oxidative phosphorylation in different diseases of gastric mucosa. Tartu, 2013, 123 p.
209. **Aili Tagoma**. Immune activation in female infertility: Significance of autoantibodies and inflammatory mediators. Tartu, 2013, 135 p.
210. **Liis Sabre**. Epidemiology of traumatic spinal cord injury in Estonia. Brain activation in the acute phase of traumatic spinal cord injury. Tartu, 2013, 135 p.
211. **Merit Lamp**. Genetic susceptibility factors in endometriosis. Tartu, 2013, 125 p.
212. **Erik Salum**. Beneficial effects of vitamin D and angiotensin II receptor blocker on arterial damage. Tartu, 2013, 167 p.
213. **Maire Karelson**. Vitiligo: clinical aspects, quality of life and the role of melanocortin system in pathogenesis. Tartu, 2013, 153 p.
214. **Kuldar Kaljurand**. Prevalence of exfoliation syndrome in Estonia and its clinical significance. Tartu, 2013, 113 p.
215. **Raido Paasma**. Clinical study of methanol poisoning: handling large outbreaks, treatment with antidotes, and long-term outcomes. Tartu, 2013, 96 p.
216. **Anne Kleinberg**. Major depression in Estonia: prevalence, associated factors, and use of health services. Tartu, 2013, 129 p.
217. **Triin Eglit**. Obesity, impaired glucose regulation, metabolic syndrome and their associations with high-molecular-weight adiponectin levels. Tartu, 2014, 115 p.
218. **Kristo Ausmees**. Reproductive function in middle-aged males: Associations with prostate, lifestyle and couple infertility status. Tartu, 2014, 125 p.
219. **Kristi Huik**. The influence of host genetic factors on the susceptibility to HIV and HCV infections among intravenous drug users. Tartu, 2014, 144 p.
220. **Liina Tserel**. Epigenetic profiles of monocytes, monocyte-derived macrophages and dendritic cells. Tartu, 2014, 143 p.
221. **Irina Kerna**. The contribution of *ADAM12* and *CILP* genes to the development of knee osteoarthritis. Tartu, 2014, 152 p.

222. **Ingrid Liiv**. Autoimmune regulator protein interaction with DNA-dependent protein kinase and its role in apoptosis. Tartu, 2014, 143 p.
223. **Liivi Maddison**. Tissue perfusion and metabolism during intra-abdominal hypertension. Tartu, 2014, 103 p.
224. **Krista Ress**. Childhood coeliac disease in Estonia, prevalence in atopic dermatitis and immunological characterisation of coexistence. Tartu, 2014, 124 p.
225. **Kai Muru**. Prenatal screening strategies, long-term outcome of children with marked changes in maternal screening tests and the most common syndromic heart anomalies in Estonia. Tartu, 2014, 189 p.
226. **Kaja Rahu**. Morbidity and mortality among Baltic Chernobyl cleanup workers: a register-based cohort study. Tartu, 2014, 155 p.
227. **Klari Noormets**. The development of diabetes mellitus, fertility and energy metabolism disturbances in a Wfs1-deficient mouse model of Wolfram syndrome. Tartu, 2014, 132 p.
228. **Liis Toome**. Very low gestational age infants in Estonia. Tartu, 2014, 183 p.
229. **Ceith Nikkolo**. Impact of different mesh parameters on chronic pain and foreign body feeling after open inguinal hernia repair. Tartu, 2014, 132 p.
230. **Vadim Brjalin**. Chronic hepatitis C: predictors of treatment response in Estonian patients. Tartu, 2014, 122 p.
231. **Vahur Metsna**. Anterior knee pain in patients following total knee arthroplasty: the prevalence, correlation with patellar cartilage impairment and aspects of patellofemoral congruence. Tartu, 2014, 130 p.
232. **Marju Kase**. Glioblastoma multiforme: possibilities to improve treatment efficacy. Tartu, 2015, 137 p.
233. **Riina Runnel**. Oral health among elementary school children and the effects of polyol candies on the prevention of dental caries. Tartu, 2015, 112 p.
234. **Made Laanpere**. Factors influencing women's sexual health and reproductive choices in Estonia. Tartu, 2015, 176 p.
235. **Andres Lust**. Water mediated solid state transformations of a polymorphic drug – effect on pharmaceutical product performance. Tartu, 2015, 134 p.
236. **Anna Klugman**. Functionality related characterization of pretreated wood lignin, cellulose and polyvinylpyrrolidone for pharmaceutical applications. Tartu, 2015, 156 p.
237. **Triin Laisk-Podar**. Genetic variation as a modulator of susceptibility to female infertility and a source for potential biomarkers. Tartu, 2015, 155 p.
238. **Mailis Tõnisson**. Clinical picture and biochemical changes in blood in children with acute alcohol intoxication. Tartu, 2015, 100 p.
239. **Kadri Tamme**. High volume haemodiafiltration in treatment of severe sepsis – impact on pharmacokinetics of antibiotics and inflammatory response. Tartu, 2015, 133 p.

240. **Kai Part**. Sexual health of young people in Estonia in a social context: the role of school-based sexuality education and youth-friendly counseling services. Tartu, 2015, 203 p.
241. **Urve Paaver**. New perspectives for the amorphization and physical stabilization of poorly water-soluble drugs and understanding their dissolution behavior. Tartu, 2015, 139 p.
242. **Aleksandr Peet**. Intrauterine and postnatal growth in children with HLA-conferred susceptibility to type 1 diabetes. Tartu. 2015, 146 p.
243. **Piret Mitt**. Healthcare-associated infections in Estonia – epidemiology and surveillance of bloodstream and surgical site infections. Tartu, 2015, 145 p.
244. **Merli Saare**. Molecular Profiling of Endometriotic Lesions and Endometria of Endometriosis Patients. Tartu, 2016, 129 p.
245. **Kaja-Triin Laisaar**. People living with HIV in Estonia: Engagement in medical care and methods of increasing adherence to antiretroviral therapy and safe sexual behavior. Tartu, 2016, 132 p.
246. **Eero Merilind**. Primary health care performance: impact of payment and practice-based characteristics. Tartu, 2016, 120 p.
247. **Jaanika Kärner**. Cytokine-specific autoantibodies in AIRE deficiency. Tartu, 2016, 182 p.
248. **Kaido Paapstel**. Metabolomic profile of arterial stiffness and early biomarkers of renal damage in atherosclerosis. Tartu, 2016, 173 p.
249. **Liidia Kiisk**. Long-term nutritional study: anthropometrical and clinico-laboratory assessments in renal replacement therapy patients after intensive nutritional counselling. Tartu, 2016, 207 p.
250. **Georgi Nellis**. The use of excipients in medicines administered to neonates in Europe. Tartu, 2017, 159 p.
251. **Aleksei Rakitin**. Metabolic effects of acute and chronic treatment with valproic acid in people with epilepsy. Tartu, 2017, 125 p.
252. **Eveli Kallas**. The influence of immunological markers to susceptibility to HIV, HBV, and HCV infections among persons who inject drugs. Tartu, 2017, 138 p.
253. **Tiina Freimann**. Musculoskeletal pain among nurses: prevalence, risk factors, and intervention. Tartu, 2017, 125 p.
254. **Evelyn Aaviksoo**. Sickness absence in Estonia: determinants and influence of the sick-pay cut reform. Tartu, 2017, 121 p.
255. **Kalev Nõupuu**. Autosomal-recessive Stargardt disease: phenotypic heterogeneity and genotype-phenotype associations. Tartu, 2017, 131 p.
256. **Ho Duy Binh**. Osteogenesis imperfecta in Vietnam. Tartu, 2017, 125 p.
257. **Uku Haljasorg**. Transcriptional mechanisms in thymic central tolerance. Tartu, 2017, 147 p.
258. **Živile Riispere**. IgA Nephropathy study according to the Oxford Classification: IgA Nephropathy clinical-morphological correlations, disease progression and the effect of renoprotective therapy. Tartu, 2017, 129 p.

259. **Hiie Soeorg**. Coagulase-negative staphylococci in gut of preterm neonates and in breast milk of their mothers. Tartu, 2017, 216 p.
260. **Anne-Mari Anton Willmore**. Silver nanoparticles for cancer research. Tartu, 2017, 132 p.
261. **Ott Laius**. Utilization of osteoporosis medicines, medication adherence and the trend in osteoporosis related hip fractures in Estonia. Tartu, 2017, 134 p.
262. **Alar Aab**. Insights into molecular mechanisms of asthma and atopic dermatitis. Tartu, 2017, 164 p.
263. **Sander Pajusalu**. Genome-wide diagnostics of Mendelian disorders: from chromosomal microarrays to next-generation sequencing. Tartu, 2017, 146 p.
264. **Mikk Jürisson**. Health and economic impact of hip fracture in Estonia. Tartu, 2017, 164 p.
265. **Kaspar Tootsi**. Cardiovascular and metabolomic profiling of osteoarthritis. Tartu, 2017, 150 p.
266. **Mario Saare**. The influence of AIRE on gene expression – studies of transcriptional regulatory mechanisms in cell culture systems. Tartu, 2017, 172 p.
267. **Piia Jõgi**. Epidemiological and clinical characteristics of pertussis in Estonia. Tartu, 2018, 168 p.
268. **Elle Põldoja**. Structure and blood supply of the superior part of the shoulder joint capsule. Tartu, 2018, 116 p.
269. **Minh Son Nguyen**. Oral health status and prevalence of temporomandibular disorders in 65–74-year-olds in Vietnam. Tartu, 2018, 182 p.
270. **Kristian Semjonov**. Development of pharmaceutical quench-cooled molten and melt-electrospun solid dispersions for poorly water-soluble indomethacin. Tartu, 2018, 125 p.
271. **Janne Tiigimäe-Saar**. Botulinum neurotoxin type A treatment for sialorrhea in central nervous system diseases. Tartu, 2018, 109 p.
272. **Veiko Vengerfeldt**. Apical periodontitis: prevalence and etiopathogenetic aspects. Tartu, 2018, 150 p.
273. **Rudolf Bichele**. TNF superfamily and AIRE at the crossroads of thymic differentiation and host protection against *Candida albicans* infection. Tartu, 2018, 153 p.
274. **Olga Tšuiko**. Unravelling Chromosomal Instability in Mammalian Preimplantation Embryos Using Single-Cell Genomics. Tartu, 2018, 169 p.
275. **Kärt Kriisa**. Profile of acylcarnitines, inflammation and oxidative stress in first-episode psychosis before and after antipsychotic treatment. Tartu, 2018, 145 p.
276. **Xuan Dung Ho**. Characterization of the genomic profile of osteosarcoma. Tartu, 2018, 144 p.
277. **Karit Reinson**. New Diagnostic Methods for Early Detection of Inborn Errors of Metabolism in Estonia. Tartu, 2018, 201 p.

278. **Mari-Anne Vals**. Congenital N-glycosylation Disorders in Estonia. Tartu, 2019, 148 p.
279. **Liis Kadastik-Eerme**. Parkinson's disease in Estonia: epidemiology, quality of life, clinical characteristics and pharmacotherapy. Tartu, 2019, 202 p.
280. **Hedi Hunt**. Precision targeting of intraperitoneal tumors with peptide-guided nanocarriers. Tartu, 2019, 179 p.
281. **Rando Porosk**. The role of oxidative stress in Wolfram syndrome 1 and hypothermia. Tartu, 2019, 123 p.
282. **Ene-Ly Jõgeda**. The influence of coinfections and host genetic factor on the susceptibility to HIV infection among people who inject drugs. Tartu, 2019, 126 p.
283. **Kristel Ehala-Aleksejev**. The associations between body composition, obesity and obesity-related health and lifestyle conditions with male reproductive function. Tartu, 2019, 138 p.
284. **Aigar Ottas**. The metabolomic profiling of psoriasis, atopic dermatitis and atherosclerosis. Tartu, 2019, 136 p.
285. **Elmira Gurbanova**. Specific characteristics of tuberculosis in low default, but high multidrug–resistance prison setting. Tartu, 2019, 129 p.
286. **Van Thai Nguyeni**. The first study of the treatment outcomes of patients with cleft lip and palate in Central Vietnam. Tartu, 2019, 144 p.
287. **Maria Yakoreva**. Imprinting Disorders in Estonia. Tartu, 2019, 187 p.
288. **Kadri Rekker**. The putative role of microRNAs in endometriosis pathogenesis and potential in diagnostics. Tartu, 2019, 140 p.
289. **Ülle Võhma**. Association between personality traits, clinical characteristics and pharmacological treatment response in panic disorder. Tartu, 2019, 121 p.
290. **Aet Saar**. Acute myocardial infarction in Estonia 2001–2014: towards risk-based prevention and management. Tartu, 2019, 124 p.
291. **Toomas Toomsoo**. Transcranial brain sonography in the Estonian cohort of Parkinson's disease. Tartu, 2019, 114 p.
292. **Lidiia Zhytnik**. Inter- and intrafamilial diversity based on genotype and phenotype correlations of Osteogenesis Imperfecta. Tartu, 2019, 224 p.
293. **Pilleriin Soodla**. Newly HIV-infected people in Estonia: estimation of incidence and transmitted drug resistance. Tartu, 2019, 194 p.
294. **Kristiina Ojamaa**. Epidemiology of gynecological cancer in Estonia. Tartu, 2020, 133 p.
295. **Marianne Saard**. Modern Cognitive and Social Intervention Techniques in Paediatric Neurorehabilitation for Children with Acquired Brain Injury. Tartu, 2020, 168 p.
296. **Julia Maslovskaja**. The importance of DNA binding and DNA breaks for AIRE-mediated transcriptional activation. Tartu, 2020, 162 p.
297. **Natalia Lobanovskaya**. The role of PSA-NCAM in the survival of retinal ganglion cells. Tartu, 2020, 105 p.

298. **Madis Rahu**. Structure and blood supply of the postero-superior part of the shoulder joint capsule with implementation of surgical treatment after anterior traumatic dislocation. Tartu, 2020, 104 p.
299. **Helen Zirnask**. Luteinizing hormone (LH) receptor expression in the penis and its possible role in pathogenesis of erectile disturbances. Tartu, 2020, 87 p.
300. **Kadri Toome**. Homing peptides for targeting of brain diseases. Tartu, 2020, 152 p.
301. **Maarja Hallik**. Pharmacokinetics and pharmacodynamics of inotropic drugs in neonates. Tartu, 2020, 172 p.
302. **Raili Müller**. Cardiometabolic risk profile and body composition in early rheumatoid arthritis. Tartu, 2020, 133 p.
303. **Sergo Kasvandik**. The role of proteomic changes in endometrial cells – from the perspective of fertility and endometriosis. Tartu, 2020, 191 p.
304. **Epp Kaleviste**. Genetic variants revealing the role of STAT1/STAT3 signaling cytokines in immune protection and pathology. Tartu, 2020, 189 p.
305. **Sten Saar**. Epidemiology of severe injuries in Estonia. Tartu, 2020, 104 p.
306. **Kati Braschinsky**. Epidemiology of primary headaches in Estonia and applicability of web-based solutions in headache epidemiology research. Tartu, 2020, 129 p.
307. **Helen Vaher**. MicroRNAs in the regulation of keratinocyte responses in *psoriasis vulgaris* and atopic dermatitis. Tartu, 2020, 242 p.
308. **Liisi Raam**. Molecular Alterations in the Pathogenesis of Two Chronic Dermatoses – Vitiligo and Psoriasis. Tartu, 2020, 164 p.
309. **Artur Vetkas**. Long-term quality of life, emotional health, and associated factors in patients after aneurysmal subarachnoid haemorrhage. Tartu, 2020, 127 p.
310. **Teele Kasepalu**. Effects of remote ischaemic preconditioning on organ damage and acylcarnitines' metabolism in vascular surgery. Tartu, 2020, 130 p.
311. **Prakash Lingasamy**. Development of multitargeted tumor penetrating peptides. Tartu, 2020, 246 p.
312. **Lille Kurvits.** Parkinson's disease as a multisystem disorder: whole transcriptome study in Parkinson's disease patients' skin and blood. Tartu, 2021, 142 p.
313. **Mariliis Põld.** Smoking, attitudes towards smoking behaviour, and nicotine dependence among physicians in Estonia: cross-sectional surveys 1982–2014. Tartu, 2021, 172 p.
314. **Triin Kikas**. Single nucleotide variants affecting placental gene expression and pregnancy outcome. Tartu, 2021, 160 p.
315. **Hedda Lippus-Metsaots**. Interpersonal violence in Estonia: prevalence, impact on health and health behaviour. Tartu, 2021, 172 p.

316. **Georgi Dzaparidze.** Quantification and evaluation of the diagnostic significance of adenocarcinoma-associated microenvironmental changes in the prostate using modern digital pathology solutions. Tartu, 2021, 132 p.
317. **Tuuli Sedman.** New avenues for GLP1 receptor agonists in the treatment of diabetes. Tartu, 2021, 118 p.
318. **Martin Padar.** Enteral nutrition, gastrointestinal dysfunction and intestinal biomarkers in critically ill patients. Tartu, 2021, 189 p.
319. **Siim Schneider.** Risk factors, etiology and long-term outcome in young ischemic stroke patients in Estonia. Tartu, 2021, 131 p.
320. **Konstantin Ridnõi.** Implementation and effectiveness of new prenatal diagnostic strategies in Estonia. Tartu, 2021, 191 p.
321. **Risto Vaikjärv.** Etiopathogenetic and clinical aspects of peritonsillar abscess. Tartu, 2021, 115 p.
322. **Liis Preem.** Design and characterization of antibacterial electrospun drug delivery systems for wound infections. Tartu, 2022, 220 p.
323. **Keerthie Dissanayake.** Preimplantation embryo-derived extracellular vesicles: potential as an embryo quality marker and their role during the embryo-maternal communication. Tartu, 2022, 203 p.